CORK STRUCTURAL CHARACTERISTICS AND THEIR INFLUENCE ON THE OXYGEN INGRESS THROUGH WINE STOPPERS

VANDA CRISTINA PAIVA TAVARES DE OLIVEIRA

ORIENTADORA: Doutora Helena Margarida Nunes Pereira

COORIENTADOR: Doutor Miguel Freire de Albuquerque Ferreira Cabral

TESE ELABORADA PARA OBTENÇÃO DO GRAU DE DOUTOR EM
ENGENHARIA FLORESTAL E DOS RECURSOS NATURAIS

2016

CORK STRUCTURAL CHARACTERISTICS AND THEIR INFLUENCE ON THE OXYGEN INGRESS THROUGH WINE STOPPERS

VANDA CRISTINA PAIVA TAVARES DE OLIVEIRA

ORIENTADORA: Doutora Helena Margarida Nunes Pereira

COORIENTADOR: Doutor Miguel Freire de Albuquerque Ferreira Cabral

TESE ELABORADA PARA OBTENÇÃO DO GRAU DE DOUTOR EM

ENGENHARIA FLORESTAL E DOS RECURSOS NATURAIS

JÚRI:

Presidente: Doutora Maria Margarida Branco de Brito Tavares Tomé, Professora Catedrática, Instituto Superior de Agronomia, Universidade de Lisboa

Vogais: Doutora Helena Margarida Nunes Pereira, Professora Catedrática, Instituto Superior de Agronomia, Universidade de Lisboa;
Mestre Luis Manuel da Costa Cabral e Gil, Investigador Principal, Direção Geral de Energia e Geologia;
Doutor Francisco Javier Vázquez Piqué, Professor Coordenador, Escuela Politécnica Superior, Universidad de Huelva, Espanha;
Doutor Miguel Freire de Albuquerque Ferreira Cabral, Professor Auxiliar, Faculdade de Farmácia, Universidade do Porto;
Doutora Ofélia Maria Serralha dos Anjos, Professora Adjunta, Escola Superior Agrária, Instituto Politécnico de Castelo Branco;
Doutor Paulo Dinis Vale Lopes, Investigador, Amorim & Irmãos, S.A., individualidade de reconhecida competência.

Este trabalho foi financiado no âmbito do projecto FCOMP-01-0124-FEDER-005421 e desenvolvido no Centro de Estudos Florestais, UI apoiada pelo financiamento nacional da FCT (PEst-OE/AGR/UI0239/2013). A doutoranda teve uma bolsa de doutoramento atribuída pela FCT (SFRH/BD/77550/2011).

2016

ACKNOWLEDGEMENTS

This research was carried out under the framework of Centro de Estudos Florestais, a research unit funded by Fundação para a Ciência e Tecnologia, Portugal (PEst OE/AGR/UI0239/2014). Financial support was given by a doctoral scholarship from FCT (SFRH/BD/77550/2011). Part of this work was carried out under the project FCOMP-01-0124-FEDER-005421 supported by FEDER funds through the Operational Programme for Competitiveness Factors–COMPETE. Part of the work was carried out under the Trees4Future project (no. 284181) with financial support from the Transnational Access to Research Infrastructures activity in the 7th Framework Programme of the EC.

First, I want to express my sincere gratitude to Professor Helena Pereira for the continuous support, advice and encouragement through all the time, much more than a supervisor has been a mentor and a true friend. It is a privilege to work with you.

I would like to thank also to Professor Miguel Cabral for the useful comments and suggestions during the work. Thanks to all my co-authors, especially to Dr. Paulo Lopes, Dr. Sofia Knapic and dr. ir. Jan Van den Bulcke. It has been a pleasure to work with you. I also thank to my colleague Lídia Silva for the support in the image analysis process and the collaboration of UAVISION in X-ray tomography image acquisition.

I would like to thank to the friends and colleagues in the Centro de Estudos Florestais that never stop helping me in different phases of this work. Special thanks to Sofia Knapic, Jorge Gominho and Ana Lourenço.

To all my friends and beloved family for believing and support me. To Ricardo and my daughters, Mafalda and Leonor, that gives me courage to go on every day.

ABSTRACT

Cork structural characteristics and their influence on the oxygen ingress through wine stoppers were studied aiming to contribute to an increased added-value of the natural cork stoppers.

The surface porosity features of cork stoppers can differentiate the three main commercial classes used nowadays: the porosity coefficient was 2.4%, 4.0% and 5.5% for premium, good and standard stoppers, respectively. Image analysis also distinguished defects in the cork structure: empty ant gallery; *Coroebus undatus* F. larvae gallery; and wetcork. Several predictive classification models of stoppers into quality classes were built using the results from cork stoppers surface characterization and a simplified model using the main discriminant features i.e. porosity coefficient and the RGB colour-type variables was presented.

X-ray tomography was used as a non-destructive technique to study the internal structure of natural cork stoppers, allowing the visualization of some defects inside the cork stopper. After characterization, the natural cork stoppers were used as closure of bottles and oxygen diffusion measurements were made along time. The kinetics of oxygen transfer was similar and could be adjusted to logarithmic models. On average 35% of the overall oxygen ingress occurred in the first 5 days, 59% in the 1st month and 78% in the first 3 months.

Microtomography images (voxel size of 50 μm) allowed the observation of lenticular channels development and geometry, and the quantification of void and high density regions (HDR) fractions. The evidence that the void fraction of lenticular channels in the innermost part of the cork stopper inserted in the bottle was strongly related to the oxygen ingress in the first month after bottling can be used for quality enhancement of natural cork stoppers with incorporation of performance requirements.

Keywords: natural cork stoppers, lenticular channels, image analysis, X-ray tomography, oxygen ingress rate

RESUMO

No presente trabalho foram estudadas as características estruturais da cortiça e a sua influência sobre a transmissão de oxigénio das rolhas de cortiça natural para o vinho com o objectivo de contribuir para um maior valor acrescentado das rolhas de cortiça natural.

As características de porosidade da superfície da rolha de cortiça podem diferenciar as três principais classes comerciais utilizadas actualmente. Através da análise de imagem consegue-se também, caso sejam visíveis à superfície, distinguir defeitos que podem ocorrer na estrutura da cortiça e que são importantes para o seu desempenho, nomeadamente, galerias de formiga, galeria de larvas de *Coroebus undatus* F. ou cortiça verde.

Foram desenvolvidos vários modelos preditivos para classificação das rolhas em classes de qualidade e é apresentado um modelo simplificado com as principais características discriminantes, isto é, o coeficiente de porosidade e as variáveis RGB relacionadas com a cor.

Neste trabalho utilizou-se tomografia de raio-X como técnica não-destrutiva útil para adquirir conhecimento sobre a estrutura interna de rolhas de cortiça natural. Esta técnica permitiu a visualização e identificação de alguns defeitos no interior da rolha de cortiça.

A medição da transmissão de oxigénio das rolhas de cortiça natural foi realizada utilizando o método colorimétrico optimizado e calibrado em estudos preliminares. A cinética da transmissão de oxigénio foi semelhante em todos os casos e pode ser expressa através de modelos logarítmicos. Em média, 35% da entrada de oxigénio total ocorre nos primeiros 5 dias, 59% no primeiro mês e 78% nos primeiros 3 meses.

Microtomografia foi aplicada a uma pequena amostra de rolhas de cortiça natural, conseguindo-se uma resolução de 50 µm o que permitiu a observação do desenvolvimento e geometria dos canais lenticulares assim como a quantificação de regiões de vazio (baixa densidade) e elevada densidade.

Os resultados sugerem que a variação de entrada de oxigénio é principalmente uma consequência das diferentes características de dimensões celulares e volume de ar existente dentro da estrutura da rolha, nomeadamente, a fracção de vazios dos canais lenticulares.

Palavras-chave: rolhas naturais de cortiça, canais lenticulares, análise de imagem, tomografia de raios-X, taxa de transmissão de oxigénio

RESUMO ALARGADO

No presente trabalho foram estudadas as características estruturais da cortiça (na superfície e no interior) e a sua influência sobre a transmissão de oxigénio das rolhas de cortiça natural para o vinho com o objectivo de contribuir para um maior valor acrescentado das rolhas de cortiça natural.

Dado que actualmente a avaliação da qualidade das rolhas de cortiça natural é feita por análise visual da sua superfície exterior, esta foi a primeira tarefa deste trabalho. Verificou-se que as características de porosidade da superfície da rolha de cortiça podem diferenciar as três principais classes comerciais utilizadas actualmente. O coeficiente de porosidade foi de 2,4%, 4,0% e 5,5% para as rolhas classificadas como *premium, good* e *standard*, respectivamente. Através da análise de imagem consegue-se também, caso sejam visíveis à superfície, distinguir defeitos que podem ocorrer na estrutura da cortiça e que são importantes para o seu desempenho, nomeadamente, galerias de formiga, galeria de larvas de *Coroebus undatus* F. ou cortiça verde.

O estudo detalhado da porosidade da superfície das rolhas permitiu também a percepção de aspectos relacionados com a formação da cortiça. A comparação da porosidade entre os dois topos confirmou a existência de variação axial na árvore e.g. um topo pode ter porosidade significativamente mais baixa do que o outro. Isto pode ser utilizado na prática na produção de rolhas, como as concebidas para engarrafamento de vinhos e bebidas espirituosas.

Utilizando os resultados obtidos na caracterização da superfície das rolhas, foram desenvolvidos vários modelos preditivos para classificação das rolhas em classes de qualidade. É apresentado um modelo simplificado com as principais características discriminantes, isto é, o coeficiente de porosidade e as variáveis RGB relacionadas com a cor.

No entanto, os estudos existentes revelaram que as diferentes classes de qualidade apresentam uma heterogeneidade considerável no que respeita à taxa de transmissão de oxigénio, uma propriedade importante das rolhas de cortiça, definidora da capacidade da rolha como vedante. A transmissão de oxigénio das rolhas de cortiça natural é independente dos parâmetros clássicos de valorização comercial: classe visual de qualidade, diâmetro, comprimento e massa volúmica, mostrando a necessidade de identificar parâmetros críticos internos que podem ser responsáveis por classes de qualidade não homogéneas.

Neste trabalho utilizou-se tomografia de raio-X como técnica não-destrutiva útil para adquirir conhecimento sobre a estrutura interna de rolhas de cortiça natural. Esta técnica permitiu a visualização e identificação de alguns defeitos no interior da rolha de cortiça.

Após aquisição das imagens de raio X, as rolhas de cortiça natural foram utilizadas para fechar garrafas onde se realizaram as medições de transmissão de oxigénio ao longo do tempo. A medição da transmissão de oxigénio das rolhas de cortiça natural foi realizada utilizando o método colorimétrico optimizado e calibrado em estudos preliminares. A cinética da transmissão de oxigénio foi semelhante em todos os casos, isto é, incluindo rolhas das três classes de qualidade e com defeitos, e pode ser expressa através de modelos logarítmicos. Existe uma entrada rápida de oxigénio nos primeiros dias após engarrafamento, com uma taxa inicial elevada, seguida por uma diminuição das taxas de transmissão após o primeiro mês e daí em diante, até ocorrer uma estabilização a taxa baixa e constante após o terceiro mês e depois disso. Em média, 35% da entrada de oxigénio ocorre nos primeiros cinco dias, 59% no primeiro mês e 78% nos primeiros três meses. Os resultados mostram que rolhas de cortiça natural brocadas de pranchas de cortiça com 27-32 mm e 45-54 mm transmitem, em média, 1,88 mg e 2,35 mg de oxigénio, respectivamente, o que representa 36-38% e 47- 50% do total do oxigénio presente teoricamente na estrutura celular da cortiça.

Os resultados encontrados corroboram a hipótese de que a elevada taxa de transmissão de oxigénio observada durante o primeiro mês após o engarrafamento é devida ao ar existente na estrutura da cortiça que é forçado a sair quando as rolhas são comprimidas no gargalo. Mais, os resultados sugerem que a variação de entrada de oxigénio é principalmente uma consequência das diferentes características de dimensões celulares e volume de ar existente dentro da estrutura da rolha.

Considerando que não foi encontrada correlação entre as características de porosidade da superfície das rolhas e a taxa de transmissão de oxigénio, e que os resultados enfatizaram a necessidade de quantificação das características de porosidade interna, efectuou-se a aquisição de imagens de raios-X com maior resolução. A resolução da imagem alcançada (tamanho do voxel de 50 µm) permitiu a observação do desenvolvimento e geometria dos canais lenticulares assim como permitiu a quantificação de regiões de vazio (baixa densidade) e elevada densidade. A fracção de vazio variou entre 0,7% a 2,3%, enquanto o volume vazio máximo de uma única estrutura variou entre 7,9 a 104,9 mm^3.

A evidência de que os canais lenticulares, nomeadamente, a sua fracção de vazio, se encontra fortemente relacionado com a entrada de oxigénio no primeiro mês após o engarrafamento

pode ser usada para a valorização das rolhas de cortiça natural com incorporação na definição de classes de qualidade de requisitos de desempenho.

Palavras-chave: rolhas de cortiça natural, canais lenticulares, análise de imagem, tomografia de raio-X, taxa de transmissão de oxigénio

TABLE OF CONTENTS

INTRODUCTION AND OBJECTIVES

1. INTRODUCTION

In Portugal, beyond the great relevance of forest and forest industry, one species – the cork oak, *Quercus suber* - and one product – cork – outstand with a determining role in the country's economy, namely regarding external trade (Pereira 2007).

The cork oak forests have a substantial ecological role *i.e.* against desertification and in maintaining animal and plant biodiversity in their restricted area of occurrence in several western Mediterranean countries, covering a total worldwide area of more than 2.1 million hectares. Portugal has 34 % of the world's area, which corresponds to about 736 thousand hectares and 23 % of the national forest (APCOR 2015). Cork is obtained from the bark of the cork oak and exploited during the tree's lifetime. It is one of the world's important non-timber forest products, with the cork industry directed towards global markets.

World cork production reached 201 thousand tonnes, with Portugal as the leader, with 49.6 % of the production. According to the foreign trade data from the National Statistics Institute (INE), Portugal exported 846 million euros (182 thousand tonnes of cork) in 2014. Cork stoppers lead the Portuguese cork exports, accounting for about 70 % of their total value (592.6 million euros), followed by cork building materials with 26 %. Within the cork stopper segment, natural corks come first with 62 % of the total value (367.2 million euros), followed by champagne stoppers with 20 % (117.1 million euros) and the other types of stoppers representing 18 % (APCOR 2015).

Cork is world known as the material used for sealing wine bottles. Cork is a cellular material with a set of specific physical and mechanical properties that provide an outstanding material when in-bottle wine aging is wanted, by combining the required minute oxygen transfer with mechanical sealing of the bottle, durability and chemical stability (Lopes et al. 2005, Pereira 2007). Cork is the closure material preferred by wine consumers, as shown by recent surveys (Bleibaum 2013, OpinionWay 2014, AstraRicerche 2014, CTR Market Research 2014, Iniciativa CORK 2012, Barber et al. 2008). However, the natural variability of cork brings some performance heterogeneity that producers and consumers would like to circumvent.

One of the most important and conspicuous characteristics of cork is the natural presence of lenticular channels crossing the cork from the outside to the inner tissue of the phellogen and containing a non-suberified filling material with darker color (Pereira 2007, Anjos et al. 2008).

Nowadays, the natural cork stoppers are graded into quality classes in function of the apparent homogeneity of their external surface which is mostly based on the extent of the visible lenticular porosity or of defects, as seen by human or machine vision (Costa and Pereira 2005, 2007, Pereira 2007). This appreciation is visual and not related with the specific physical and mechanical properties that provide cork with its outstanding sealing performance, and a great range of porosity can be found in each commercial quality class of natural stoppers.

Moreover, the different quality classes present a considerable heterogeneity in oxygen transmission rate, one important property of cork stoppers, defining its ability as sealant. Recent studies have shown that the oxygen transmission rate of natural corks stoppers is independent of the classic parameters of valorisation, visual quality grades, diameter, length and density (Lopes et al. 2006). The cork stoppers are essentially impermeable to atmospheric oxygen, but transmit oxygen from its own cellular structure to the wine (Lopes et al. 2007).

These results emphasize the need to identify internal critical parameters that may be responsible for the heterogeneity within quality classes and to elucidate the internal porosity spatial distribution.

It was in this context that the research project INCORK (FCOMP-01-0124-FEDER-005421) was developed with the participation of Amorim & Irmãos, Centro de Estudos Florestais, and New Jersey Institute of Technology. INCORK aimed at the development of a new integrated system for non-destructive evaluation of the internal structure and the outer surface of cork stoppers that would allow optimizing their quality grading and oxygen transmission.

It was in the framework of INCORK that the present work was carried out. The study encompasses a detailed characterization of the surface of natural cork stoppers using image analysis, the use of X-ray tomography as non-destructive technique for material internal characterization, and the determination of the oxygen transmission rate after bottling.

2. OBJECTIVES AND OVERVIEW

The research carried out in this work aimed to contribute to the natural cork stoppers valorisation by modelling their oxygen transmission performance using modern techniques for non-destructive analysis. This knowledge will allow achieving higher levels of quality and consistency in performance by developing an integrative quality classification based on visual quality and sealing performance.

The specific objectives were:

i. To determine the internal structure of the natural cork stoppers, namely through the identification and dimension of heterogeneity zones (porosity and inclusions, for example);

ii. To understand how internal structural features, namely porosity distribution and critical defects, may be related to oxygen transfer properties;

iii. To understand if the internal structural features can be inferred by natural cork stoppers surface features;

iv. To develop three-dimensional modelling of the natural cork stoppers internal structure needed to achieve higher levels of quality and consistency in performance.

The operational objectives were:

i. Characterization of the natural cork stoppers by non-destructive methods:
    a. Natural cork stoppers surface by image analysis; and
    b. Natural cork stoppers internal structure by X-ray tomography;

ii. Determination of the oxygen transmission rate after bottling;

iii. Statistical analysis of correlation between the internal structure of natural cork stoppers and the features of its outer surface with the oxygen transmission results into the wine after bottling.

This thesis is structured in chapters, with the results presented as internationally refereed papers published in scientific journals of the specific areas.

The present chapter intends to be a brief introduction of the thesis with description of the main objectives and list of publications.

The second chapter presents the state of the art related to the subjects dealt with in this work. It gives a general description of the cork oak tree and the sustainable management practice for cork production, and reviews the formation and structure of cork. Because the work focused on natural cork stoppers, cork processing and industry is presented with emphasis on natural cork stopper production and quality (visual and oxygen permeability). Finally, the use of X-ray tomography is reviewed as a non-destructive technique for the analysis of materials.

The third chapter presents the original research starting with an outline, followed by the material and methods used in this work, and the results that encompass a total of five articles published in international journals with referee. In sequence an integrative discussion of all the results is presented, and at last the conclusions are highlighted with the perspective of future works.

3. LIST OF PUBLICATIONS AND PRESENTATIONS

This thesis is based on the following peer-reviewed publications:

I. **Oliveira V**, Knapic S, Pereira H (2012) Natural variability of surface porosity of wine cork stoppers of different commercial classes. Journal International des Sciences de la Vigne et du Vin, 46(4): 331-340

II. **Oliveira V**, Knapic S, Pereira H (2015) Classification modelling based on surface porosity for the grading of natural cork stoppers for quality wines. Food and Bioproducts Processing, 93:69-76. DOI: 10.1016/j.fbp.2013.11.004

III. **Oliveira V**, Lopes P, Cabral M, Pereira H (2013) Kinetics of Oxygen Ingress into Wine Bottles Closed with Natural Cork Stoppers of Different Qualities. American Journal of Enology and Viticulture, 64(3): 395-399. DOI: 10.5344/ajev.2013.13009

IV. **Oliveira V**, Van den Bulcke J, Van Acker J, de Schryver T, Pereira H (2016) Cork structural discontinuities studied with X-ray microtomography. Holzforschung, 70(1): 87-94. DOI: 10.1515/hf-2014-0245

V. **Oliveira V**, Lopes P, Cabral M, Pereira H (2015) Influence of cork defects in the oxygen ingress through wine stoppers: insights with X-ray tomography, Journal of Food Engineering, 165:66-73. DOI: 10.1016/j.jfoodeng.2015.05.019

All publications are reproduced here with the permission of the publishers.

The results from this work were also accepted for oral presentations in the following conferences:

I. Oliveira V and Pereira H (2015) Transferência de oxigénio para o vinho em garrafas com rolhas de cortiça natural. Ciclo de Sessões: Da investigação à aplicação "O Montado e a Cortiça", Sept 25, Instituto Superior de Agronomia, Lisboa, Portugal. http://www.repository.utl.pt/handle/10400.5/9280

II. Oliveira V and Pereira H (2014) Conhecer as rolhas de cortiça: exterior, interior e permeabilidade ao oxigénio em garrafa. Ciclo de Sessões: Da investigação à aplicação "O Montado e a Cortiça", Jan 31, Instituto Superior de Agronomia, Lisboa, Portugal. http://www.repository.utl.pt//handle/10400.5/6758

III. Oliveira V, Knapic S, Pereira H (2013) The porosity of natural cork stoppers. 7th National Forest Congress. Forests-Knowledge and Innovation, June 5-8, Vila Real and Bragança, Portugal. http://www.spcflorestais.pt/index.php/76-7-congresso-florestal-nacional-2013

IV. Oliveira V, Knapic S, Pereira H (2012) The surface porosity of natural cork stoppers produced from cork boards of different calliper. IUFRO Conference. Division 5 Forest Products, July 8-13, Lisboa, Portugal. http://www.cabdirect.org/abstracts/20123419612.html

STATE OF THE ART

1. THE SUSTAINABLE MANAGEMENT OF CORK PRODUCTION

Cork is a product obtained from the cork oak (*Quercus suber* L.), a species spreading around the western Mediterranean basin, and of crucial importance to the economy and ecology of several Mediterranean countries, covering a worldwide area of 2 139 942 hectares of which Portugal has 736 thousand hectares (34% of the world's area and 23% of the national forest). The world cork production totals more than 201 thousand tonnes, with Portugal being responsible for around 49.6% and 100 thousand tonnes (APCOR 2015).

Internationally, cork oak forests are acknowledge for cork production but also for their role in environmental protection against soil erosion and desertification, their specificity and value as a particular landscape, their biodiversity preservation, aesthetic and identity values, attractiveness for recreation and environmental balance (Costa et al. 2009; Surová and Pinto-Correia 2008; Pinto-Correia et al. 2011; Surová et al. 2011).

Cork oak forests are often a part of a multifunctional agro-forestry-pastoral system called «*montado*» that is considered a High Nature Value Farming System, according to the European classification proposed by the European Environmental Agency (Pinto-Correia et al. 2011). These ecosystems are also recognized as habitats of conservation value listed in the Habitats Directive (Catry et al. 2012).

In this non wood forest production system, cork harvesting is still the major economic activity, and cork the most valuable product. The entire cork chain from the forest to the consumer relies on the regular and sustainable production of cork. To maintain cork production capacity and provide the mentioned environmental services, it is necessary that cork oak forests are adequately managed, being the sustainability a matter of general concern (Pereira 2007).

The exploitation of the cork oak as a cork producer needs its periodical removal from the stem and branches in a degree that is considered well-suited with the maintenance of the tree in good physiological conditions (Pereira 2007). Cork production yields depend not only on the tree growth and cork growth, as well as on management variables such as intensity of cork extraction and the interval between strippings that are regulated with strict rules by the Portuguese legislation (Decreto-Lei n.º 155/2004).

The production of cork relies on a specific forest management and silvicultural model, often called subericulture that is based on the biological characteristics of the cork-oak bark development (Pereira and Tomé 2004). The extraction of cork, or cork stripping, is done

manually by cutting large rectangular planks and pulling them out of the tree when the cork oak is physiologically active in late spring and early summer. By law, young trees can only be stripped when they reach at least 70 cm of perimeter at 1.3 m of height, corresponding to about 25 years of age. Moreover, cork cannot be stripped above a stem height equal to twice the perimeter of the stem in the first stripping, or not more than three times, for a mature tree in full production, the so called stripping coefficient.The trees are then debarked every 9 years (the legal minimum allowed in Portugal and Spain) or more, called the production cycle. The decision of longer production cycles is often related to an adjustment to cork growth and productivity in order to achieve a minimum cork plank thickness.

This means that in cork management planning cork growth is the main criteria to consider since it determines the thickness of the cork plank that is available for industrial processing, which is primarily oriented towards the production of wine stoppers (requiring a minimum thickness of 27 mm after the cork boiling operation).

The annual cork growth during a production cycle varies with the number of years (growth is usually higher in the first years of the cycle) and is influenced by environmental and tree conditions (Costa et al. 2002, Ferreira et al. 2000). Pereira (2007) refers that, in a study considering 30 locations in Portugal, the annual cork growth was on average 3.5 mm, ranging from 2.1 and 4.6 mm. In a recent study encompassing a large time span (24 years) and sampling (1584 cork samples), it was found an average annual cork-ring width ranging from 1.2 to 7.3 mm with an average value of 3.3 mm (Oliveira et al. 2016). Both studies reveal differences between sites that could be explained by climatic factors, especially due to water availability (Caritat et al. 2000; Costa et al. 2002; Oliveira et al. 2016).

Cork oaks show high resiliency to inter-annual precipitation variability, with rapid and complete recovery from extreme dry years or from rainfall exclusion, but have a high sensitivity to the amount and timing of late spring precipitation (Besson et al. 2014). In Mediterranean conditions access to water resources and the relationship to soil-site conditions are key factors for cork oak development (Costa et al. 2009). Soils with low depth and high compactness have a negative influence on the development of the cork oak deep root system, thereby diminishing the access to direct ground water resources, namely during summer drought (Costa et al. 2008; David et al. 2007, 2013).

Taking into consideration that future climate scenarios predict a reduction of spring precipitation and greater severity of droughts in the Iberian Peninsula (Miranda et al. 2006, Gea-Izquierdo et al. 2013, Granda et al. 2013), a cork growth decrease is expected, with

narrower annual rings and a consequent decrease of cork thickness. This will have implications regarding the raw-material adequacy to the cork industry, and the need for a potential adjustment of the silvicultural cork management.

A recent study demonstrated that in the cork stoppers supply chain it is the forest management stage that has the largest contribution to the environmental impact in the majority of the impact categories, namely due to the pruning and spontaneous vegetation cleaning operations (Demertzi et al. 2016). Moreover, several factors such as pests and diseases or over-harvesting are endangering cork oak forests, by affecting tree health and increasing vulnerability to wildfires that are exacerbated by climate changes (Catry et al. 2012). In a climate change environment, adaptive management concepts are needed so as to maintain cork oak woodland systems sustainable (Ribeiro et al. 2010).

2. THE FORMATION AND STRUCTURE OF CORK

2.1. The cork formation

Cork is a protective tissue located in the outer bark of the cork oaks where it is part of the periderm. The formation of cork in the periderm is the result of the activity of a secondary meristem, the phellogen: each phellogen mother-cell originates by cellular division cork cells that grow unidirectionally outwards in the tree's radial direction and phelloderm cells to the inside (Graça and Pereira 2004). In the cork oak, the first phellogen maintains its activity year after year, producing successive layers of cork. The phellogen may be functional for many years, probably during the tree's life, although the intensity of its activity decreases with age (Pereira 2007).

If the cork layer of the initial periderm (virgin cork) formed in the young cork oaks is removed (an operation called cork stripping), a new phellogen is formed inside the phloem and rebuilds a traumatic periderm and its subsequent cork layer (second cork). At this time of life in young cork oaks, the radial growth of the stem is still important and the second cork external regions are subject to a large tangential stress that may result into deep fractures of the cork (Fortes and Rosa 1992).

If the second cork is removed, the process is repeated with the formation of a new phellogen and the production of a new cork layer (reproduction cork). Upon removal of this reproduction cork, the process is repeated, therefore allowing an exploitation during the tree's lifetime by successive removals of the reproduction cork. The second and reproduction corks are covered at the outside by a lignocellulosic layer of phloem, corresponding to the part of the phloem that remained to the outside when the traumatic phellogen was regenerated inside the phloem.

The cork oak periderm has lenticels that are created by the activity of particular regions of the phellogen, called lenticular phellogen. The activity of lenticular phellogen is maintained year after year and therefore the lenticels prolong radially from the phellogen to the external surface of the periderm forming approximate cylinders of complementary tissue, named lenticular channels (Pereira 2007). The lenticular channels are loosely filled with a lenticular filling tissue of rigid unsuberified cells with thick walls and shows ruptures and intercellular voids in a great extent (Pereira 2007). The region bordering the lenticular channels has often

higher density than the surrounding material due to the presence of lignified and thick-walled cells at their borders.

The lenticular channels are the most important and characteristic features of cork heterogeneity, variable in number and dimension between trees, and are related directly to the quality and value of the cork material (cork porosity) (Pereira 2007, Ferreira et al. 2000, Lauw et al. submitted).

2.2. The structure of cork

The description of the cork structure requires its location in space and in relation to its original position in the tree, as represented in Figure 1. The sections are named as: (a) the transverse section is perpendicular to the axial direction (*x*-*y* plane); (b) the tangential section is perpendicular to a radial direction (*x*-*z* plane); and (c) the radial section contains the axial direction and is perpendicular to the tangential direction (*z*-*y* plane).

The structure of cork observed by scanning electron microscopy in the three principal sections is shown in Figure 2. The three-dimensional structure of cork is compact and may be described as an array of prismatic, on average hexagonal cells stacked base-to-base making rows oriented in the radial direction of the tree and assembled side by side, forming a honeycomb-type structure (Figure 3). In adjacent rows, the prism bases of neighbour cells most often lay in staggered positions. The cell volume is on average 1.7×10^{-5} mm^3, and the solid cell-wall content 10%. The cork cell-walls, especially those that constitute the lateral prism faces, show *ab initio* some bending and undulations of varying intensity that can attain strong corrugation derived from constraints during cork growth in the tree (Pereira et al. 1987; Fortes and Rosa 1992). Table 1 summarise the main structural features of cork.

Cork also shows a layered structure, corresponding to the biological annual rhythm of formation of cork rings (Figure 4): the cells formed in the main growth period (earlycork cells) have larger height and thinner walls than those formed at the end of the growth period, which are smaller and thicker-walled (latecork cells) (Pereira et al. 1987).

Cork cell-walls are composed of a suberinic secondary wall and are flexible enough to undulate or corrugate with variable intensity under compression without fracture. The smaller and thick-walled latercork cells are much more rigid and stronger when compared to earlycork cells, and do not show any undulations. When the phellogen starts its meristematic activity at the beginning of the growing season, the first cork cells formed are pushed against the existing

cork layers and compressed against the previous year's latecork cells causing the undulation of the cell walls (Pereira 2007).

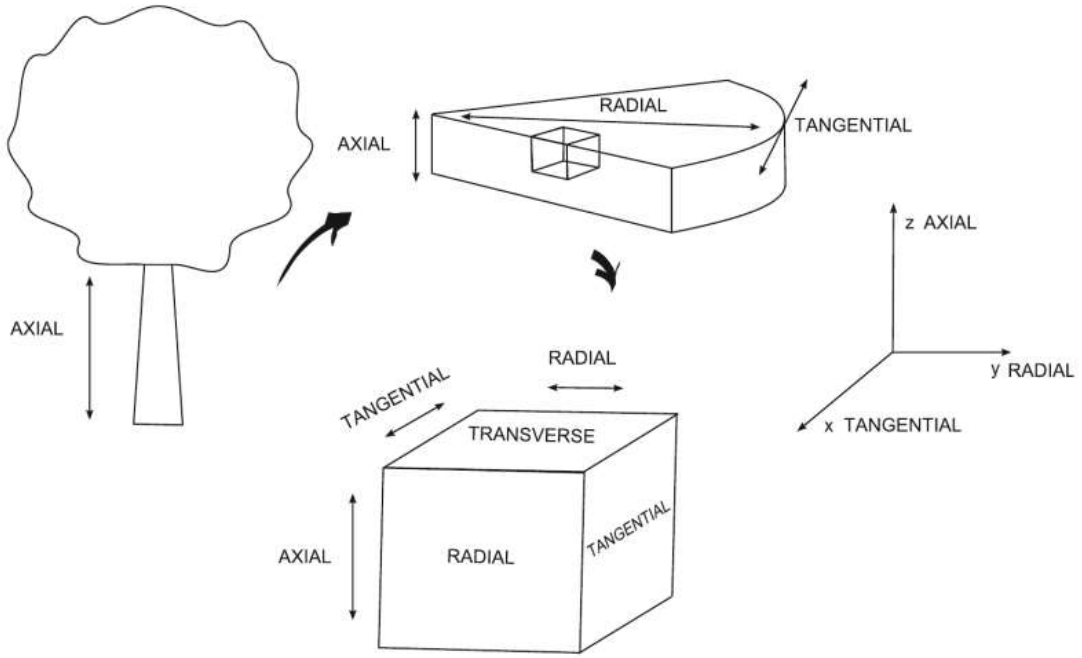

Figure 1. Diagram for the spatial description of cork structure showing the axis system and sections nomenclature as used in plant anatomy (Pereira 2007).

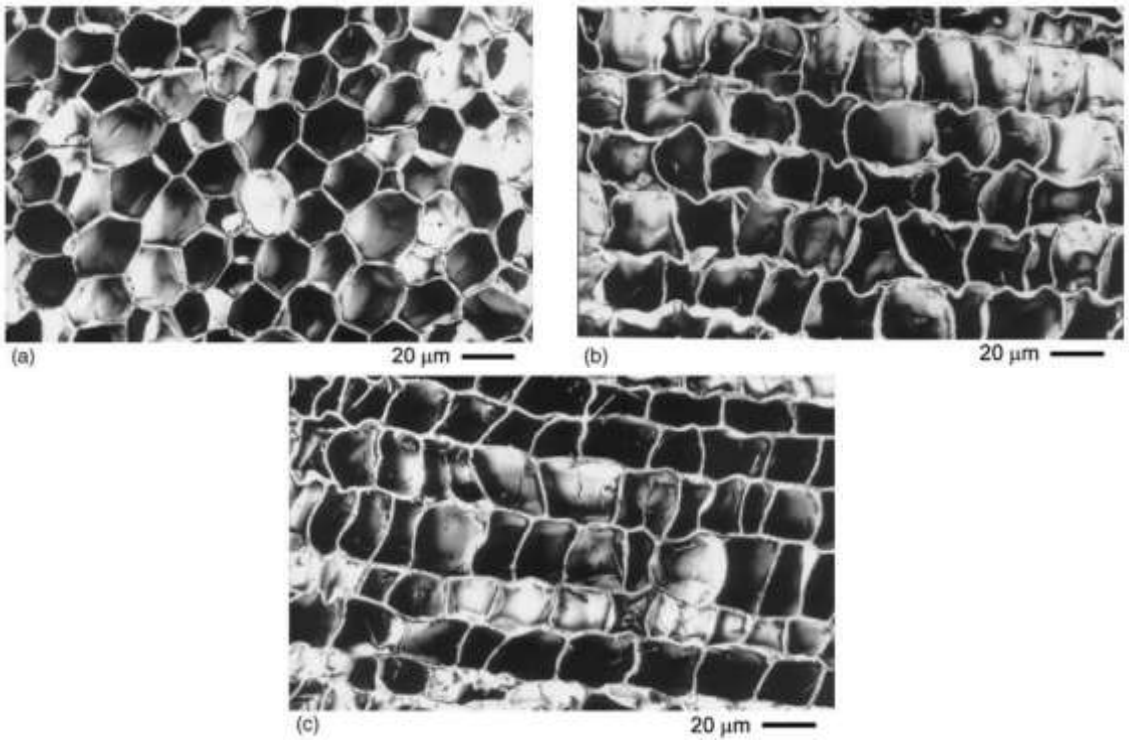

Figure 2. Scanning electron micrographs of sections of reproduction cork:
(a) tangential; (b) radial; and (c) transverse sections (Pereira 2007).

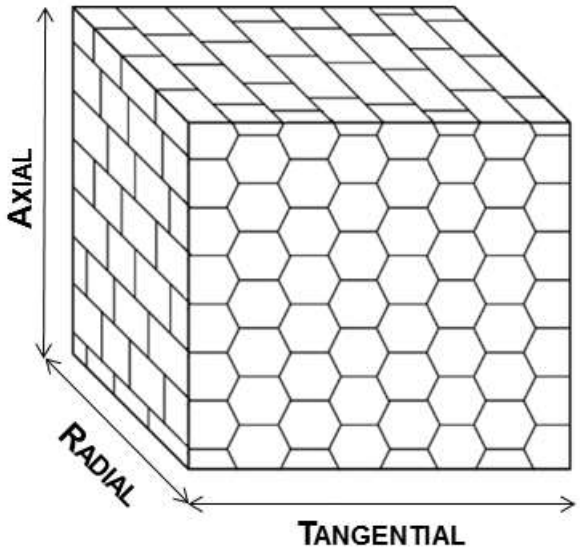

Figure 3. Schematic representation of the cellular structure of cork (Oliveira et al. 2014).

Table 1. Main characteristics of cork structure (Pereira 2007)

Material	Natural suberized lignocellulosic composite
Density	120-170 kg m^{-3}
Mean edges/face	*n*=6
Mean faces/cell	*f*=14
Individual cell shape	Hexagonal prism
Symmetry of structure	Axisymmetric
Cell thickness	1-1.5 µm
Fraction of solid material	10%
Largest principal cell dimension	40 µm
Smallest principal cell dimension	20 µm
Intermediate principal cell dimension	30 µm
Shape anisotropy ratios	R_{13}=1.5-1.7, R_{12}=1-1.1
Other specific features	Growth rings, lenticular channels

As referred previously, the cork tissue is not completely homogeneous and the cellular structure contains discontinuities that influence several properties of the material and the in-use performance of cork products, and are thereby closely associated with the commercial value of raw cork and of cork products (Pereira 2007).

The occurrence of lenticular channels crossing radially the cork tissue is one of the most important features of cork heterogeneity: they cross the cork layers from the outside to the inner tissue and are loosely filled with a dark brown coloured, unsuberified material, usually conspicuous to visual observation (Pereira et al. 1996).

The lenticular channels appear differently shaped in the three sections of cork: (a) in the transverse and radial sections they are thin elongated rectangular channels oriented radially; and (b) in the tangential section they present circular to elliptical form. This feature contributes to increase cork structural anisotropy (Figure 4).

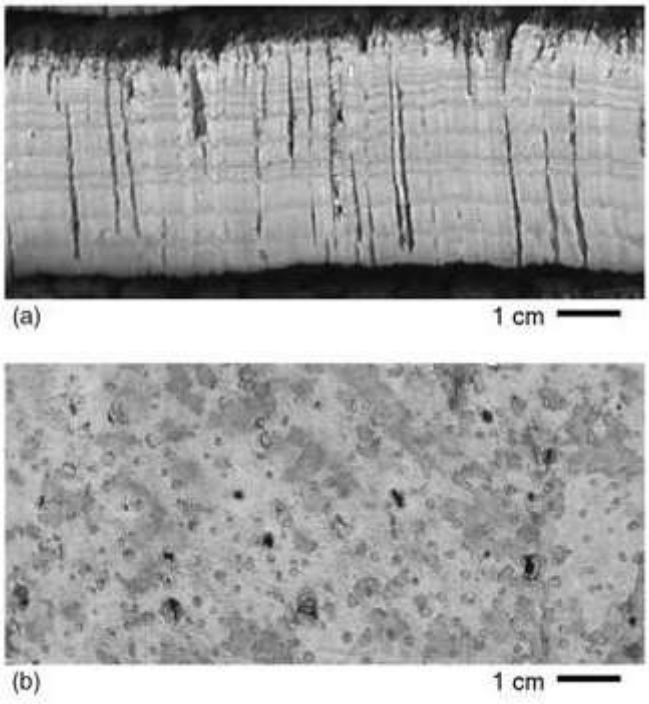

Figure 4. Lenticular channels crossing the cork layer: (a) in cross-section; and (b) in the tangential section of the belly (Pereira 2007).

3. PRODUCTION AND QUALITY OF NATURAL CORK STOPPERS

The industrial production is organized generally in two streamlines: (a) the production of stoppers and discs of natural cork and (b) the production of agglomerates of cork particles, with or without the addition of binding materials (Pereira 2007). Because the primarily goal is the production of stoppers and discs, the planks of reproduction cork are the prime raw material for the industrial processing, and their technological quality has a major role in the overall economy of the cork sector.

In the industrial processing for production of natural cork stoppers, two main factors determine its economic feasibility: the yield of production, *i.e.* the efficiency of raw material use, and the quality of the obtained stoppers (Costa and Pereira 2010).

3.1. Industrial production of natural cork stoppers

After reception at the mill, the raw cork planks are stored at the mill yard until being submitted to the preparation process which consists essentially in the boiling in water, the trimming and the classification of cork planks.

The water boiling of all reproduction cork planks is a treatment by immersion in water at 95^{o}C for 1 h in closed stainless steel closed autoclave with a water filtration circuit. The goal is to clean the cork plank, to extract water-soluble substances, to increase the thickness and to improve cork flexibility and elasticity (Celiège 2013). The combination of heat and water allows the relief of growth stresses in the cork cells, with the decrease of cell-wall corrugations and the increase of cellular structure uniformity (Pereira 2007). As a result of the cell-wall straightening, there is a volume increase of about 20%: approximately 15% in thickness (radial expansion) and 6% in tangential and axial directions (Rosa et al. 1990). Cumbre et al. (2000) found that the coefficient of porosity decreases with the water boiling operation. Thus we could say that water boiling increases the technological quality of cork planks by increasing the plank thickness and decreasing the cork porosity.

After water boiling there is a stabilisation step with cork planks left to air dry until a homogeneous moisture content of 8-16%, considered adequate for working (Celiège 2013). Subsequently the cork planks are individually observed, trimmed and cut in more homogeneous sub-planks for further processing. The cutting of the raw cork planks into cork boards produces on average 5% of by-products (Costa and Pereira 2004).

The planks aimed for the cork stopper sector are separated according to their thickness and quality (visual aspect). The trimming of cork planks also allows the separation of all the cork pieces with defects and unsuitable to be used for cork stoppers and discs production.

Cork planks with stains (yellow and marble stain) that result from microbial attacks are discarded for the production of cork stoppers to avoid eventual contamination with off-flavours and taints (Pereira 2007). Moreover, cork may sporadically include defects of biological or external origin that will influence the performance of cork products, namely of wine stoppers. If present in a natural cork stopper, some defects will disqualify it from its wine sealant functions, e.g. the presence of wetcork spots, insect galleries or microbial stains.

The selected and prepared cork planks with a thickness greater than 27 mm produce cork stoppers following a general flowchart. Figure 5 shows the flowchart from Amorim group. They are cut into strips (transversal perpendicular sections) and punched with a machine to extract the cylindrical cork stopper without deformation and within the dimensional limits required. The dimensions of the stoppers are rectified by mechanical operations of sanding of both tops and body (including chamfering).

The production of natural cork stoppers originates a large amount of by-products for the cork agglomerates industry. The production yield of stoppers is directly related to the size and shape of the cork board (Costa and Pereira 2004) and represents only 22% to 24% of the initial cork with net productions of 98 stoppers/kg and 747 stoppers/m^2 (Pereira et al. 1994, Fortes et al. 2004, Pereira 2007).

The finishing operations of the cork stoppers include a washing and bleaching stage to ensure the cleaning, dusting and disinfecting of the stoppers, with the subsequent drying by applying a thermal treatment. Nowadays the usual cork bleaching is done by hydrogen peroxide or peracetic acid, and the treatment should not leave peroxide residue greater than 0.2 mg/stopper (Celiège 2013).

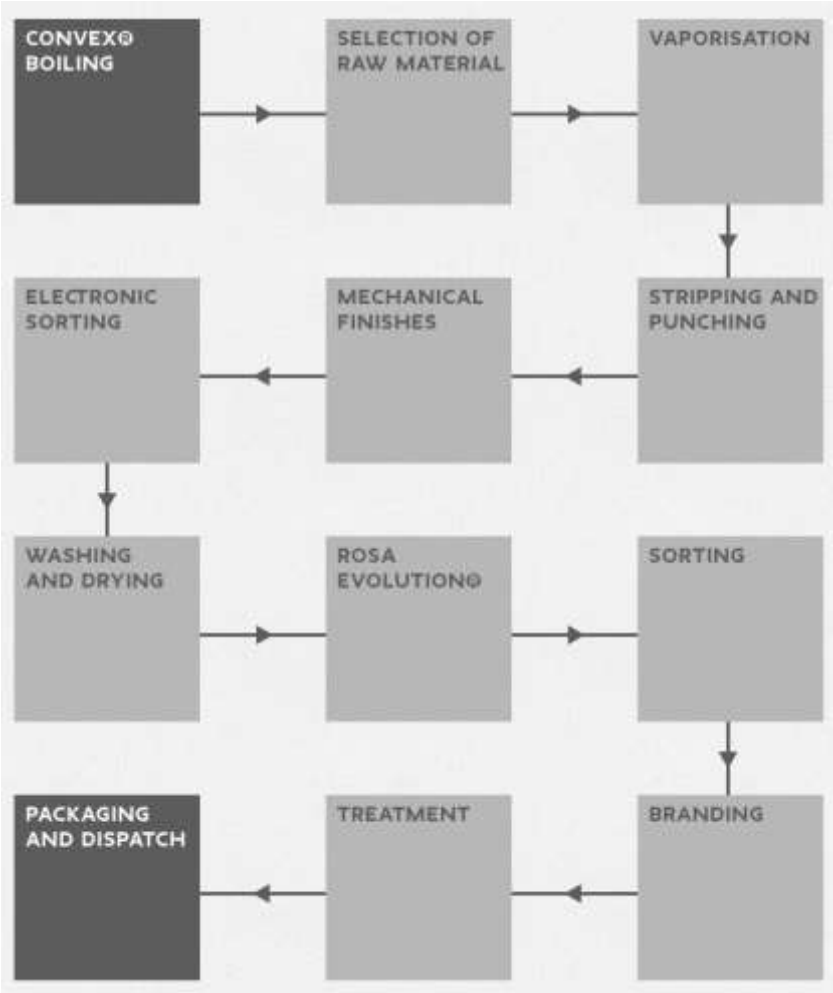

Figure 5. Flowchart from Amorim group of the industrial production of cork stoppers from boiled cork planks.

In the classification step, natural cork stoppers are separated into quality classes in function of the apparent homogeneity of their external surface, as seen by human or machine vision (Fortes et al. 2004, Pereira 2007). The quality profile of the cork stoppers depends on the quality of cork planks (Pereira et al. 1994, Pereira 2007) and is an important factor for the economic feasibility of the industrial production since the price value for the different cork stoppers grades is very different: the price of a good quality stopper can be five times higher than that of a low quality stopper (Costa and Pereira 2010).

The purpose of the surface treatment of cork stoppers is to coat the stopper with a lubricant film in order to reduce friction, thereby allowing an easier insertion and extraction into and out of the bottle (Fortes et al. 2004, Pereira 2007). The stoppers with poor aspect are often subjected to colmation, which consists in covering the pores with a mixture constituted by an adhesive and cork powder, to improve the visual appearance.

3.2. Visual quality of natural cork stoppers

The stoppers are punched out from the cork strips so that their cylindrical axis is parallel to the axial direction of cork. Therefore, the surface of the cork stoppers is not homogeneous relative to the section of cork: (a) the circular tops correspond to transverse sections with the lenticular channels crossing the surface as thin rectangular channels perpendicular to the growth rings; and (b) the lateral surface of the body range from regions corresponding to tangential and radial sections of cork. The lenticular channels appear differently shaped in these two sections: in the radial section they look like elongated rectangular channels and in the tangential section they have an approximately circular to elliptical form (Pereira 2007).

Nowadays the evaluation of cork quality is made by visual analysis of the outer surface (lateral body surface and tops) using automated image-based inspection systems with high throughput rates based on line-scan cameras and a computer embedded in an industrial sorting machine capable of acquiring and processing in real-time the surface image of the stoppers (Lima and Costa 2006).

The heterogeneity of the cork surface is given primarily by the presence of lenticular channels, as well as by woody inclusions, small fractures or other defects, that can be visually and out singled from the cork surface and are named as the porosity of cork (Gonzalez-Adrados and Pereira 1996, Pereira et al. 1996). The systems allow an identification of surface defects and quantification of porosity features, e.g. total area, number or concentration of pores (Chang et al. 1997, Jordanov and Georgieva 2009, Pereira et al. 1994, Raveda et al. 2002).

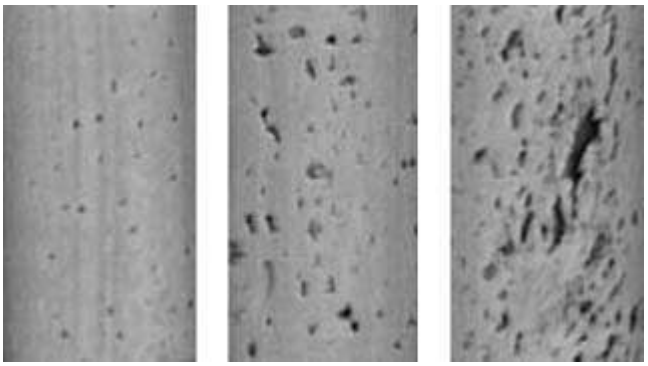

Figure 6. Cylindrical surface (bodies) of cork stoppers from three quality groups ordered from best to worst quality (from left to right) (Costa and Pereira 2007).

The traditional classification system used to evaluate cork quality is divided into a total of nine classes (flor, extra, superior, 1st to 6th), although a three-class system, i.e., premium, good and standard, might be better adapted to reality and performance requirements (Figure 6) (Costa and Pereira 2005, 2007, Pereira 2007).

It is known that the underlying criteria for the quality classification of cork stoppers are subjective to some extent, with no grading standards defined by the cork industry or the consumers and, therefore, tends to vary between experts and even within individual on different occasions (Pereira 2007). Quantification of this subjectivity showed that the disparity is higher in the mid-quality range (Melo and Pinto 1989) and that the larger the set of classes considered, the more difficult and subjective is the classification.

Several studies have been published with the quantitative description of porosity and their contribution for the grading of cork stoppers (Costa and Pereira 2009, 2007, 2006, 2005), as well as of cork discs (Lopes and Pereira 2000) and cork planks (Benkirane et al. 2001, Gonzalez-Adrados et al. 2000, Gonzalez-Adrados and Pereira 1996, Pereira et al. 1996). Costa and Pereira (2007) published porosity coefficients of 1.6%, 4.6% and 7.4% for superior (extra, superior and 1st classes), standard (2nd and 3rd) and inferior (4th and 5th) grades, respectively. These authors also reported values of 1.4% for extra, 2.1% and 2.3% for superior and 1st, and 4.2% and 4.5% for 2nd and 3rd quality classes, respectively (Costa and Pereira 2009).

Other studies have been published focusing on modelling the classification of cork stoppers and discs. Chang et al. (1997) proposed a cork stopper quality classification system based on features extraction and a fuzzy neural network, with 6.7% of rejection after re-evaluation of the results by human experts. Vega-Rodríguez et al. (2001) presented a system for image processing using reconfigurable hardware and an algorithm for the cork stoppers classification that uses a simplified set of porosity features (defect area, size of the biggest defect and area occupied by defects of different sizes) for the two tops. Vitrià et al. (2007) presented a cork stopper classification model based on feature extraction and class-conditional independent component analysis, reaching an average error rate of 2%. Paniagua et al. (2011) developed for cork discs a neurosystem to model the human cork quality classification. Other techniques such as Synchrotron, Compton and Terahertz tomography were recently applied for a non-destructive evaluation of natural cork in order to refine the visual classification and leading to a better understanding of their inner structure but without identification and classification of defects (Brunetti et al. 2002; Donepudi et al. 2010; Hor et al. 2008; Mukherjee and Federici 2011).

3.3. Quality control parameters of natural cork stoppers

The properties required for a wine closure are its sealing capability, inertness towards the liquid content, durability along storage and possibility of removal with acceptable effort. Cork stoppers are controlled using standard protocols, i.e. ISO standards or country specific standards in relation to physical and chemical properties that potentially impact on their performance as wine closures (Pereira 2007). These standard properties for certification include dimensions characteristics, like length, diameter and ovality, moisture, extraction force, peroxide and dust content and visual grade (Table 2).

Because of the subjectivity inherent to quality classification and in order to overcome this problem, the visual quality is usually based on reference samples showing the range of quality variation that can be found in the consignment for a given client (Lopes and Pereira 2000).

The specifications and methods used to certify the dimension characteristics, moisture content, liquid seal capability, dimensional recovery after compression, extraction force, and dust content are defined in ISO 9727:2007. ISO 21128:2006 is applicable to cork stoppers washed with peroxide to determine the peroxide remaining in the cork after processing since a high level of residual peroxide may impact adversely on the level of sulphur dioxide in the wine.

Portuguese standards include other tests, for instance, NP 2803-6:2015-pt that defines the torsion test, NP 2803-7:2013-pt for boiling water resistance determination, or NP 2803-5:1996-pt where is defined the tests for sealing behavior determination.

Certification and the reinforcement of quality requirements and control have increased due to the necessity of the cork industry to demonstrate that the taints and off-flavours that sporadically spoil the wine are not due to cork. One of the important taints in wine is a mouldy taste and aroma due to the presence of halonisoles, namely of the 2,4,6-trichloroanisole (TCA). The formation of TCA occurs when micro-organisms, such as fungi, come into contact with chlorine-based compounds, usually chlorophenols. The TCA in wine may be due to the contamination of oak barrels or cork stoppers, winemaking machinery and bottling equipment or other sources of contamination in wineries and cellars.

In cork stoppers, TCA was primarily found on the external surface indicating that most of the contamination occurred after the punching of cork planks (Pereira et al. 2000). In order to reduce TCA incidence, the cork industry has invested in R&D and adopted measures to prevent

cork contamination with chlorinated compounds and to avoid microbial growth on cork as well as increased quality management. Hypochlorite bleaching, considered the main source of chlorophenols, was eliminated. Nowadays the storage and processing of cork are controlled in order to avoid microbial development and contamination (ISO 10718:2015).

Table 2. Published standards under the direct responsibility of ISO/TC 87 Secretariat related to cork stoppers

ISO standard	**Description**
ISO 9727-1:2007	Cylindrical cork stoppers -- Physical tests -- Part 1: Determination of dimensions
ISO 9727-2:2007	Cylindrical cork stoppers -- Physical tests -- Part 2: Determination of mass and apparent density for agglomerated cork stoppers
ISO 9727-3:2007	Cylindrical cork stoppers -- Physical tests -- Part 3: Determination of humidity content
ISO 9727-4:2007	Cylindrical cork stoppers -- Physical tests -- Part 4: Determination of dimensional recovery after compression (NP ISO 9727-4:2014-pt)
ISO 9727-5:2007	Cylindrical cork stoppers -- Physical tests -- Part 5: Determination of extraction force
ISO 9727-6:2007	Cylindrical cork stoppers -- Physical tests -- Part 6: Determination of liquid tightness
ISO 9727-7:2007	Cylindrical cork stoppers -- Physical tests -- Part 7: Determination of dust content
ISO 10106:2003	Cork stoppers -- Determination of global migration
ISO 10718:2015	Cork stoppers -- Characterization of a low-in-germs stopper, through the enumeration of colony-forming units of yeasts, moulds and bacteria, capable of both being extracted and growing in alcoholic medium
ISO 20752:2014	Cork stoppers -- Determination of releasable 2, 4, 6-trichloroanisol (TCA)
ISO 21128:2006	Cork stoppers -- Determination of oxidizing residues -- Iodometric titration method
ISO 22308:2005	Cork stoppers -- Sensory analysis

The Amorim group has patented the ROSA® (Rate of Optimal Steam Application) which uses controlled steam to eliminate any trace of TCA. The quality control is performed at molecular level using high precision gas chromatography/mass spectrometry (GC-MS) machines. GC-MS analysis is more objective, precise and reliable than the sensory analysis (ISO 22308:2005).

Recently a standard was established with the determination of releasable TCA (ISO 20752:2014). GC-MS analysis is able to detect releasable TCA levels below 0.5 parts per trillion (0.5 ng L^{-1}), which are much lower than the sensory detection levels. A recent study (Lopes et al. 2011) indicated that cork stoppers are an effective barrier against the transmission of TCA, contrary to what happens with artificial closures, and are able to ensure protection from the external environment.

Very recently, Amorim group have launch NDtech, the state-of-the-art system to strengthen quality control measures by screening individual cork stoppers on the production line to eliminate the risk of any natural cork stopper contaminated with releasable TCA reaching winemakers.

The cork stoppers quality control can include a capillarity test to determine the efficiency of the surface treatment. There should be no surface migration of wine up the cork surface when the bottom of the cork is in contact with a liquid, under standard conditions, and held in contact with the liquid for 24 h at 20 +/- 2ºC.

Surface treatments are applied to lubricate the cork stopper contributing to sealing, insertion during the bottling and cork extraction. The quantity and composition of the surface treatment applied depends on customer requirements. Gonzalez-Adrados et al. (2012) applied Fourier transform infrared spectroscopy (ATR-FTIR) to determine the type of surface treatment and dose used on cork stoppers, demonstrating the value of this non-destructive technique to improve quality control of stoppers.

The certification system SYSTECODE was established by CELIÈGE (The European Cork Federation) and is nowadays the quality assurance system for the cork industry. Since 2011, CELIÈGE has implemented a “Premium Systecode” certification for companies that meet more requirements, namely in terms of hygiene and food safety, sustainable development and environmental impact. According to APCOR, in 2014, 204 Portuguese companies applied for the “basic” certification and 38 for the “premium” certification.

3.4. Oxygen permeability of natural cork stoppers

The contact between wine and oxygen is of critical importance for wine conservation and bottle ageing processes during which the wine characteristics evolve towards the appearance of the so-called developed characters (Godden et al. 2005). Wine post-bottling development is

complex and differs between red and white wines: red wines benefit from a small degree of oxygenation as it contributes to colour stabilization, astringency reduction and aroma improvement (Lopes et al. 2005, Silva et al. 2011, Gómez-Plaza and Cano-López 2011, Han et al. 2015); white wines are less resistant to oxygen, leading to oxidative off-flavours and browning that reduce wine quality (Escudero et al. 2002, Karbowiak et al. 2010). However, a tight sealing and lack of oxygen can also lead to negative sensory attributes (Karbowiak et al. 2010). Wine tastings pay a special attention to reduced or oxidized tastes related to oxygen ingress into the bottle, even if quantitative information on this matter is rather scarce.

The closure is the most obvious factor that influences in-bottle wine development. The main function of a closure is to ensure an appropriate seal, avoiding liquid leakage and preventing organoleptic deterioration during storage. The sealing performance of closures is strictly related to their permeability properties that are commonly used for evaluating their barrier efficiency (Godden et al. 2005, Karbowiak et al. 2010). Exposure to oxygen of bottled wines is usually low, but can be quite variable depending on: (1) the amount of oxygen in the headspace at bottling; (2) oxygen ingress into the bottle through the closure; (3) oxygen ingress into the bottle through the interface closure/bottle; and (4) from the closure into the bottle, as a consequence of compression during bottling (Caillé et al. 2010, Mas et al. 2002, Lopes et al. 2005, 2006, Kontoudakis et al. 2008, Silva et al. 2011).

Several studies have been published about the mechanisms and main routes of oxygen ingress through closures. Waters et al. (2001) revealed that the main route for oxygen entering into the wine is through the glass/cork interface but data interpretation must be made with great caution due to the small sample size. On the other hand, Lopes et al. (2007) found no significant differences in the oxygen ingress rates of cork stopped bottles when comparing uncovered, interface-covered, and fully covered natural cork stoppers, suggesting that oxygen diffuses mainly out of the cork into the wine due to the high pressure in the cork cells. The high internal pressure (from 0.6 to 0.9 MPa) created when natural cork stoppers are compressed into the bottleneck could force the air out of the cork structure, preferentially during the first 12 months (Fortes et al. 2004, Lopes et al. 2007). Natural cork stoppers with 24 mm diameter x 45 mm length have a volume of 20.4 mL, of which 80-85% is air contained in the cell lumen, implying the existence of 4.9-5.2 mg of oxygen within the stopper's structure (Fortes et al. 2004).

The kinetics of oxygen ingress through natural cork stoppers present a common behavior along time corresponding to a logarithmic behavior with time. There is a quick and high oxygen

ingress in the first month after bottling, with an initial high ingress rate, followed by a decreasing ingress rate, until stabilizing at a low and rather constant ingress rate from the 3rd to the 12th month. Lopes et al. (2005) published values of 35.8-64.6 µg/day in the first month, and ranging from 2.43 to 8.73 µg/day from the 2nd to 12th months for bottles stored horizontally (Figure 7). Godden et al. (2005) reported a mean oxygen permeation of 25.6 µg/day, with a range from 0.1 to 175.7 µg/day, tested after approximately 36 months post-bottling.

The permeability to oxygen of natural cork stoppers decreases along time, as shown by Lopes et al. (2006) during a 36-month wine storage experiment: 1.0 to 1.86 mg O_2 in the first month, 0.04 to 0.24 mg/month between the 2nd and 12th month, and 0.003 to 0.10 mg/month between the 12th and the 36th month, totalling 2.43 and 3.29 mg of oxygen for cork stoppers of two visual quality grades (flor and first, respectively). In relation to the theoretically estimated total oxygen within the stoppers, the average oxygen ingress into the wine bottles in the first month of storage represents 27-29% (1.43 mg). Of notice is the fact that no significant differences were found in the overall oxygen diffusion of stoppers of different quality (Figure 7) (Lopes et al. 2005).

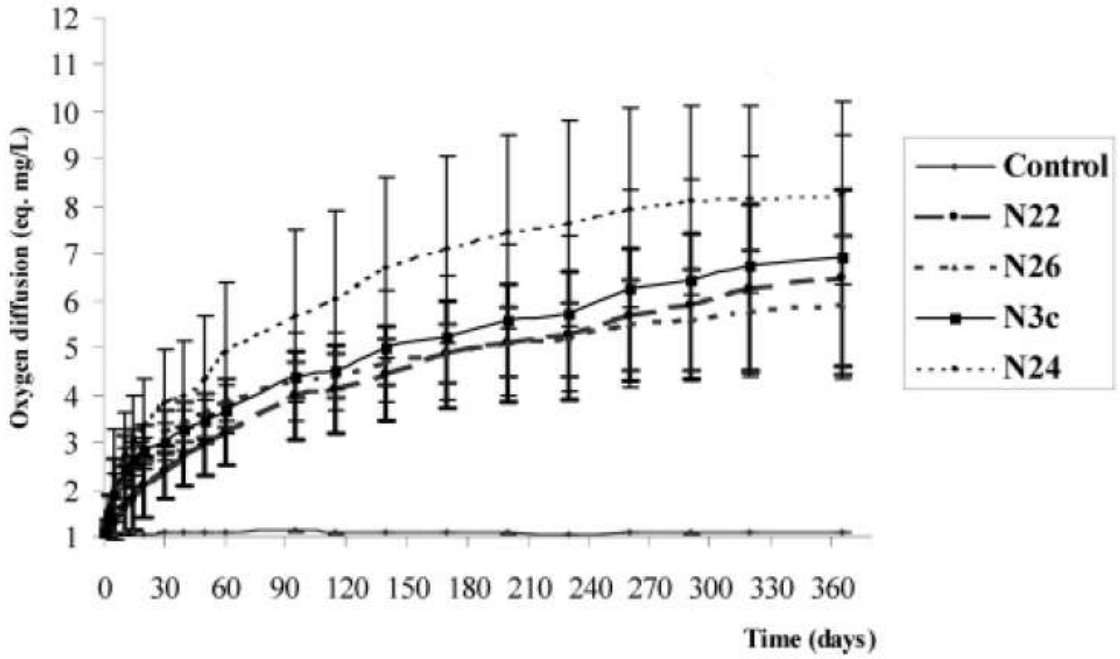

Figure 7. Kinetics of oxygen through natural cork closures. Commercial bottles were stored horizontally over a period of 365 days. N22, natural cork, first-grade closure, diameter 22 mm; N24, natural cork, first-grade closure, diameter=24 mm; N26, natural cork, first-grade closure, diameter=26 mm; N3c, natural cork, third-grade colmated (Lopes et al. 2005).

Understanding how oxygen transport is made through the cork stopper is important to find discriminant parameters that help to understand why some cork stoppers are better than others independently of their visual quality.

In a recent study, Faria et al. (2011) investigated the permeability of gases through uncompressed cork, suggesting that the gas transport mechanism is due mainly through the minute channels present in the cork cells walls, the plasmodesmata that cross the wall and have a diameter of about 0.1 µm (Figure 8) (Teixeira and Pereira 2009). Faria et al. (2011) also noted that samples from thinner planks on average permeate less than those from thicker planks. Brazinha et al. (2013) modelled this gas permeation transport through the plasmodemata following a Knudsen mechanism. However, in other studies, Lequin et al. (2012) and Lagorce-Tachon et al. (2014) concluded that the transfer of oxygen in raw cork is essentially controlled by a mechanism of diffusion through the cork cell walls following a Fickian law.

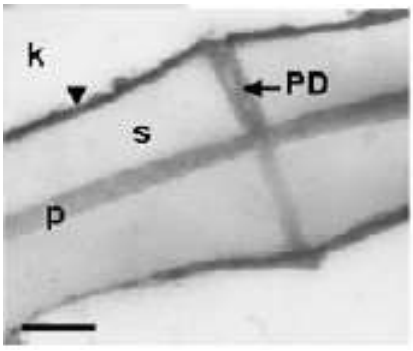

Figure 8. Cell wall of virgin cork from *Q. suber* L. showing a translucent secondary suberized cell wall. Plasmodesmata (PD) can be observed crossing both cell walls (arrow) (Teixeira and Pereira 2010).

Recently synthetic closures, technical stoppers and screwcaps with different oxygen barrier properties were developed with the goal of allowing winemakers the possibility of developing different wine styles and lengths of aging (Vidal and Aagaard 2008, Ugliano et al. 2009). The existence of closures with controlled levels of oxygen permeation will be a new challenge in quality control.

4. X-RAY (MICRO)TOMOGRAPHY AND 3D IMAGING

X-ray imaging is a transmission-based technique in which X-rays from a source pass through a sample and are detected either by film or an ionization chamber on the opposite side of the sample. The contrast in the image between the different tissues arises from differential attenuation of X-rays in the sample (Webb 2003).

In planar X-ray radiography, the image produced is a simple two-dimensional projection of the tissues lying between the X-ray source and the film. X-ray imaging in its two dimensional form is widely used in wood science for microdensitometry studies (Boden et al. 2012, Helama et al. 2012, Ikonen et al. 2008, Knapic et al. 2014).

X-ray microtomography has its origins in Computerized Axial Tomography (CT) that have been used for medical imaging over 40 years. More recently industrial X-ray tomography scanners are used in forestry for determination of wood properties by detecting internal log features such as pith, growth rings, heartwood and sapwood, knots and decay (Longuetaud et al. 2012, Wei et al. 2011). In a very recent study, Stängle et al. (2015) concluded that sawing optimisation of beech logs using a CT scanning system to detect log internal defects, followed by sawing simulation, can increase volume and value yield (Figure 9).

X-ray microtomography is a radiographic imaging technique that can produce 3D images of a material's internal structure at a spatial resolution below 1 micrometer. The sample preparation is usually minimal, and for many materials the technique is non-destructive, allowing many scans to be made of the same sample under different conditions (Landis and Keane 2010).

X-ray microtomography combine information from a series of 2D X-ray absorption images recorded in sequence as the object is rotated about a single axis or holding the object stationary while the X-ray source and detector are rotated around the object.

The reconstruction of the image requires computation of the inverse Radon transform (backprojection or filtered backprojection algorithms) of the acquired projection data in order to produce a three-dimensional digital image where each voxel (volume element or 3D pixel) represents the X-ray absorption at that point. Because different material features and phases often have different X-ray absorption properties related to their density, the 3D internal structure can be inferred from the images, with identification and positioning of the different

internal features. The resulting 3D images are typically displayed as a series of 2D “slices” (Landis and Keane 2010). The process is schematically illustrated in Figure 10.

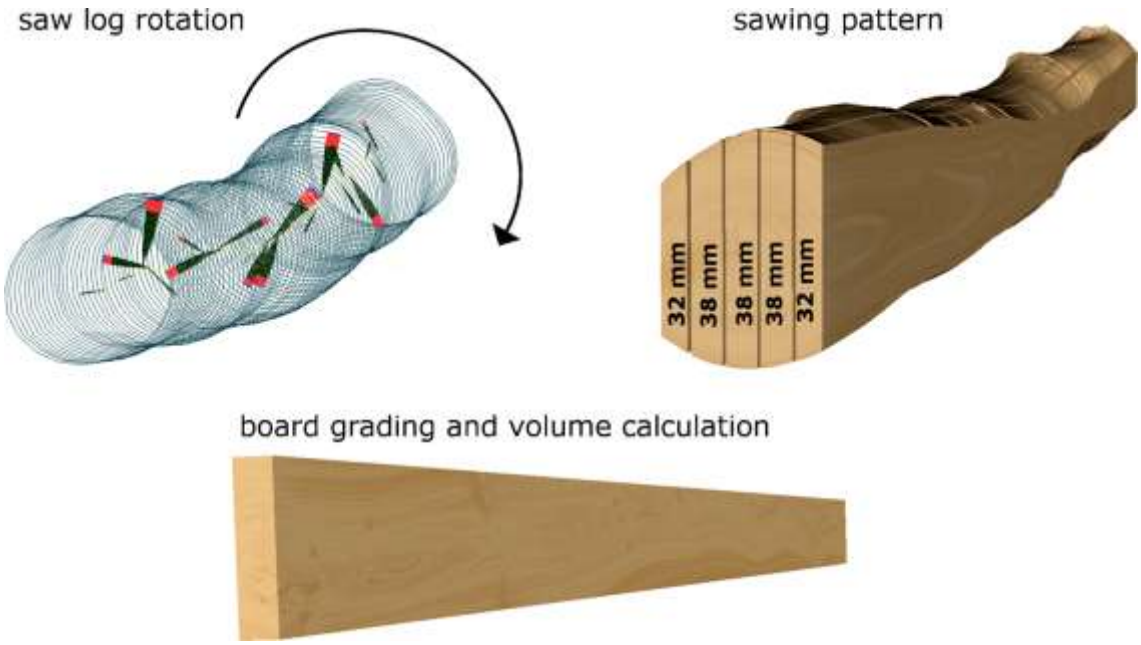

Figure 9. Cutting simulation with InnoSIM: 3D saw log model that includes information on log shape and its knots (upper left); pseudocolour computed tomography (CT) reconstruction of a log and the chosen sawing pattern (upper right); a board that has been graded automatically according to its appearance (bottom) (Stängle et al. 2015).

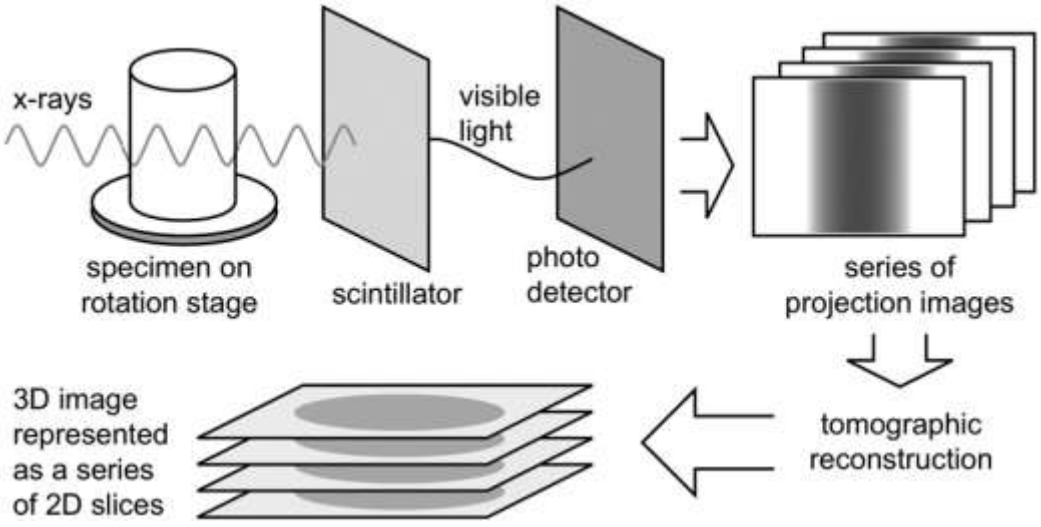

Figure 10. Schematic illustration of X-ray CT acquisition and reconstruction processes (Landis and Keane 2010).

X-ray microtomography has been used in many different fields from biomedical (Kim et al. 2014) to geoscience (Cnudde and Boone 2013) up to material science (Česen et al. 2013, Dewanckele et al. 2012). 3D X-ray microtomography has seen a widespread use in wood science and is employed to study various features: the shrinkage behaviour of cellular materials (Taylor et al. 2013), the analysis of coatings (Bessières et al. 2013, Van den Bulcke et al. 2010), the compressive behaviour of low-density fibreboard (Tran et al. 2013), wood anatomical analysis (Figure 11) (Van den Bulcke et al. 2009), the characterization of paper pore structure (Axelsson and Svensson 2010), wood composites (Wieland et al. 2013), and also dendrochronological studies (Van den Bulcke et al. 2014).

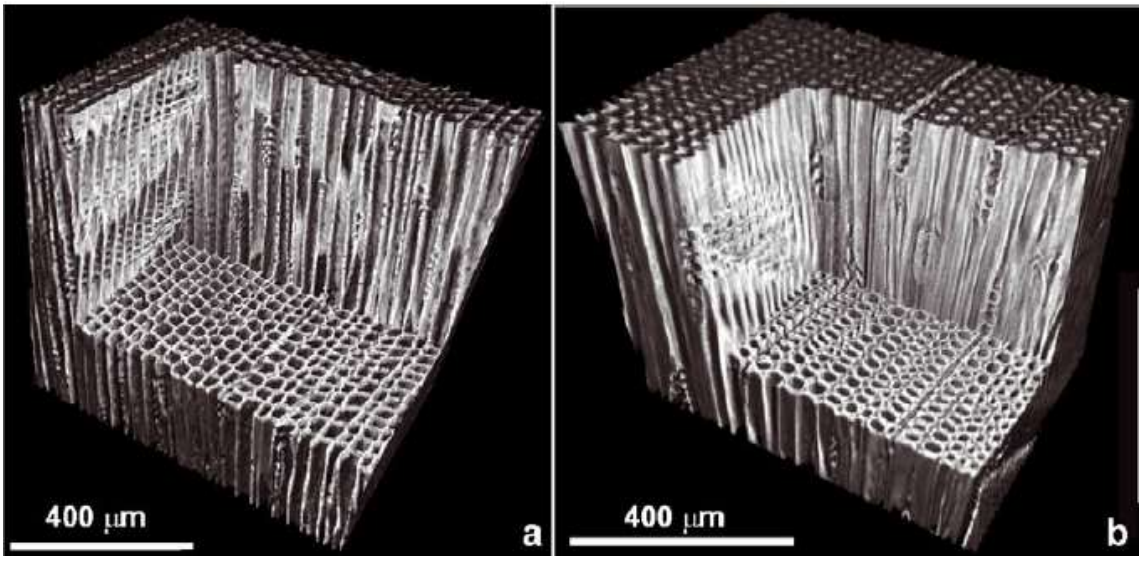

Figure 11. Overview with cut out giving a clear view on the internal anatomy of *Pinus silvestris* L. (a) earlywood and (b) latewood (Van den Bulcke et al. 2009).

As referred previously, techniques such as Synchrotron, Compton and Terahertz tomography were recently applied for a non-destructive evaluation of natural cork in order to refine the visual classification and leading to a better understanding of their inner structure but without identification and classification of defects.

Brunetti et al. (2002) reported the application of Compton tomography in the study of cork stoppers density. Those experiments have shown how the green cork differs from mature cork, allowing to easily discriminate a small zone of green cork inside a mature volume. The authors meant by green cork, the defect known as wet cork that appears occasionally in small regions and is characterized by a high moisture content leading upon drying to collapsed cork regions.

Hor et al. (2008) applied terahertz (THz) spectroscopy and imaging to non-destructively evaluate natural cork. Mukherjee and Federici (2011) were able to clearly distinguish between defective and non-defective corks using the reconstructed images of natural cork by pulsed Terahertz tomography. Donepudi et al. (2010) visualized images of cork stoppers with a novel imaging technology, called diffraction-enhanced imaging (DEI).

In a very recent study, Lagorce-Tachon et al. (2015) compares two techniques: digital photography and neutron imaging (radiography and tomography) to identify and quantify the lenticular channels present in different classes of cork stoppers (Figure 12).

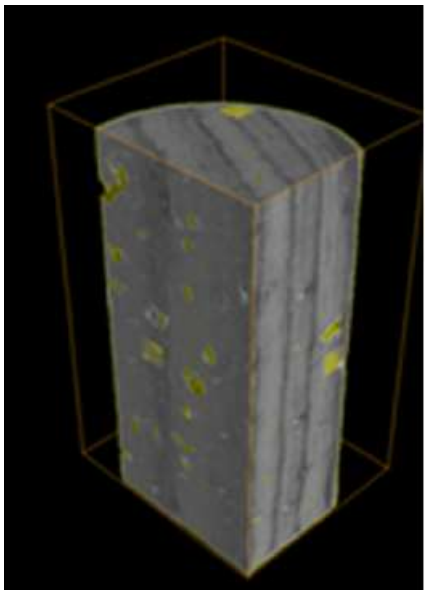

Figure 12. Visualization in 3 dimensions of a natural cork stopper (grade 0) obtained by neutron tomography (Lagorce-Tachon et al. 2015).

1. RESEARCH OUTLINE

The research carried out in this work aimed at a valorisation of the natural cork stoppers by modelling their oxygen transmission performance using modern techniques for non-destructive analysis. To achieve this objective several tasks were outlined after sample definition.

Since natural cork stoppers are nowadays classified into quality classes in function of the apparent homogeneity of their external surface, the first task characterized the variability and quantified the surface porosity of wine cork stoppers from different commercial classes using image analysis techniques. The aim was a better understanding and definition of the quality grading of natural cork stoppers. Two publications were written with the obtained results: (a) one with the detailed characterization of porosity of stoppers of different quality classes, as well as of the stopper itself i.e. of the different cork sections (Publication I); and (b) one with the analyses of the contribution of each porosity feature to the quality classification of cork stoppers (Publication II).

Considering that previous studies suggested that oxygen diffuses mainly out of the cork itself into the wine and that oxygen permeability is not related with commercial quality classes, the acquisition of knowledge on the internal structure of natural cork stoppers seemed to be the obvious objective in a second task by application of non-destructive techniques based on X-ray tomography.

In the third task, the natural cork stoppers were used for the closure of bottles and oxygen diffusion measurements were made along time. This information gave rise to Publication III with information on the kinetics of oxygen ingress into wine bottles and its variability between cork stoppers from different commercial quality classes.

Complementarily to the elucidation of several features of the internal structure of cork stoppers using X-ray tomography, microtomography was used to achieve a higher resolution. The image resolution allowed the visualization and quantification of cork structural discontinuities that are decisive for the commercial value of raw cork and of cork products because they can be an easy pathway for air diffusion as well as a preferential impregnation route for liquids or microbial penetration. These results are presented in Publication IV where it was possible to establish a relationship of internal features with oxygen diffusion measurements.

The final publication ascertains the impact of some defects (wetcork and insect galleries) that are visually observable in the performance of the natural cork stoppers in the bottle as regards oxygen ingress. The corresponding publication (Publication V) encompasses results from all the tasks.

2. MATERIAL AND METHODS

2.1. Sampling natural cork stoppers

The natural cork stoppers used in this work were supplied by Amorim & Irmãos, S.A. (Santa Maria de Lamas, Portugal).

A total of 600 natural cork stoppers with 24 mm diameter and 45 mm length were selected: 300 stoppers were punched out from corkboards of calliper 27-32 mm and 300 stoppers from corkboards of calliper 45-54 mm. The stoppers were randomly taken from the production line after grading by the automated vision system, subsequently inspected by skilled operators, and final graded into three reference quality classes, coded as premium (including the traditional "flor" and extra commercial classes), good (superior and 1st commercial classes) and standard (2nd and 3rd commercial classes) (Figure 13). These classes correspond to the presently used commercial classification for the quality wine bottling market. From each class 100 stoppers were taken before washing and surface treatment. The callipers 27-32 mm and 45-54 mm were selected because are the extremes of the callipers used for cork stoppers production.

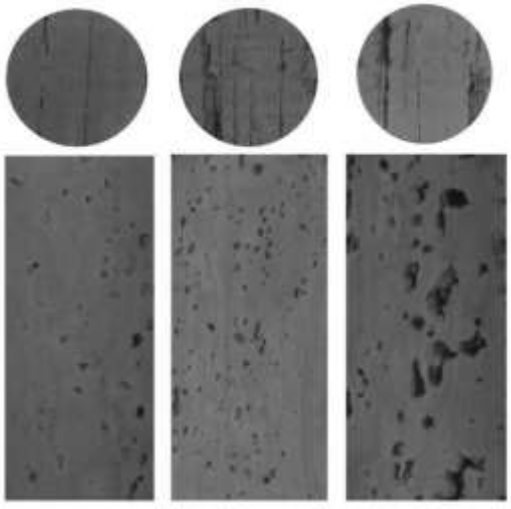

Figure 13. Images from cork stoppers belonging to the reference quality classes ordered from best to worst quality (from left to right): premium, good and standard.

Moreover, a total of 150 natural cork stoppers with 24 mm diameter and 45 mm length with defects were selected: 50 stoppers with the presence of ant (*Crematogaster scutellaris*) galleries, 50 stoppers with *Coroebus undatus* larvae galleries and 50 stoppers with wetcork spots (Figure 14).

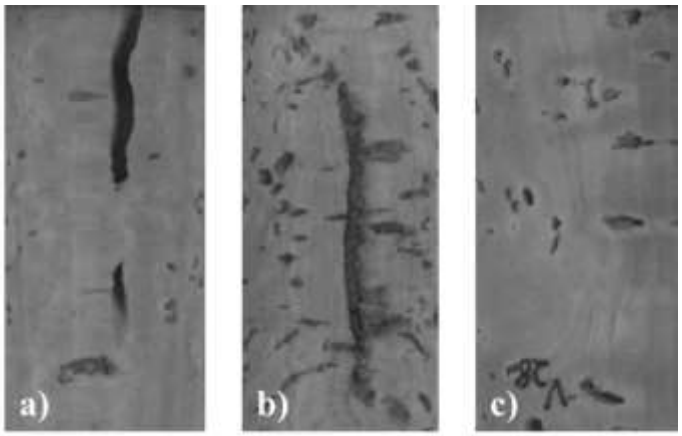

Figure 14. Image of the lateral body surface of cork stoppers showing defects in the cork structure: a) empty ant gallery; b) *Coroebus undatus* F. larvae gallery; and c) wetcork.

The physical parameters were collected for all the cork stoppers using the MedCork equipment, a totally automatic, intelligent and integrated system created to measure length, diameter, weight and moisture of cork stoppers, following rigorous metrological techniques and the present standards.

2.2. Surface image analysis of natural cork stoppers

The totality of the natural cork stoppers (600+150 samples) were individually analysed and their image surface (cylindrical lateral surface and circular bases) acquired with an image analysis system. The system included a digital 7 mega pixels in macro stand solution set on an acquisition Kaiser RS1 Board with a controlled illumination apparatus, connected to a computer using AnalySIS® image processing software (Analysis Soft Imaging System GmbH Münster, Germany, version 3.1) (Figure 15).

The image acquisition covered 100% of the lateral area by using eight successive frames of the cylindrical lateral surface of the body, named A to H. The first frame (A) was acquired parallel to cork growth rings and the others subsequently taken by rotating the stopper by 45^{o}. Two circular frames were acquired for the two tops corresponding to 96% of the total area. Due to the way stoppers are punched out from the cork strip, the tops correspond to transversal sections of cork while the lateral surface of the stopper includes tangential and radial sections of cork and all the in-between sections (Figure 16) (Pereira 2007, Pereira et al. 1987).

Figure 15. Image analysis system used for the surface observation of cork stoppers.

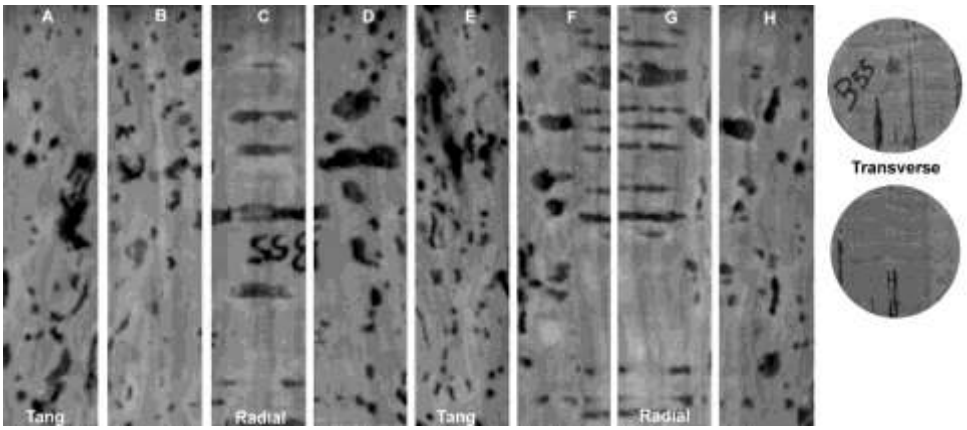

Figure 16. Image analysis frames (eight frames in the lateral surface and two tops) and the corresponding cork sections.

The object extraction was carried out inside two predefined regions of interest, one rectangular, 45.05 mm long and 9.41 mm wide (area 423.92 mm^2), for the lateral surface, and another circular for the tops with 23.51 mm diameter (area 433.92 mm^2). The image threshold was adjusted individually for each image. A set of variables was collected automatically for each pore as resumed in Table 3, grouped in three types: dimension, shape and colour.

These data were filtered and only pores with area equal or superior to 0.1 mm^2 were considered for the analysis. The pixel size was 0.05 mm and therefore the lowest pore area that could be confidently resolved was 0.02 mm^2 corresponding to eight contiguous pixels.

The variables collected for each pore were processed and used to calculate several variables for each frame:

- porosity coefficient (%), defined as the proportion of the area occupied by pores;
- total number of pores and number of pores by dimension classes;
- total area of pores (mm^2), sum of the area of all pores in the frame;

- average pore area (mm^2), calculated as the arithmetic mean of the area of all pores in the frame;
- maximum pore area (mm^2), defined as the area of the biggest pore in the frame;
- mean diameter, calculated as the mean diameter average of all pores;
- maximum diameter, defined as the biggest of all pores maximum diameter;
- mean rectangle, calculated as the arithmetic mean of the mean rectangle of all pores in the frame;
- maximum rectangle, defined as biggest of all pores maximum rectangle.

Table 3. List and description of the variables collected through the image analysis system that was applied for the observation of cork stoppers.

Class	**Variables**	**Description**
Dimension	area	calculated by the number of pixels of the particle times the calibration factors (mm^2)
	mean diameter	the arithmetic mean of all diameters of a particle (range angles between 0^o and 179^o, with step width of 1^o) (mm)
	maximum diameter	maximum diameter of all maximum diameters determined at each angle (varies in 1^o steps) (mm)
	mean rectangle	defined as the area of the mean rectangle which sides consist of tangents to the particle borders (mm^2)
	maximum rectangle	area of the biggest rectangle which sides consist of tangents to the particle borders (mm^2)
Shape	shape factor	(area/perimeter^2)*4π, measuring the roundness of the pores
	sphericity	describes the elongation of the pore by using central moments (value of 1 for a perfect circular particle)
	convexity	the fraction of the pore area and the area of its convex hull (ranging between 0 and 1)
	aspect ratio	the maximum ratio between width and length of a bounding rectangle of the pore
Colour	RGB	mean value of all red, green and blue intensities in each pore

The shape-variables (shape factor, sphericity, aspect ratio and convexity) and the colour-variables (red, green and blue) from pores were averaged into frame variables.

Moreover, these variables were averaged and transformed into cork stopper variables: transverse (two tops), tangential (frames A and E) and radial (frames C and G) sections and cork stopper body variables (considering the eight frames of the stoppers lateral surface).

Several graphical and descriptive statistical analyses were carried out for the characterization of the three reference quality classes, the variation between tops and the body lateral surface and the establishment of the variation within the body lateral surface due to the presence of two different cork sections.

In order to differentiate between quality classes and to predict the class of a future observation, several predictive classification models of stoppers were built based on their surface characteristics using stepwise discriminant analysis (SDA). For the models construction, the sample was randomly divided into two groups: 70% of the cork stoppers were used to estimate the discriminant functions and produced the classification models (modeling set), and 30% of the stoppers were used for external validation of the models (validation set). All the statistical analysis was performed using SPSS® statistical software (version 19.0; SPSS Inc., Chicago IL).

2.3. Oxygen ingress measurements

The kinetics of oxygen ingress into bottles closed with natural cork stoppers was investigated by a non-destructive colorimetric method using the oxidation of an indigo carmine solution. The procedure for reduction and oxidation of indigo carmine solution in the calibration bottle, here transcribed, was originally described and developed by Lopes et al. (2005).

2.3.1 Calibration procedure

The oxidation solution was prepared by dissolving 250 mg of indigo carmine (oxidized compound) and 5 g of sodium benzoate (antimicrobial properties) in 1 L of purified water. The obtained solution exhibited an indigo blue colour.

A calibration bottle without bottleneck was used for the calibration procedure. This bottle had exactly the same dimensions, volume capacity and glass thickness than the “Extra-white” (colorless) “bordelaise” classic bottles (375 mL) with no bore neck containing two openings in

the body of the bottle, which were closed by closures with silicone rings of 5 mm of thickness (Figure 17).

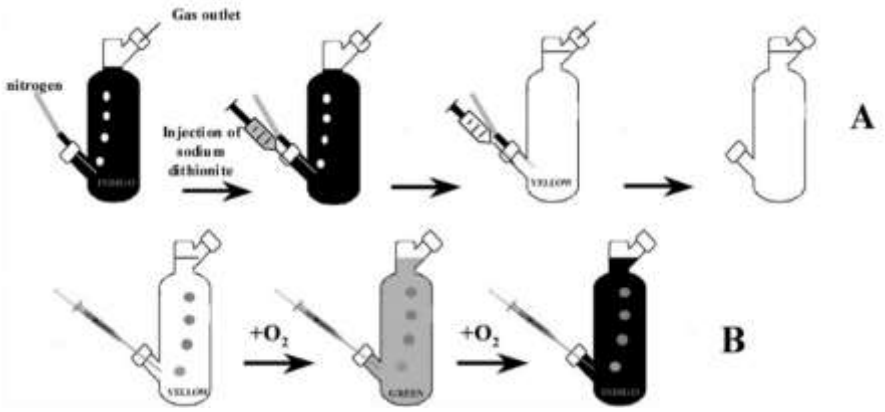

Figure 17. Diagram of the calibration procedure: reduction of indigo carmine in the bottle (A) and bottle-controlled oxidation of reduced indigo carmine by injection of microquantities atmospheric oxygen (B) (Lopes et al. 2005).

Figure 17A shows the several steps in the reduction procedure of indigo carmine in the calibration bottle. The calibration bottle was filled with 350 mL of indigo carmine solution, and both openings were sealed. The bottle was flushed for 15 min with nitrogen gas at a pressure of 0.2 bar to remove all of the oxygen present. A syringe was filled with aqueous sodium dithionite solution (2.25 g/L) and injected into the lower silicone bottle ring. The procedure described by Lopes et al. (2005) was adapted by adding sodium dithionite in a controlled excess pre-determined to correspond to the necessary amount to consume the oxygen that enters into the bottle due to the bottling operation (1.4 to 1.9 mg). The solution's colour changed from indigo blue to yellow.

After the indigo carmine reduction, the colour of the bottle was evaluated by tristimulus measurements (*L**, *a**, *b**, CIELAB76). These measurements were carried out in the upright position at 5 cm from the base of the bottle. Four body measurements were collected by rotating the bottle 90° on its vertical axis. All measurements were made in the dark at room temperature (18 ± 4°C). The average of the four collected values was used.

For calibration, controlled amounts of oxygen were injected along 28 different times into the reduced indigo carmine bottled solution (Figure 17B). After each oxygen injection, the bottle was shaken vigorously by hand to homogenize the indigo carmine solution. Until 1.9 mg of oxygen the colour solution did not change since the oxygen was being consumed by the excess of dithionite. Once the excess of sodium dithionite was consumed, the reduced indigo carmine starts to consume the oxygen resulting in a colour change to the original indigo blue colour of

the carmine. Colour changes were measured with a colorimeter apparatus as described previously. During this period the bottle was stored in a nitrogen atmosphere. Each point of the calibration curve was obtained by calculating the mean of five replicates. The calibration curve is valid up to a maximal limit of oxygen quantification of 5.7 mg, which is the amount necessary to fully oxidize the excess of sodium dithionite and to reduce the indigo carmine (Figure 18).

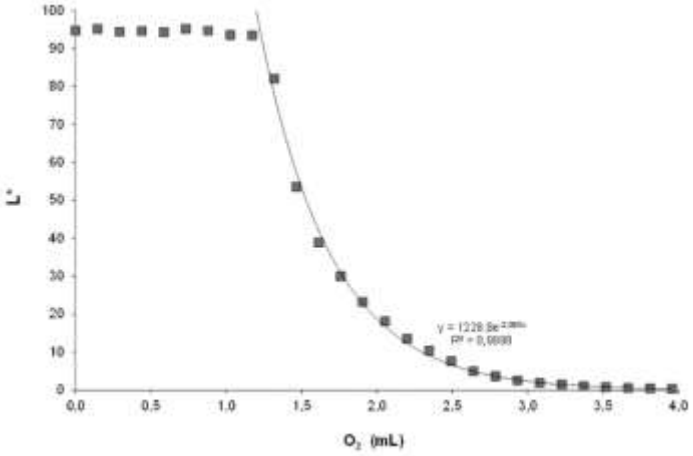

Figure 18. Relationship between *L** colorimetric parameter and the quantities of atmospheric oxygen injected.

2.3.2. Bottling procedure and storage

For the bottling trials, 750 sterilized “Extra-white” (colorless) “bordelaise” classic bottles (375 mL) for cylindrical closures were used. This bottle size was selected in order to reduce experimental costs. However, the bottleneck dimensions complied with the CETIE specifications: a diameter of 18-19 mm at a depth of 3 mm and a diameter of 19-21 mm at a depth of 45 mm from the bottle entrance. All bottles were supplied by Saint-Gobain Glass Packaging (Cognac, France).

These bottles were filled with indigo carmine solution that was reduced with 20 mL sodium dithionite solution (2.9 g/L). Bottles were then sealed with the natural cork stoppers using a single headed corker Bertolazo Epsilon R/S. All closures were compressed to a diameter of 16 mm before insertion under vacuum into bottles (Figure 19). The internal pressure 2 h after bottling was 0 bar. These measurements were carried out in 30 bottles specially prepared to this purpose using a pressure gauge. The final filling level for each bottle was 65 ± 3 mm from the top of the bottle. The temperature of the indigo carmine solution ranged from 17.2 to 21.1°C.

All bottles were left upright for 24 h after bottling and then stored horizontally over 12 months. All bottles were stored under room conditions where temperature varied from a maximum of 27.8°C and minimum of 13.6°C.

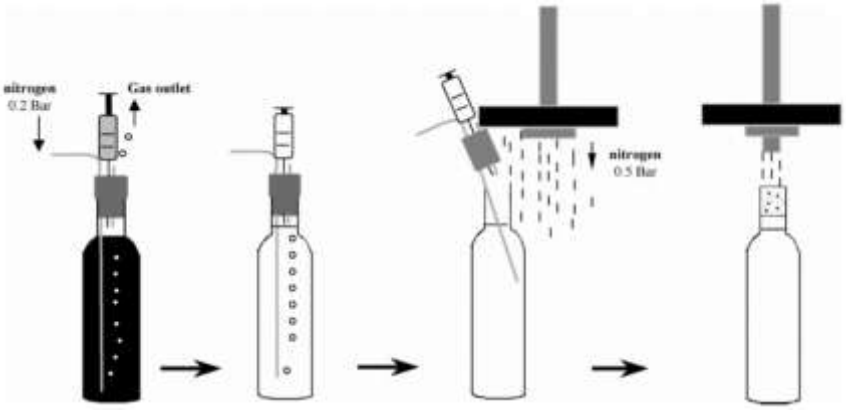

Figure 19. Diagram of the reduction of indigo carmine in commercial bottles and the sealing procedure of the natural cork stoppers (Lopes et al. 2005).

The CIELAB measurements of the parameters *L**, *a**, *b** were performed by directly scanning the bottled solutions with a Minolta series CM-508i spectrocolorimeter equipped with a transmittance accessory CM-A76 (Osaka, Japan). These measurements were obtained using illuminant D65 and a 10° observer according to the CIELAB76 (McLaren 1980).

A clean Pyrex bottle filled with water was used to carry out autozero calibration (blank). All bottles were cleaned with ethanol and dried before CIELAB measurements. These measurements were carried out in the upright position at 5 cm from the base of the bottle. Four body measurements were collected by rotating each bottle 90° on its vertical axis. All positions were marked on the bottleneck to allow consistent measurement over time. All measurements were made in the dark at room temperature (18 ± 4°C).

The calculation of the oxygen ingress into the bottle after closure with the cork stopper was made by deducting the oxygen that was already present in the bottle headspace to the values obtained by the colorimetric measurement. This means that the value of 1.50 mg of oxygen (present in the bottle headspace due to the bottling process) was withdrawn from all measurements, corresponding to the assumption of the quick and total consumption of this oxygen by the indigo carmine (the bottles were shaken immediately after bottling and before each colour measurement). Therefore the oxygen ingress was set at zero at time 0. The limit of oxygen measurement by the method was reached at 4.2 mg of oxygen. This value corresponds to the amount of oxygen that can be consumed after the oxygen is introduced due to bottling.

Oxygen ingress rates were calculated on a day basis (µg/day) and on a month basis (mg/month).

For data analysis, the 600 natural cork stoppers from the three reference quality classes were clustered into five oxygen ingress classes in function of the total oxygen measured at 12 months. The clustering was done by ensuring that the distribution of the number of stoppers was approximately the same in the different oxygen ingress classes. To ascertain if corkboard calliper and stoppers quality classes are significant factors influencing oxygen ingress into bottle was applied a two-way analysis of variance.

For the 150 cork stoppers with different type of defects was applied a one-way analysis of variance to find differences between types of defect. All the statistical analysis was performed using SPSS® statistical software (version 19.0; SPSS Inc., Chicago IL).

2.4. X-ray tomography methodology

The totality of the cork stoppers were scanned using a medical X-ray CT scanner Philips Tomoscan AV, with an X-ray source of 130 kV high voltage generators and a current of 140 mA. The greyscale images (512x512 pixels) are composed of a set of consecutive 2D slices, spaced by 2 mm, and the grey levels correspond to density computed in Hounsfield units (HU). On this scale, typical densities are 0 HU for water and -1000 HU for air. The spatial resolution of 2 mm/voxel allows the visualization of structures larger than 4 mm^2 when seen in 2D or 8 mm^3 in 3D.

In the resulting grey images the voids will appear as dark regions while the high density areas will appear as brighter regions. Segmentation was performed by means of an automated thresholding base on the modified isodata algorithm implemented in Fiji image processing package (Schindelin et al. 2012). The resulting binary images were used for 3D reconstruction, performed using the 3D viewer plugin for ImageJ (Schmid et al. 2010).

The results allowed an understanding of the inner structure of the cork stoppers but, due to the low resolution of the images obtained with the medical CT, porosity quantification by determination of volume was not possible. This quantification was possible for a selected sample of 10 cork stoppers that were scanned using a high resolution prototype X-ray equipment built at the Centre for X-ray Computed Tomography (UGCT, Ghent University, Belgium; www.ugct.ugent.be). The scanner used at Woodlab-UGent (Nanowood) is specifically designed to obtain very high resolution scans as well as scans of larger objects. It has a generic

in-house developed CT scanner control software platform (Dierick et al. 2010) that allows full control of the scanner hardware. A detailed description and performance assessment of nanowood can be found in Dierick et al. (2014).

For all the stoppers of the selected sample, a total of 900 projections were acquired over an angle of 360°. The reconstructions were done using Octopus 8.6, a server/client tomography reconstruction package for parallel and cone beam geometry (Vlassenbroeck et al. 2007), resulting in a voxel size of 50 µm for a scan covering the entire stopper.

The reconstructed images were further manipulated with the Fiji image processing package (Schindelin et al. 2012) and Morpho+ (Vlassenbroeck et al. 2007, Brabant et al. 2011), aiming at noise removal, image enhancement and features extraction.

Morpho+ was used to apply a bilateral filter (non-linear, edge-preserving and noise-reducing smoothing filter) and to perform histogram equalization to improve the contrast.

For features extraction with Fiji, a circular region of interest was manually selected within each stack to represent the transverse cork stoppers section. Segmentation was performed using automated thresholding based on the isodata algorithm (Ridler and Calvard 1978). A single threshold level was selected for pores and one for high density regions through the entire volume. When studying the void fraction, every data point was assigned to either background (solid material) or foreground (voids) and the closing mathematical morphology operator was applied to the binary images to fill misclassified pixels inside the pores as well as to maintain pore connections.

The void volume was calculated using the “3D Object Counter” plugin (Bolte and Cordelières 2006). The 3D void fraction coefficient was calculated by dividing the total volume of voids by the volume of interest. The same analysis was done for the 3D characterization of high density regions (HDR). The results from the analysis of the X-ray volumes were compared with data from previous measurements of surface image analysis, density and oxygen ingress using Pearson's correlation analysis.

Using the reconstructed images and Fiji image processing package it was possible to create movies that show the inside of the cork stopper by travelling through a series of 2D “slices”. These movies show the orthogonal planes and the lenticular channel development in the corresponding cork section. Movies were also created that show the 3D distribution of voids and high density regions.

PUBLICATION I.

NATURAL VARIABILITY OF SURFACE POROSITY OF WINE CORK STOPPERS OF DIFFERENT COMMERCIAL CLASSES

NATURAL VARIABILITY OF SURFACE POROSITY OF WINE CORK STOPPERS OF DIFFERENT COMMERCIAL CLASSES

Vanda OLIVEIRA*, Sofia KNAPIC and Helena PEREIRA

Centro de Estudos Florestais, Instituto Superior de Agronomia, Universidade Técnica de Lisboa
Tapada da Ajuda, P-1349-017 Lisboa, Portugal

Abstract

Aim: The aim of this study was to characterize the variability and to quantify the surface porosity of wine cork stoppers of different quality classes.

Methods and results: The porosity of 300 cork stoppers was characterized by image analysis on the lateral surface and tops. Porosity coefficient was 2.4 %, 4.0 % and 5.5 % for premium, good and standard stoppers, respectively. The lateral surface of stoppers was heterogeneous with respect to porosity features: the tangential regions presented higher porosity while the radial regions had larger pores.

Conclusion: The quality classes of cork stoppers can be differentiated by the mean values of the main porosity features of their surface. There is a natural heterogeneity of the porosity features over the external surface of cork stoppers that can be traced back to the biological basis of cork formation and the production process.

Significance and impact of the study: Natural cork stoppers are the premium product of the cork industry, with worldwide recognition of quality and performance as wine sealant. Due to the large sampling and detailed observation, the results presented in this study may be used for reinforcing quality requirements, e.g., with definition of standards to improve the classification system. A better understanding of cork intrinsic variability and of the anisotropy of porosity features shown by cork stoppers is important for performance development.

Key words: natural cork stoppers, quality classes, porosity, image analysis, lateral surface

Résumé

Objectif: L'objectif de ce travail a été de caractériser la variabilité et de quantifier la porosité de la surface des bouchons de liège de différentes catégories de qualité.

Méthodes et résultats: La porosité de 300 bouchons de liège a été caractérisée par analyse d'images de la surface latérale et des deux bases circulaires. Le coefficient de porosité était 2.4 %, 4.0 % et 5.5 %, respectivement pour les bouchons de qualité première, bonne et standard. La surface latérale des bouchons était hétérogène par rapport aux caractéristiques de porosité: les régions tangentielles présentaient une porosité plus élevée tandis que les régions radiales avaient des pores plus grands.

Conclusion: Les catégories de qualité des bouchons de liège peuvent être différenciées par les valeurs moyennes des caractéristiques principales de la porosité de leur surface. Les caractéristiques de la porosité ont une hétérogénéité naturelle sur la surface des bouchons qui est le résultat de la biologie de la formation du liège et de la méthode de production.

Signification et impact de l'étude: Les bouchons de liège sont le premier produit de l'industrie du liège avec une qualité et une performance reconnues mondialement pour la fermeture des bouteilles de vin. Basés sur un grand échantillonnage et une observation détaillée, les résultats de cette étude peuvent être utilisés pour le renforcement des critères de qualité, par exemple par la définition de standards de classification. La compréhension de la variabilité intrinsèque du liège et de l'anisotropie des caractéristiques de la porosité des bouchons de liège est importante pour le développement de leur performance.

Mots clés: bouchons en liège naturel, classes de qualité, porosité, analyse d'image, surface latérale

manuscript received 12th October 2011 - revised manuscript received 20th February 2012

*Corresponding author: vandaoliveira@isa.utl.pt

J. Int. Sci. Vigne Vin, 2012, **46**, n°4, 331-340

INTRODUCTION

Natural cork stoppers are the premium product of the cork industry, and the commercial value of cork is determined by its suitability for the production of stoppers (Pereira, 2007).

Cork is a biological material with cellular structure, chemical inertia and specific mechanical behavior that provide an unmatched closure for bottles with worldwide recognition for its quality and performance as wine sealant (Pereira, 2007; Fortes *et al.*, 2004; Pereira, 1988; Pereira *et al.*, 1987). However, some cases of negative evolution of bottled wines have been attributed to cork stoppers as a result of their intrinsic variability. Although the underlying factors are still poorly understood, this variability has been used as an argument in some wine markets to replace cork stoppers for non-biological sealants such as synthetic stoppers and aluminum screw caps.

The response of the cork industry has been to reinforce quality requirements and control. The natural cork stoppers are classified into quality classes in function of the homogeneity of their external surface, which is mostly based on the extent of the apparent lenticular porosity, as seen by human or machine vision (Pereira, 2007; Fortes *et al.*, 2004). The traditional classification system used to evaluate cork quality is divided into a total of nine classes (flor, extra, superior, 1st to 6th), although a three-class system, i. e., premium, good and standard, might be better adapted to reality and performance requirements (Costa and Pereira, 2005, 2007; Pereira, 2007). It is empirically known that the quality classification of cork stoppers is subjective and therefore tends to vary between experts and even within individual on different occasions (Pereira, 2007). Quantification of this subjectivity showed that the disparity is higher in the mid-quality range (Melo and Pinto, 1989) and that the larger the set of classes considered, the more difficult and subjective is the classification.

Nowadays the evaluation of cork quality is made by visual analysis of the outer surface (lateral body surface and tops) using automated systems based on empirical algorithms using the results of image analysis. Several studies led to improvements in cork quality classification algorithms (Chang *et al.*, 1997; Vega-Rodríguez *et al.*, 2001; Radeva *et al.*, 2002; Costa and Pereira, 2006; Vitrià *et al.*, 2007; Jordanov and Georgieva, 2009; Paniagua *et al.*, 2010, 2011). The quantitative description of porosity has been made only recently by analyzing tops and lateral surface of stoppers of different quality classes (Costa and Pereira, 2005, 2006, 2007, 2009). The best classes include stoppers with few and very small lenticular channels, while the lower quality stoppers contain a noticeable porosity with greater pores sizes, but intra-quality grade variability was found to be high. Since the sampling in these studies was limited in the number of cork stoppers (i. e., 24 cork stoppers per class) and in the surface area covered by image analysis (i. e., 51 % of the stopper lateral surface), the question remains on the reasons underlying the variation in performance.

To overcome the limitations of the previous studies, this paper presents the results of a detailed observation of cork stoppers based on a large sample in order to encompass natural variability and to allow a broad confidence in the results. Moreover, this study was performed on the total external surface (lateral surface and tops) of stoppers of the three major quality grades: premium (including the top two commercial classes, flor and extra), good (superior and 1st) and standard (2nd and 3st). Such classification follows the most actual tendency regarding cork stopper use by the quality wine markets. The goal was to characterize the variability and to quantify the surface porosity of wine cork stoppers from different commercial classes aiming at a better understanding and definition of the quality grading of natural cork stoppers. The wine bottling industry may therefore better establish their requirements for the quality classification of the stoppers.

MATERIALS AND METHODS

1. Data collection

A set of 300 stoppers (24 mm diameter x 45 mm length) was distributed equally into three quality classes: premium (flor and extra), good (superior and 1st) and standard (2nd and 3st). The natural cork stoppers were collected at a major cork industrial unit before washing and surface treatment. They were randomly sampled after grading by the automated vision system and subsequently inspected by skilled operators, and finally graded into the three quality classes considered.

2. Image acquisition and processing

The surface image of the body (cylindrical lateral surface) and of the tops (circular bases) of the natural cork stoppers was acquired with an image analysis system that includes a digital 7 mega pixels in macro stand solution set on an acquisition Kaiser RS1 Board with a controlled illumination apparatus, connected to a computer using AnalySIS® image processing software (Analysis Soft Imaging System GmbH, Münster, Germany, version 3.1).

The visualization of all the stoppers was made using the same calibration and light intensity. The defects extraction was carried out inside two predefined regions of interest, one rectangular, for the lateral surface, with 423.92 mm^2, and another circular, for the tops, with 433.92 mm^2. Mean magnification values for stopper bodies and tops were 0.42440 and 0.36151, respectively. The image threshold

was adjusted individually for each image and ranged in a RGB system from 65 to 135 for red, 60 to 115 for green, and 65 to 120 for blue.

The natural cork stoppers were individually analyzed. Two circular frames were acquired for the two tops, corresponding to 96 % of the total top area. The cylindrical lateral surface of the body was analyzed by acquiring eight successive frames, covering 100 % of the total lateral area, named A to H. The first frame (A) was set perpendicular to the cork growth rings and the others were subsequently taken by rotating the stopper 45° (Figure 1).

Knowing that the stoppers are punched out with the cylinder axis in the axial direction of the cork strip, the lateral surface of a stopper includes the tangential (frames A and E) and radial (frames C and G) sections of cork and all the in-between sections (frames B, D, F and H), while the tops correspond to transversal sections of cork (Pereira, 2007; Pereira *et al.*, 1987).

3. Data analysis

The layer of the extracted pores can be measured and quantitatively characterized as individual objects, while a defined observation area may be characterized by the mean values of its pores or by their concentration (Pereira, 2007).

The set of variables that characterize each pore as measured by image analysis was classified into dimension-, shape- and color-type variables. The dimension-type variables included: area; mean and maximum diameter, defined as the arithmetic mean and the maximum of all diameters (angle range between 0° and 179°, with step width of 1°); and mean and maximum rectangle, defined as the rectangle whose area is the average or the maximum of all rectangles. The shape-type variables included: shape factor, defined as (area/perimeter^2)*4π, measuring the roundness of the pores; sphericity, which describes the elongation of the pore (value of 1 for the perfect circular particle); convexity; aspect ratio, defined as the maximum ratio between width and length of a bounding rectangle of the pore; and orientation, measuring the angle of the longest chord linking the gravity centre to the periphery. The color-type variables included the value of red, green and blue (RGB system) for each pore.

These data were filtered and only pores with area equal or superior to 0.1 mm^2 were considered for the analysis. The pixel size was 0.05 mm and therefore the lowest pore area that could be resolved was 0.02 mm^2. The pores with an area inferior to 0.1 mm^2 represented on average 2.8 %, 1.9 % and 1.7 % of the total porosity and 42.2 %, 40.7 % and 46.5 % of the total number of pores for the premium, good and standard quality classes, respectively. Previous works from our laboratory considered only porosity superior to 0.5 mm^2 because small porosity is functionally and aesthetically irrelevant and only brings higher variance and variability to the sample (Costa and Pereira, 2006, 2007, 2009; Gonzalez-Adrados *et al.*, 2000; Pereira *et al.*, 1996; Lopes and Pereira, 2000).

Each frame of the lateral surface, the tops and the full lateral body of each stopper were characterized by several calculated variables: total area of pores, total number of pores, largest pore area, mean and maximum rectangle, mean and maximum diameter, porosity coefficient (defined as the proportion of the area occupied by pores), and number of pores per 100 mm^2. All the other dimension-, shape- and color-type variables collected for pores were averaged and transformed into cork stopper lateral section, top and body variables.

RESULTS AND DISCUSSION

1. Characterization of cork stopper quality classes

The different cork stopper quality classes were differentiated by the mean values of the main porosity features of their surface, namely by dimension and concentration variables, which are summarized in Table 1. There was an increasing trend in both lateral surface and tops, from the premium to standard quality class, for the dimension variables (number of pores, total area of pores, mean and maximum rectangle and diameter, and largest pore area) as well as for the concentration variables (porosity coefficient and number of pores per 100 mm^2). The premium stoppers showed less and smaller pores.

No between-class trend was found for the values of shape and color variables. The shape variables (shape factor, sphericity, convexity, aspect ratio) presented identical values between quality classes. This performance of shape variables was previously reported by Gonzalez-Adrados and Pereira (1996) and Costa and Pereira (2009). The color-type variables showed differences between classes although without a trend.

The mean porosity coefficient calculated for the lateral surface of the stoppers was 2.4 %, 4.0 % and 5.5 % for premium, good and standard quality classes, respectively (Table 1). At the 95 % confidence level, the porosity coefficient ranged from 2.2 to 2.5 % for premium stoppers, 3.7 to 4.3 % for good stoppers, and 5.1 to 5.8 % for standard stoppers. These values are within the range and exhibit similar trends to those reported in the literature. Costa and Pereira (2007) published porosity coefficients of 1.6 %, 4.6 % and 7.4 % for superior (extra, superior and 1st classes), standard (2nd and 3rd) and inferior (4th and 5th) grades, respectively. These authors also reported values of 1.4 % for extra, 2.1 % and 2.3 % for superior and 1st, and 4.2 % and 4.5 % for 2nd and 3rd quality classes, respectively (Costa and Pereira, 2009).

Table 1 - Mean (n=100) and standard deviation (in parentheses) of the independent variables of the lateral surface and tops for the three quality classes of natural cork stoppers.

	Prenium	Good	Standard
Lateral surface			
Porosity coefficient (%)	2.4 (0.8)	4.0 (1.4)	5.5 (1.9)
Number of pores per 100 mm^2	4.6 (1.5)	5.6 (1.8)	5.9 (1.6)
Number of pores	156 (51)	190 (60)	201 (55)
Total area of pores (mm^2)	80.5 (28.3)	135.6 (48.6)	184.9 (65.8)
Mean rectangle (mm^2)	1.3 (0.5)	1.8 (0.6)	2.4 (0.8)
Maximum rectangle (mm^2)	20.8 (12.0)	39.4 (25.4)	53.9 (23.5)
Mean diameter (mm)	1.0 (0.2)	1.2 (0.2)	1.3 (0.2)
Maximum diameter (mm)	5.6 (1.7)	7.7 (2.4)	8.9 (2.1)
Largest pore area (mm^2)	5.7 (2.8)	10.6 (6.2)	16.1 (8.8)
Mean shape factor	0.5 (0.0)	0.5 (0.0)	0.5 (0.0)
Mean esfericity	0.3 (0.0)	0.3 (0.0)	0.3 (0.0)
Mean aspect ratio	2.0 (0.3)	2.1 (0.2)	2.1 (0.1)
Mean convexity	0.8 (0.0)	0.8 (0.0)	0.8 (0.0)
Mean red	64.6 (6.9)	74.4 (2.9)	61.5 (2.7)
Mean green	50.2 (7.9)	61.5 (3.1)	46.0 (2.6)
Mean blue	56.4 (6.9)	65.8 (2.4)	51.3 (2.2)
Tops			
Porosity coefficient (%)	2.1 (1.3)	3.1 (1.8)	3.7 (2.0)
Number of pores per 100 mm^2	2.5 (1.2)	3.3 (1.5)	3.5 (1.3)
Number of pores	22 (10)	29 (13)	30 (11)
Total area of pores (mm^2)	17.4 (10.9)	26.8 (15.5)	32.4 (17.4)
Mean rectangle (mm^2)	4.9 (5.7)	5.9 (5.5)	5.9 (4.8)
Maximum rectangle (mm^2)	58.3 (55.4)	86.8 (71.9)	89.7 (70.5)
Mean diameter (mm)	2.0 (1.0)	2.1 (1.0)	2.1 (0.8)
Maximum diameter (mm)	9.5 (4.7)	11.7 (5.4)	12.0 (5.1)
Largest pore area (mm^2)	5.7 (4.5)	9.0 (6.8)	10.2 (6.8)
Mean shape factor	0.4 (0.1)	0.3 (0.1)	0.3 (0.1)
Mean esfericity	0.2 (0.1)	0.2 (0.1)	0.2 (0.1)
Mean aspect ratio	3.7 (1.1)	3.6 (1.2)	3.4 (0.8)
Mean convexity	0.7 (0.0)	0.7 (0.0)	0.7 (0.0)
Mean red	63.5 (5.3)	64.2 (3.0)	61.2 (10.1)
Mean green	48.7 (5.1)	49.9 (3.3)	48.7 (11.2)
Mean blue	54.0 (3.5)	54.5 (2.8)	53.3 (9.0)

The differences between the values presented here and those published in other studies (Costa and Pereira, 2006, 2007, 2009) can be explained by the differences in the sampling size, which was much larger in the present study, and the fact that pore sizes superior to 0.1 mm^2 were considered instead of 0.5 mm^2, therefore allowing a more comprehensive and accurate characterization. In the present study, the proportion of pores between 0.1 mm^2 and 0.5 mm^2 that were discarded in the previous studies represented, on average, for the lateral surface, 23.7 %, 15.9 % and 11.6 % of the total porosity and 68.7 %, 62.9 % and 60.3 % of the total number of pores for premium, good and standard classes, respectively (Figures 2 and 3), while for the tops it represented 13.5 % of the total porosity in premium, 10.9 % in good and 9.0 % in standard stoppers. In both cases, there was a significant proportion of the total porosity that should be considered in a detailed characterization of stoppers,

notwithstanding the irrelevant visual impact that such small pores might have.

The results obtained for cork stoppers tops had the same trend as described for the lateral surface. The porosity coefficient was 2.1 %, 3.1 % and 3.7 % for premium, good and standard quality classes, respectively (Table 1). These results can be compared with the values published by Costa and Pereira (2009), which ranged from 1.1 % for extra stoppers to 4.7 % for 5th quality stoppers.

For the body lateral surface, the large pores with size greater than 5 mm² represented on average 8.2 %, 20.6 % and 33.0 % of the total porosity for premium, good and standard quality classes, respectively (Figure 2), while corresponding only to 0.6 %, 1.8 % and 3.2 % of the total number of pores (Figure 3). For the tops, this class size represented 30.6 %, 44.6 % and 46.0 % of the total porosity for premium, good and standard quality classes, respectively.

In premium cork stoppers, small pores (area < 2 mm²) represented 95.3 % in the body lateral surface and 89.3 % in the tops, which corresponds to 69.2 % and 39.7 % of the total porosity, respectively. On the other hand, in standard stoppers the small porosity represented only 40.6 % and 30.4 % of the total area of pores but 88.6 % and 86.9 % of the total number of pores in the body and tops, respectively.

The shape factor plotted as a function of pore size presented a decreasing trend in both lateral surface and tops for the three quality classes (Figure 4). On the contrary, the aspect ratio increased with increasing pore size, although this trend was more pronounced in tops (Figure 5).

The mean size of the largest pores in the lateral surface of cork stoppers was 5.7 mm², 10.6 mm² and 16.1 mm² for premium, good and standard classes, respectively (Table 1). These values are within the reported range of 3.5 mm² and 25.5 mm² for superior and inferior classes (Costa and Pereira, 2007) or the 3.1 mm² and 26.5 mm² range for extra and 5th class stoppers, respectively (Costa and Pereira, 2009).

The average RGB of pores was 74.4, 61.5 and 65.8 for good, and 61.5, 46.0 and 51.3 for standard stoppers (Table 1). The pores of premium stoppers presented a much larger scattering of RGB values than the other classes.

These results can be used to establish better requirements for the quality classification of the stoppers. The increasing trend shown by dimension and concentration variables, both in lateral surface and tops, suggests that these are the best variables to distinguish the quality classes. The porosity coefficient is probably the most important single

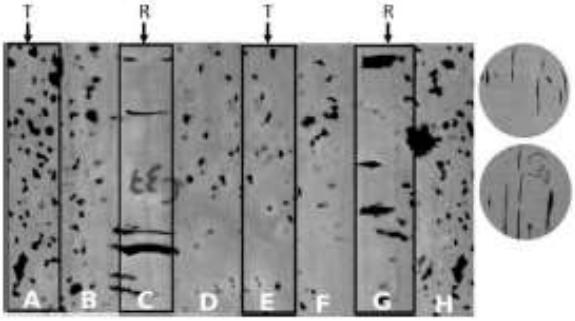

Figure 1 - Photographs of the cylindrical lateral surface (as a composition of eight successive pictures – frames A to H) and the two circular tops of one cork stopper. Arrows mark out the position of the different cork sections (T: tangential, R: radial).

variable since it expresses the extent of porosity and is correlated to size variables. On the contrary, shape variables do not seem to have discriminating power. These assumptions are in accordance with the variables selected by the classification system based on canonical and stepwise discriminant analysis presented by Costa and Pereira (2006). The color variables showed differences between classes. This observation suggests that they could be used in the quality classification and is accordance with Gonzalez-Adrados and Pereira (1996), who reported that color visual systems enable a better separation of the inferior quality class due to a more accurate detection of the pores.

The standard deviation for the dimension and concentration variables presented, with few exceptions, an increasing trend from best to worst quality class (e.g., the standard deviation of the porosity coefficient of the lateral surface was 0.8 % and 1.9 % for the premium and standard quality class, respectively) (Table 1). The standard deviation values also demonstrated a large variation between stoppers in the same quality class. For instance, the number of pores for the premium class presented a standard deviation of 51 pores, which means that approximately 68 % of the stoppers had between 105 and 207 pores in their lateral surface. This large range of values can be explained by the cork intrinsic variability. This variability between and within the three quality classes further corroborates that the traditional quality grading into nine classes is excessive in relation to the reality of cork variability (Costa and Pereira, 2005, 2007). Costa and Pereira (2006) reported that a classification in three quality classes improves the classification accuracy. This has been recognized by the industry and costumers and the present trade practice for the quality wines is to sort stoppers in premium-good-standard classes.

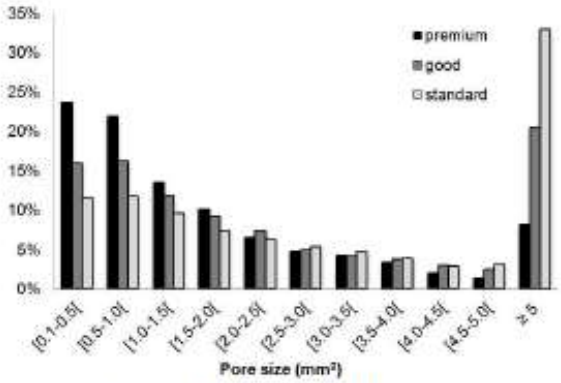

Figure 2 - Distribution of total porosity in the lateral surface as a function of pore size for the three quality classes of natural cork stoppers.

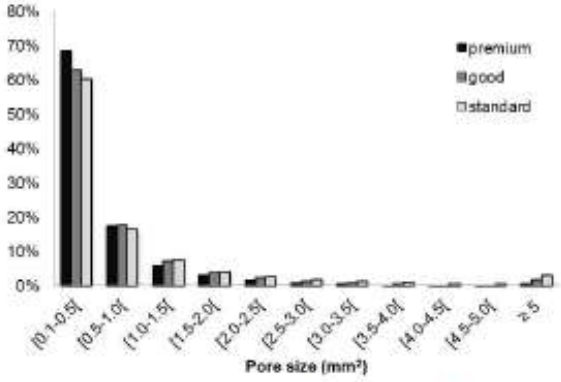

Figure 3 - Distribution of the number of pores in the lateral surface as a function of pore size for the three quality classes of natural cork stoppers.

On average, the stoppers belonging to each quality class can be described and distinguished from each other according to the characteristics of their pores. The stoppers from the premium class are characterized by an average porosity coefficient of 2.4 % and 2.1 % in their body and tops, respectively, with pores smaller than 5.7 mm² and with approximate 69 % of the porosity resulting from pores smaller than 2 mm². For the good quality class it will be expected to find, on average, a porosity coefficient of 4.0 % and 3.1 % in the lateral surface and tops, respectively, with pores up to 10.6 mm² and 9.0 mm². Stoppers belonging to the standard class will have a porosity coefficient of 5.5 % and 3.7 % in the lateral surface and tops, respectively, with pores smaller than 16.1 mm² and nearly 40 % of the porosity resulting from pores smaller than 2 mm².

2. Variation between tops and lateral surface

Tops showed different porosity features when compared to those observed in the lateral surface of the stopper (Table 1). Tops had a lower porosity coefficient and the difference increased with decreasing quality grade (12 %, 22 % and 33 % lower coefficient in relation to the lateral surface for premium, good and standard grade, respectively), and they had less pores per unit area (about 60 % of that in the lateral surface).

Pores in the tops were more elongated than in the lateral surface (Figures 4 and 5). For instance, the mean aspect ratio was 3.6 in the tops and 2.1 in the lateral surface (Figure 5, Table 1), and, on average, the pores were large (mean rectangle of 4.9 mm² in the tops and 1.3 mm² in the lateral surface for the premium grade).

These differences along with the relatively higher importance given by the human visual inspection to the lateral surface compared with tops suggest that the image analysis of the porosity features of the tops is of lesser impact for the quality classification and only of an aesthetical concern, as stated by Costa and Pereira (2006).

These differences are closely related to the biological development of the lenticular channels within the corkboard and the orientation of the cutting process for the production of stoppers (Pereira, 2007). The tops section the lenticular channels along their longitudinal axis, which runs approximately parallel to this section, thereby showing them as thin but long lines, as clearly seen in Figure 1.

The comparison of porosity between the two tops confirmed the existence of axial variation in the tree since both tops showed different porosity coefficients. A porosity ratio calculated between the top with the highest porosity and the other one showed a median value of 2.1, but extreme between-top differences could be found (e.g., 15.3 % and 0.2 % in the two tops of the same stopper). This variation can be practically used in the production of cork stoppers that have one of the tops covered with a covering cap, such as those designed for bottling fortified wines and spirits, i. e., by selecting the top with the lowest porosity as the apparent top.

3. Variation within the lateral surface

The stoppers are punched out from the cork strips so that their cylindrical axis is parallel to the axial direction of cork. Therefore, the lateral surface of the cork stoppers is not homogeneous relative to the section of cork and ranges from regions corresponding to tangential and radial sections of cork (Fortes *et al.*, 2004). The lenticular channels appear differently shaped in these two sections: in the radial section they look like elongated rectangular channels and in the tangential section they have an

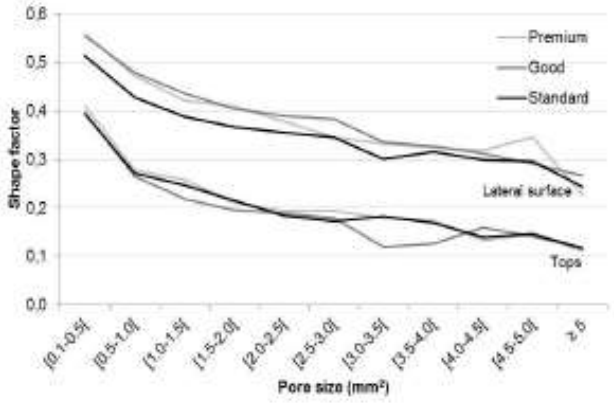

Figure 4 - Shape factor variation in lateral surface and tops as a function of pore size for the three quality classes of natural cork stoppers.

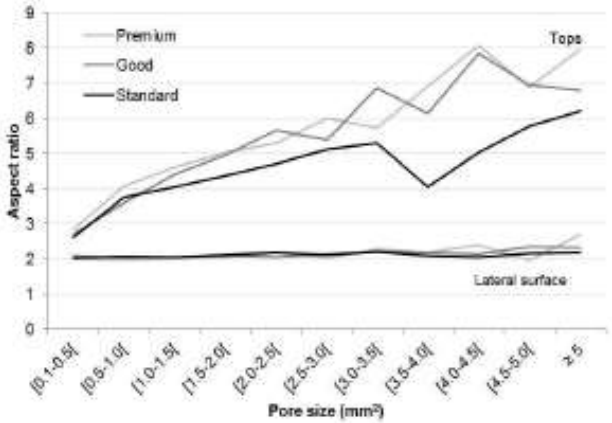

Figure 5 - Aspect ratio variation in lateral surface and tops as a function of pore size for the three quality classes of natural cork stoppers.

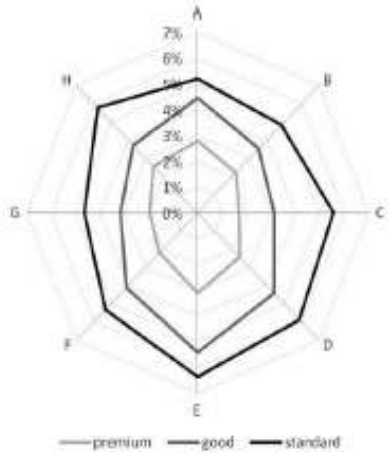

Figure 6. Variation of the porosity coefficient in the cork stoppers lateral surface (frames A to H) for the three quality classes. Mean (n=100).

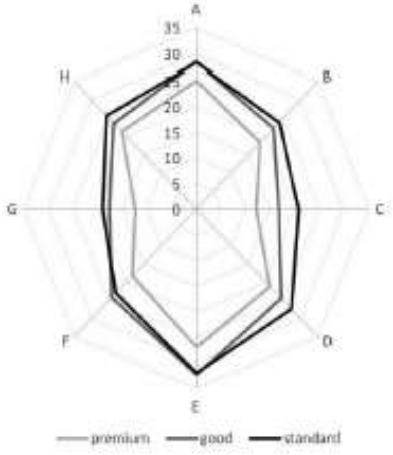

Figure 7. Variation of the number of pores in the cork stoppers lateral surface (frames A to H) for the three quality classes. Mean (n=100).

approximately circular to elliptical form (Pereira, 2007). The eight frames acquired by image analysis on the lateral surface of the cork stoppers represent the tangential (frames A and E) and radial sections (frames C and G) and the in-between sections (B, D, F and H), as shown in Figure 1. The described features of the sectioned lenticular channels are clearly visible in Figure 1: the along-the-channel development of the lenticular channels is well visualized in the tops, and a part of this path is seen in the radial frames C and G, while the cross-sectional image of the lenticular channel is shown in the tangential frames A and E.

The present investigation has shown that the lateral surface of the cork stoppers is not homogeneous with regard to the distribution and characteristics of the lenticular channels. The most relevant results of the variation of pore features along the lateral surface of the stopper are shown graphically in Figures 6 to 11. These are star-type graphs where eight axes represent the different frames with a scale adequate for the variable under study. This type of representations allows a rapid grasp of the variation of the corresponding variable.

The dimension and concentration variables showed differences between frames in the three quality classes: frames A and E, corresponding to the tangential sections of cork, had a higher porosity coefficient and a higher number of pores when compared with frames C and G, corresponding to the radial sections of cork. These frames also presented higher values for the largest pore area and mean pore area.

Regarding the porosity coefficient, there was variation when moving around the lateral surface of the stopper,

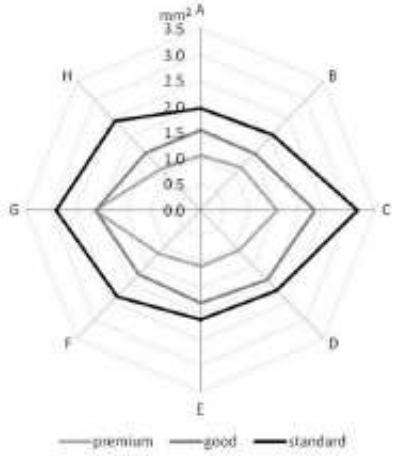

Figure 8 -Variation of the medium rectangle in the cork stoppers lateral surface (frames A to H) for the three quality classes. Mean (n=100).

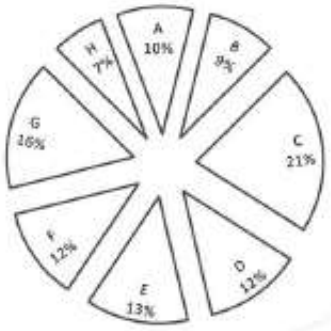

Figure 9 - Distribution for cork stoppers lateral surface (frames A to H) of the biggest pore (% of the total stoppers).

with maximal values for frames A and E (Figure 6). This was enhanced for the premium and good stoppers, for which the coefficient of porosity in frames A and E was 1.6 times superior to the value observed in frames C and G. For the standard stoppers, there was a more homogeneous distribution of porosity around the stopper (5.8 % in frames A and E, and 5.1 % in frames C and G).

The number of pores had a clear anisotropy in their distribution on the lateral surface of the cork stoppers, reaching maximal values in the A and E tangential frames and minimal values in the C and G frames (Figure 7). There was no significant difference between the three quality grades of stoppers. However, the mean values showed statistically significant differences between frames of the lateral surface, allowing the identification of three different groups: i) radial frames; ii) in-between frames; and iii) tangential frames.

Regarding the distribution of the mean dimension of the pores in the lateral surface, the radial frames (C and G) presented a significantly higher medium rectangle in all the quality classes, with values of 1.8 mm², 2.2 mm² and 3.1 mm² for premium, good and standard classes, respectively, in comparison with 1.1 mm², 1.7 mm² and 2.1 mm² in the A and E frames. Statistically significant differences occurred between the radial frames and all the others. The biggest pore was also preferentially located in the radial frames: 37 % of the largest pores lied in these two frames (Figure 9).

The distribution of porosity as a function of pore size showed different patterns for large, medium and small pores (Figure 10). The largest pores (above 5 mm²) were located preferentially in the C and G frames, the smallest pores (below 1 mm² and from 1 to 2 mm²) were located mostly in the A and E frames, while the medium sized pores (from 2 to 5 mm²) were more evenly distributed along the lateral surface of the stopper.

Figure 11 shows that the distribution of pores as a function of orientation was independent of quality class. However, there was a clear difference between the orientation of the main axis of the pores around the stopper: in the radial frames (C and G) more than 55 % of the pores were approximately oriented parallel to the tops of the stopper (i. e., 0° to 45° and 135° to 180° orientation), while in the tangential frames (A and E) almost 80 % of total number of pores were approximately oriented along the stopper's axis (i.e., between 45° and 135°).

Independently of quality class, the shape factor was, on average, slightly higher in the tangential section than in the radial section (0.5 and 0.4, respectively). This can be explained by the fact that pores in the tangential section have an approximately circular to elliptical form while in the radial sections they are elongated rectangular channels.

There are no published data for the different sections in the lateral surface of cork stoppers. However, results can be compared with the data reported for the tangential and radial surfaces of cork planks and the rationale of the orientation of the stopper when bored from the cork plank (Pereira, 2007; Pereira *et al.*, 1996).

The pore features presented variation along the lateral surface of cork stoppers, which is not homogeneous in this aspect as it is clearly seen in the example shown in Figure 1. The main differences were observed between radial and tangential sections. In radial sections the lenticular channels are cut by a plane parallel or with a small angle with respect to its radial development axis, which leads to the occurrence of pores approximately

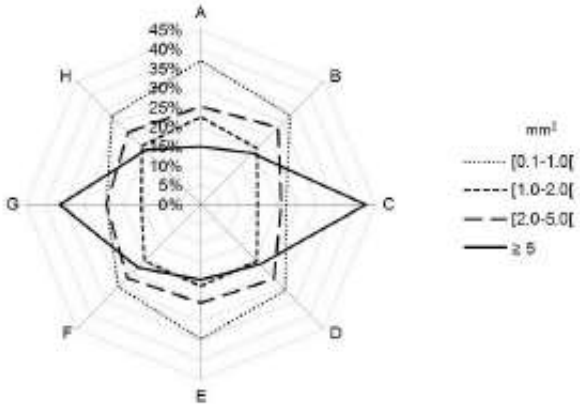

Figure 10 - Distribution of total porosity by pore dimension classes for the eight frames of the natural cork stoppers lateral surface.

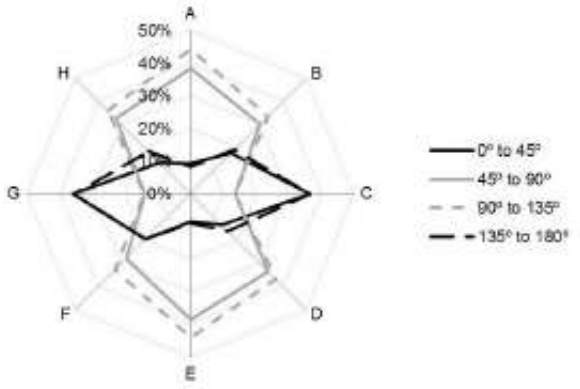

Figure 11 - Distribution of the total number of pores by pore orientation classes for the eight frames of the natural cork stoppers lateral surface.

parallel to the tops of the stopper and with an elongated shape, on average larger but fewer. On the other hand, the tangential sections present the cross-sectional image of the lenticular channel leading to pores that are oriented along the stopper's axle, in higher number and are visualized with an approximately circular to elliptical form (shape factor of 0.5). This surface variation of pore features was observed for the three quality classes with an increasing trend from best to worst quality class, namely for porosity coefficient and medium rectangle.

These results point out the importance of radial and tangential sections for the detailed characterization of cork stoppers porosity. Variables like tangential porosity coefficient, radial medium rectangle or the radial largest pore may therefore improve the accuracy of quality classification algorithms.

The variation of pore features along the lateral surface of cork stoppers can be related to their sealing performance as regards the leakage between stopper and bottleneck, which is evaluated by the liquid penetration in the interface (Fortes *et al.*, 2004). The highest depth of penetration should therefore occur in radial sections and the lowest in tangential sections.

The results obtained in this investigation may be used for reinforcing quality requirements of cork stoppers, including definition of standards, since the large sampling that encompassed the natural variability of cork and the detailed observation of surface porosity allow a broad confidence. Therefore the results may be used to develop better decision models for the quality classification of natural cork stoppers, i. e., by adding new decision variables or redefining class boundaries.

CONCLUSIONS

Quality classes of cork stoppers can be differentiated by mean values of the main porosity features of their surface, namely dimension and concentration variables, considering either the lateral surface or tops. These features showed an increasing trend from the premium to standard quality class.

Variation of pore features occurred along the lateral surface of cork stoppers, mainly between radial and tangential sections. Radial sections presented pores approximately parallel to the tops of the stopper, in a smaller number but with superior dimension and elongated shape. Tangential sections had pores oriented along the stopper's axis, in higher number and with circular to elliptical form.

The anisotropy of porosity features shown by cork stoppers is a consequence of the biological development of cork and of their production method. Understanding this variation is a relevant component in the analysis of performance of stoppers as wine sealants.

Acknowledgements: This work was supported by FEDER funds through the Operational Programme for Competitiveness Factors – COMPETE and by National Funds under the project FCOMP-01-0124-FEDER-005421. Centro de Estudos Florestais is a research unit supported by national funding from FCT – Fundação para a Ciência e Tecnologia (PEst-OE/AGR/UI0239/2011). The authors acknowledge the collaboration of Amorim & Irmãos, S.A. in the material supply and the assistance of our colleague Lídia Silva in the image analysis. The first and second authors acknowledge a scholarship from FCT.

REFERENCES

Chang J., Han G., Valverde J.M., Griswold N.C., Duque-Carrillo J.-F. and Sanchez-Sinencio E., 1997. Cork

quality classification system using a unified image processing and fuzzy-neural network methodology. *IEEE Trans. Neural Netw.*, **8**, 964-974.

Costa A. and Pereira H., 2005. Quality characterization of wine cork stoppers using computer vision. *J. Int. Sci. Vigne Vin*, **39**, 209-218.

Costa A. and Pereira H., 2006. Decision rules for computer-vision quality classification of wine natural cork stoppers. *Am. J. Enol. Vitic.*, **57**, 210-219.

Costa A. and Pereira H., 2007. Influence of vision systems, black and white, colored and visual digitalization, in natural cork stopper quality estimation. *J. Sci. Food Agric.*, **87**, 2222-2228.

Costa A. and Pereira H., 2009. Computer vision applied to cork stoppers inspection. *In: Cork oak woodlands and cork industry: present, past and future*. Ed. Santiago Zapata, Barcelona, Spain, pp. 394-405.

Fortes M.A., Rosa M.E. and Pereira H., 2004. *A Cortiça*. Ed. IST Press, Lisbon, Portugal, 259 p.

Gonzalez-Adrados J.R. and Pereira H., 1996. Classification of defects in cork planks using image analysis. *Wood Sci. Technol.*, **30**, 207-215.

Gonzalez-Adrados J.R., Lopes F. and Pereira H., 2000. Quality grading of cork planks with classification models based on defect characterisation. *Holz Roh Werkst.*, **58**, 39-45.

Jordanov I. and Georgieva A., 2009. Neural network classification: a cork industry case. *In: IEEE International Symposium on Industrial Electronics*. Ed. IEEE Computer Society, Seoul, Korea. pp.232-237.

Lopes F. and Pereira H., 2000. Definition of quality classes for champagne cork stoppers in the high quality range. *Wood Sci. Technol.*, **34**, 3-10.

Melo B. and Pinto R., 1989. Análise de diferenças nos critérios de classificação qualitativa das rolhas. *Cortiça*, **601**, 293-302.

Paniagua B., Vega-Rodríguez M.A., Gómez-Pulido J.A. and Sánchez-Pérez J.M., 2010. Improving the industrial classification of cork stoppers by using image processing and Neuro-Fuzzy computing. *J. Intell. Manuf.*, **21**, 745-760.

Paniagua B., Vega-Rodríguez M.A., Gómez-Pulido J.A. and Sánchez-Pérez J.M., 2011. Automatic texture characterization using Gabor filters and neurofuzzy computing. *Int. J. Adv. Manuf. Technol.*, **52**, 15-32.

Pereira H., Rosa M.E. and Fortes M.A., 1987. The cellular structure of cork from *Quercus suber* L. *IAWA Bull.*, **8**, 213-218.

Pereira H., 1988. Chemical composition and variability of cork form *Quercus suber* L. *Wood Sci. Technol.*, **22**, 211-218.

Pereira H., Lopes F. and Graça J., 1996. The evaluation of the quality of cork planks by image analysis. *Holzforschung*, **50**, 111-115.

Pereira H., 2007. *Cork: Biology, Production and Uses*. Ed. Elsevier B.V., Amesterdam, The Netherlands, 336 p.

Radeva P., Bressan M., Tovar A. and Vitrià J., 2002. Bayesian classification for inspection of industrial products. *In: Proceedings of the 5th Catalonian Conference on Artificial Intelligence*, Castellon, Spain. Eds. M.T. Escrig et al., Springer-Verlag, Heidelberg, pp. 399-407.

Vega-Rodríguez M.A., Sánchez-Pérez J.M. and Gómez-Pulido J.A., 2001. Cork stopper classification using FPGAs and digital image processing techniques. *In: Proceedings of the Euromicro Symposium on Digital Systems Design*. Ed. IEEE Computer Society, Washington, DC, pp. 270-275.

Vitrià J., Bressan M. and Radeva P., 2007. Bayesian classification of cork stoppers using class-conditional independent component analysis. *IEEE Trans. Syst. Man Cybern. – Part C: Applications and Reviews*, **37**, 32-38.

PUBLICATION II.

CLASSIFICATION MODELLING BASED ON SURFACE POROSITY FOR THE GRADING OF NATURAL CORK STOPPERS FOR QUALITY WINES

FOOD AND BIOPRODUCTS PROCESSING 93 (2015) 69–76

Contents lists available at ScienceDirect

Food and Bioproducts Processing

journal homepage: www.elsevier.com/locate/fbp

Classification modeling based on surface porosity for the grading of natural cork stoppers for quality wines

Vanda Oliveira, Sofia Knapic, Helena Pereira*

Universidade de Lisboa, Instituto Superior de Agronomia, Centro de Estudos Florestais (CEF), Tapada da Ajuda, P-1349-017 Lisboa, Portugal

ABSTRACT

The natural cork stoppers are commercially graded into quality classes according with the homogeneity of the external surface. The underlying criteria for this classification are subjective without quantified criteria and standards defined by cork industry or consumers. Image analysis was applied to premium, good and standard quality classes to characterize the surface of the cork stoppers and stepwise discriminant analysis (SDA) was used to build predictive classification models. The final goal is to analyze the contribution of each porosity feature and propose an algorithm for cork stoppers quality class classification. This study provides the knowledge based on a large sampling to an accurate grading of natural cork stoppers.

In average all the models presented accuracy in relation to the commercial classification over 68% with a higher mismatch in the mid-quality range. Color showed an important discriminating power, increasing the accuracy in 10%. The main discriminant features were porosity coefficient and color variables, calculated for the lateral surface. A quality classification algorithm was presented based on a simplified model with an accuracy of 75%. The classification based on color vision systems can ensure improved quality class uniformity and a higher transparency in trade.

Keywords: Natural cork stoppers; Quality classes; Image analysis; Porosity; Discriminant analysis; Classification algorithm

1. Introduction

Natural cork is an outstanding material for the closure of wine bottles combining physical performance and durability, and allowing a balanced development of wine during bottle aging through its oxygen transfer characteristics (Lopes et al., 2005). Cork is the closure material preferred by wine consumers, as shown by recent surveys (Barber et al., 2009). Natural cork stoppers have also a very favorable footprint and are associated to cork oak forests, a sustainable ecosystem with high biodiversity richness.

Cork is a cellular material with chemical inertia and a set of specific physical and mechanical properties that provide an unmatched closure for bottles and for high performance insulation, with natural cork stoppers as the premium product of the cork industry (Fortes et al., 2004; Pereira, 2007).

Natural cork stoppers are graded into quality classes in function of the apparent homogeneity of their external surface, as seen by human or machine vision (Fortes et al., 2004; Pereira, 2007). The heterogeneity of the cork surface is given primarily by the presence of lenticular channels, as well as by woody inclusions, small fractures or other defects, that can be visually outsingled from the cork surface and are named as the porosity of cork (Gonzalez-Adrados and Pereira, 1996; Pereira et al., 1996). This evaluation is made using automated image-based inspection systems with high throughput rates based on line-scan cameras and a computer embedded in an industrial sorting machine capable of acquiring and processing in real-time the surface image of the stoppers (Lima and Costa, 2006). The systems allow an identification of surface defects and quantification of porosity features, e.g. total area, number or concentration of pores (Chang et al., 1997; Jordanov

* *Corresponding author*. Tel.: +351 21 365 3491; fax: +351 21 365 3338.
E-mail address: vandaoliveira@isa.ulisboa.pt (V. Oliveira).
Received 18 January 2013; Received in revised form 5 November 2013; Accepted 15 November 2013
Available online 24 November 2013
0960-3085/$ – see front matter
http://dx.doi.org/10.1016/j.fbp.2013.11.004

and Georgieva, 2009; Pereira et al., 1994; Radeva et al., 2002).

However, it is known that the underlying criteria for the quality classification of cork stoppers are subjective to some extent and no standards were defined by the cork industry or the consumers to grade sorting (Pereira, 2007). The classification is usually based on reference samples showing the range of quality variation that can be found in the consignment for a given client (Lopes and Pereira, 2000).

Several studies have been published on identifying the contribution of each porosity feature for the grading of cork stoppers (Costa and Pereira, 2005, 2006, 2007, 2009), as well as of cork discs (Lopes and Pereira, 2000) and cork planks (Benkirane et al., 2001; Gonzalez-Adrados et al., 2000; Gonzalez-Adrados and Pereira, 1996; Pereira et al., 1996). All the studies have shown that there is overlap between classes and that the role of non-quantified features, i.e. related to operator or industry is significant. However, the sampling used in these studies was limited, e.g. in number of cork stoppers and in the surface area covered by image analysis, and doubts may remain regarding the selected features since the natural variability in cork is high. A recent study analyzed in detail the porosity of a large sample of natural cork stoppers, showing that variation of some of the pores characteristics throughout the lateral surface of the stopper is important (Oliveira et al., 2012).

Other studies have been published focusing on modeling the classification of cork stoppers and discs. Chang et al. (1997) proposed a cork stopper quality classification system based on features extraction and a fuzzy neural network, with 6.7% of rejection after reevaluation of the results by human experts. Vega-Rodríguez et al. (2001) presented a system for image processing using reconfigurable hardware and an algorithm for the cork stoppers classification that uses a simplified set of porosity features (defect area, size of the biggest defect and area occupied by defects of different sizes) for the two tops. Vitrià et al. (2007) presented a cork stopper classification model based on feature extraction and class-conditional independent component analysis, reaching an average error rate of 2%. Paniagua et al. (2011) developed for cork discs a neurosystem to model the human cork quality classification. Other techniques have been applied to cork classification such as X-ray Compton tomography (Brunetti et al., 2002) or terahertz/millimeter wave spectroscopy (Hor et al., 2008) in order to refine the visual classification with inclusion of possible voids, cracks, and defects inside the stopper. Recently, Gómez-Sánchez et al. (2013) used colorimetric image analysis techniques with application of segmentation algorithms to measure the porosity of cork samples. They obtained the best NIRS calibrations by measuring the porosity into three classes of color, matching the results obtained by image analysis.

This paper analyses in detail the porosity features of cork stoppers in the grades used today by the quality wine markets: three major quality grades, of premium, good and standard stoppers. The study was made on the total external surface (lateral surface and tops) of the stoppers, and was based on a large sample in order to encompass the cork natural variability and to allow better confidence in the results. The contribution of each porosity feature to quality classification is analyzed using adequate statistical validation, the significant indicators for the grading selected and a classification algorithm is proposed for cork stoppers quality classification using today's quality grades. The final goal is to define a simple and objective classification that could be used by the industry in order to ensure improved quality class uniformity and a higher transparency in trade, and additionally generate knowledge on the key features of the raw material that may be used in the research, development and enhancement of new products.

2. Materials and methods

2.1. Sampling

The natural cork stoppers (24 mm diameter × 45 mm length) used in this study were collected from one major Portuguese cork industrial unit. The stoppers were randomly sampled (before washing and surface treatment) after a first step grading by the automated vision system used routinely in the industrial production line. The criteria considered in such automated grading include total area and number of pores, area of the largest pores, pore concentration level, location of defects, vertical and horizontal projection of pores, and the presence of cracks. Subsequently they were inspected by skilled operators and graded into three references quality classes as required today by the wine market, coded as premium (including the traditional "flor" and extra commercial classes), good (superior and 1st commercial classes) and standard (2nd and 3rd commercial classes). After this manually validated classification, a sample of 200 cork stoppers of each quality class was randomly taken and used as the reference for the classification modeling.

2.2. Image acquisition

The natural cork stoppers were individually analyzed and their image surface (cylindrical lateral surface and circular bases) acquired with an image analysis system that included a digital 7 mega pixels in macro stand solution set on an acquisition Kaiser RS1 Board with a controlled illumination apparatus, connected to a computer using AnalySIS® image processing software (Analysis Soft Imaging System GmbH Münster, Germany, version 3.1).

The image acquisition covered 100% of the lateral area by using eight successive frames of the cylindrical lateral surface of the body. The first frame was acquired parallel to cork growth rings and the others subsequently taken by rotating the stopper 45° (Fig. 1). Two circular frames were acquired for the two tops corresponding to 96% of the total area. Due to the way stoppers are punched out from the cork strip, the tops correspond to transversal sections of cork while the lateral surface of the stopper includes tangential and radial sections of cork and all the in-between sections (Pereira, 2007; Pereira et al., 1987).

The object extraction was carried out inside two predefined regions of interest, one rectangular, 45.05 mm long and 9.41 mm wide (area 423.92 mm^2), for the lateral surface, and another circular for the tops with 23.51 mm diameter (area 433.92 mm^2). The image threshold was adjusted individually for each image and ranged in a RGB system from 65 to 135 for red, from 60 to 115 for green, and from 65 to 120 for blue.

2.3. Image data analysis

A set of variables was collected automatically for each pore: area (mm^2), calculated by the number of pixels of the particle times the calibration factors; mean diameter (mm), defined as the arithmetic mean of all diameters of a particle (range angles between 0° and 179°, with step width of 1°); maximum diameter (mm), is the maximum diameter of all maximum

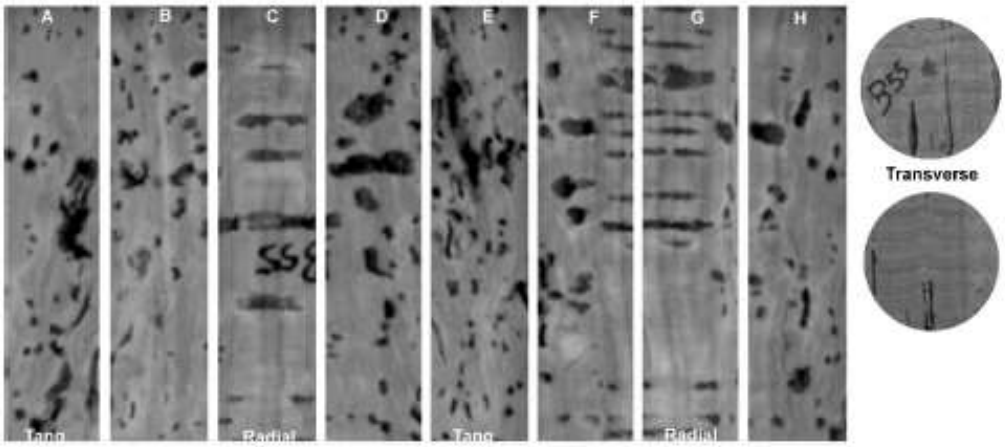

Fig. 1 – Photographs of the cylindrical lateral surface (composition of eight successive pictures) and the two circular tops (transverse section). Frames A and E represent tangential section while frames C and G represents cork radial section.

diameters determined at each angle (varies in 1° steps); mean rectangle, defined as the area of the mean rectangle which sides consist of tangents to the particle borders; maximum rectangle, defined as the area of the biggest rectangle which sides consist of tangents to the particle borders; shape factor, defined as (area/perimeter^2) $\times 4\pi$, measuring the roundness of the pores; convexity, defined as the fraction of the pore area and the area of its convex hull (ranging between 0 and 1); aspect ratio, as the maximum ratio between width and length of a bounding rectangle of the pore; sphericity, that describes the elongation of the pore by using central moments (value of 1 for a perfect circular particle); and mean value of all red, green and blue intensities in each pore.

These data were filtered and only pores with area equal or superior to 0.1 mm^2 were considered for the analysis. The pixel size was 0.05 mm and therefore the lowest pore area that could be confidently resolved was 0.02 mm^2 corresponding to eight contiguous pixels. Previous studies considered only porosity superior to 0.5 mm^2 on the assumption that small porosity is functionally and esthetically irrelevant, and only brings higher variance and variability to the sample (Costa and Pereira, 2005, 2006, 2007, 2009; Gonzalez-Adrados et al., 2000; Lopes and Pereira, 2000; Pereira et al., 1996).

The variables collected for each pore were processed and originate several calculated variables for each frame: porosity coefficient (%), defined as the proportion of the area occupied by pores; total number of pores and number of pores by dimension classes; total area of pores (mm^2), sum of the area of all pores in the frame; average pore area (mm^2), calculated as the arithmetic mean of the area of all pores in the frame; maximum pore area (mm^2), defined as the area of the biggest pore in the frame; mean diameter, calculated as the mean diameter average of all pores; maximum diameter, defined as the biggest of all pores maximum diameter; mean rectangle, calculated as the arithmetic mean of the mean rectangle of all pores in the frame; maximum rectangle, defined as biggest of all pores maximum rectangle; the shape-variables (shape factor, sphericity, aspect ratio and convexity) and the color-variables (red, green and blue) from pores were averaged into frame variables. Moreover, these variables were averaged and transformed into cork stopper transverse (two tops), tangential (frames A and E) and radial (frames C and G) section and cork stopper body variables (considering the eight frames of the stoppers lateral surface).

2.4. *Statistical analysis*

Several graphical and descriptive statistical analyses were carried out for the characterization of the quality classes and of the stoppers lateral surface.

In order to differentiate between quality classes and to predict the class of a future observation, several predictive classification models of stoppers were built based on their surface characteristics using stepwise discriminant analysis (SDA). Discriminant analysis is the appropriate statistical technique when the dependent variable is categorical and the independent variables are quantitative. Discriminant analysis assumes that data come from a multivariate normal distribution and that the covariance matrices of the groups are equal (Sharma, 1996). Another characteristic of the data that can affect the results is multicollinearity among the independent variables. The stepwise method can be useful when in the presence of many predictors by automatically selecting the "best" variables to use in the model. The stepwise selection begins with no variables in the discriminant function, and at each step a variable is either added or removed, if it adds the most discriminating power or if it does not significantly lower the discriminating power, as measured by the statistical criterion. The procedure stops when at a given step no variable is added or removed from the discriminant functions (Sharma, 1996). The statistical criterion used to measure variable discriminating power was Wilks' Λ value ($p < 0.05$). All the statistical analysis was performed using SPSS® statistical software (version 19.0; SPSS Inc., Chicago IL).

The sample was randomly divided into two groups: 70% of the cork stoppers were used to estimate the discriminant functions and produced the classification models (modeling set), and 30% of the stoppers were used for external validation of the models (validation set).

These models were analyzed and compared, and a simplified model and a classification algorithm for cork stoppers quality class classification were proposed.

3. Results

3.1. *Characterization of quality classes*

The three quality classes of natural cork stoppers are characterized in Table 1 for the lateral surface.

Table 1 – Mean ($n = 200$) and standard deviation (in brackets) of the independent variables of the lateral surface for the three reference quality classes of natural cork stoppers.

	Premium	Good	Standard
Porosity coefficient (>0.1 mm²) (%)	2.4 (0.8)	4.0 (1.4)	5.6 (2.0)
Porosity coefficient (>0.5 mm²) (%)	2.0 (0.8)	3.5 (1.4)	5.0 (2.0)
Number of pores			
Total	135 (48)	167 (58)	193 (54)
0.1–0.5 mm²	86	99	112
0.5–1.0 mm²	26	31	35
1.0–2.0 mm²	15	20	23
2.0–5.0 mm²	7	13	16
>5.0 mm²	1	4	7
Total area of pores (mm²)	82.7 (28.8)	135.1 (47.6)	191.2 (69.1)
Average pore area (mm²)	0.6 (0.2)	0.9 (0.3)	1.1 (0.4)
Maximum pore area (mm²)	6.5 (3.2)	11.3 (6.0)	18.0 (9.9)
Average pore shape factor	0.6 (0.1)	0.5 (0.0)	0.5 (0.1)
Average pore aspect ratio	2.0 (0.3)	2.1 (0.2)	2.1 (0.2)
Average pore Red	93 (29)	96 (21)	91 (30)
Average pore Green	71 (22)	77 (16)	69 (24)
Average pore Blue	76 (20)	80 (14)	73 (22)

The average porosity coefficient including all pores above 0.1 mm² was 2.4%, 4.0% and 5.6%, respectively, for premium, good and standard class. When considering only pores above 0.5 mm², the values decreased to 2.0%, 3.5% and 5.0%, respectively.

The small porosity (between 0.1 and 0.5 mm²) represented on average an increase of 0.5% in the porosity coefficient and represented 63.9%, 59.4% and 58.1% of the total number of pores for the premium, good and standard quality classes, respectively.

The standard deviation of the porosity coefficient of the lateral surface was 0.8%, 1.4% and 2.0% for the premium, good and standard quality class, respectively, regardless of the minimum pore area considered for the porosity coefficient calculations (0.1 or 0.5 mm²).

The maximum pore area in the lateral surface of cork stoppers differed significantly between classes with 6.5 mm², 11.3 mm² and 18.0 mm² for premium, good and standard classes, and the average pore area also increased from 0.6 mm² to 0.9 mm² and 1.1 mm², respectively.

The shape variables presented identical values between quality classes. The RGB of the pores was, on average, 93 red, 71 green and 76 blue for premium class, 96 red, 77 green and 80 blue for good class and 91 red, 69 green and 73 blue for the standard class.

Fig. 2 presents the variation of the porosity coefficient and the average pore area in the transverse, tangential and radial sections for the three quality classes of natural cork stoppers. These sections correspond respectively to the tops (transverse), frames A and E (tangential) and frames C and G (radial).

The porosity coefficient ranged between 3.1% and 6.2% in the tangential section, respectively, for premium and standard quality class, and 1.9% and 5.3% in the radial section (Fig. 2a). The premium class had average pore areas of 0.6 mm², 0.8 mm² and 1.3 mm² for the, tangential, radial and transverse section, respectively. The corresponding values for the standard quality class were 0.9, 1.4 and 1.7 mm² (Fig. 2b).

3.2. *Quality classification models*

Five predictive classification models of stoppers into quality classes were analyzed and their differences characterized. Table 2 shows the variables selected by SDA to build each model and Table 3 presents the results of the classification of cork stoppers into the three quality classes considered in this study.

The multivariate normality assumption was investigated by the application of Kolmogorov–Smirnov test with Lilliefors significance correction to the independent variables and there was no reason to believe that was violated. Box's M test was used to verify if the variance–co-variance matrices are equivalent. Although M was significant ($p < 0.00$), with large samples, a significant result is not regarded as too important.

Models 1 and 2 were built with the application of SDA to the variables used traditionally in the automated image-based inspection systems, i.e. dimension, concentration and shape

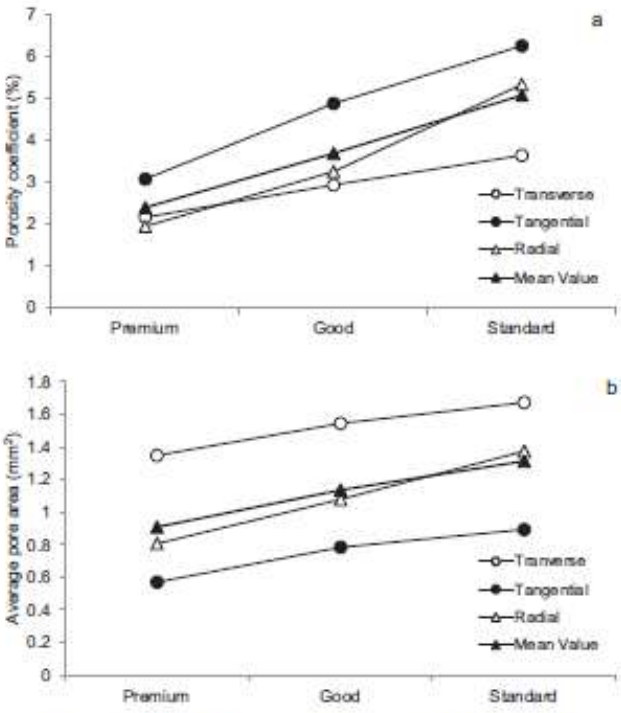

Fig. 2 – Variation in the transverse, tangential and radial sections and mean value for the three quality classes of natural cork stoppers: (a) porosity coefficient and (b) average pore area.

Table 2 – Type and variables selected by SDA for each predictive classification model.

Variables	Models							
	Model 1	Model 2		Model 3	Model 4		Model 5	
	Body	Body	Tops	Body	Body	Tops	Tang	Rad
Concentration and dimension								
Porosity coefficient	x	x	x	x	x		x	x
Total number of pores	x	x		x		x		x
Mean pore area						x		x
Maximum pore area	x	x		x	x			
Mean diameter	x	x		x	x		x	
Maximum diameter	x	x						
Mean rectangle							x	
Maximum rectangle	x	x						x
Shape								
Shape factor	x	x						
Sphericity	x	x			x		x	
Aspect ratio	x	x			x			
Convexity				x	x		x	
Color								
Average pore Red				x	x	x	x	
Average pore Green				x	x	x	x	
Average pore Blue				x	x	x	x	

variables averaged for the body lateral surface and tops. In both models the body variables selected by SDA were porosity coefficient, shape-variables (shape factor, sphericity and aspect ratio) and dimension-variables (maximum pore area, mean and maximum diameter, total number of pores and maximum rectangle). In both models the average accuracy for modeling and validation set was 69.5% and 68.3%, respectively. The good quality class showed the lowest accuracy of 60.0% and 62.9% for, respectively, models 1 and 2, while premium and standard quality classes had accuracy values above 70%.

Models 3 and 4 are comparable to models 1 and 2 with the addition of pores color-variables. The independent variables selected by SDA for model 4 were porosity coefficient, maximum pore area, mean diameter, total number of pores, convexity and average pore red, green and blue. These color variables were selected by SDA leading to an accuracy of 80.0% for model 3 and 84.1% for model 4. The good class accuracy increased to 70.7% and 78.6% for models 3 and 4, respectively. The validation set showed an average accuracy over 73% for both models with the highest value of 85.0% for the standard

Table 3 – Classification of cork stoppers into three quality classes using discriminant analysis in percentage of the initial number of stoppers in each quality class (modeling set). In brackets is the classification of the validation set. Bold corresponds to the match of classifications.

Original quality class	Predicted quality class			
	Premium	Good	Standard	Mean accuracy
Model 1				
Premium	75.7 (70.0)	20.7 (30.0)	3.6 (0.0)	
Good	21.4 (20.0)	60.0 (61.7)	18.6 (18.3)	
Standard	5.7 (8.3)	21.4 (18.3)	**72.9 (73.3)**	69.5 (68.3)
Model 2				
Premium	**74.3 (70.0)**	22.9 (30.0)	2.9 (0.0)	
Good	20.0 (20.0)	**62.9 (60.0)**	17.1 (20.0)	
Standard	5.0 (6.7)	23.6 (18.3)	**71.4 (75.0)**	69.5 (68.3)
Model 3				
Premium	**84.3 (73.3)**	13.6 (25.0)	2.1 (1.7)	
Good	23.6 (23.3)	**70.7 (61.7)**	5.7 (15.0)	
Standard	10.7 (10.0)	4.3 (6.7)	**85.0 (83.3)**	80.0 (72.8)
Model 4				
Premium	**85.0 (66.7)**	12.9 (30.0)	2.1 (3.3)	
Good	17.1 (21.7)	**78.6 (68.3)**	4.3 (10.0)	
Standard	7.1 (8.3)	4.3 (6.7)	**88.6 (85.0)**	84.1 (73.3)
Model 5				
Premium	**80.0 (61.7)**	15.7 (31.7)	4.3 (6.7)	
Good	20.0 (20.0)	**73.6 (65.0)**	6.4 (15.0)	
Standard	13.6 (10.0)	3.6 (6.7)	**82.9 (83.3)**	78.8 (70.0)
S. model				
Premium	**84.3 (70.0)**	13.6 (28.3)	2.1 (1.7)	
Good	20.7 (25.0)	**68.6 (63.3)**	10.7 (11.7)	
Standard	14.3 (16.7)	10.0 (5.0)	**75.7 (78.3)**	76.2 (70.6)

Table 4 – Structure matrix.

	Function 1	Function 2
Porosity coefficient (>0.1 mm²) (%)	0.762*	0.562
Average pore Red	−0.080	0.225*
Average pore Green	−0.097	0.150*
Average pore Blue	−0.041	0.078*

* Largest absolute correlation between each variable and any discriminant function.

class in model 4. In model 3 the good quality class had the lowest accuracy of 70.7% and 61.7% for the validation set and the standard quality class had the highest accuracy for validation set with 83.3%.

Model 5 considered dimension, concentration, shape and color variables calculated for radial and tangential sections of cork. The variable with the highest discriminating power was the porosity coefficient from both sections. The other variables of the tangential section selected for the model by SDA were: color (RGB), shape (sphericity and convexity) and mean dimension variables (diameter and rectangle). For the radial section the variables selected were: total number of pores, average pore area and maximum rectangle. The average accuracy for modeling and validation set was 78.8% and 70.0%, respectively.

Two discriminating functions were fitted automatically for all the models, but nearly all the variance explained in terms of differences between classes by the models was due to the first discriminant function. In all the models both functions were considered relevant for the discriminating power.

3.3. *Quality classification algorithm*

A simplified model was made using the main discriminant features, i.e. porosity coefficient and the RGB color-type variables calculated for the body lateral surface. The analysis of the structure matrix table (Table 4) reveals that porosity coefficient is highly related with function 1 while function 2 explains essentially the color variability.

Fig. 3 illustrates the distribution of the discriminant functions scores for each predicted group. Reading the scores ranges on the axes and the overlaps of the graphs, a substantial discrimination is revealed. Function 1 discriminates the standard quality class from premium and good stoppers (Fig. 3a), whereas function 2, that represents color variability, has discriminating power between premium and good stoppers (Fig. 3b).

Fisher's classification function coefficients were used to classify the cases between the quality classes. The coefficients of the independent variables shown in Table 5 were used to construct a discriminant function for each quality class. To

Table 5 – Classification function coefficients (Fisher's linear discriminant functions).

	Quality class		
	Premium	Good	Standard
Porosity coefficient (>0.1 mm²) (%)	1.283	1.727	2.695
Average pore Red	−1.689	−1.981	−1.332
Average pore Green	−2.198	−1.854	−2.090
Average pore Blue	4.948	4.995	4.312
(Constant)	−34.033	−37.037	−32.853

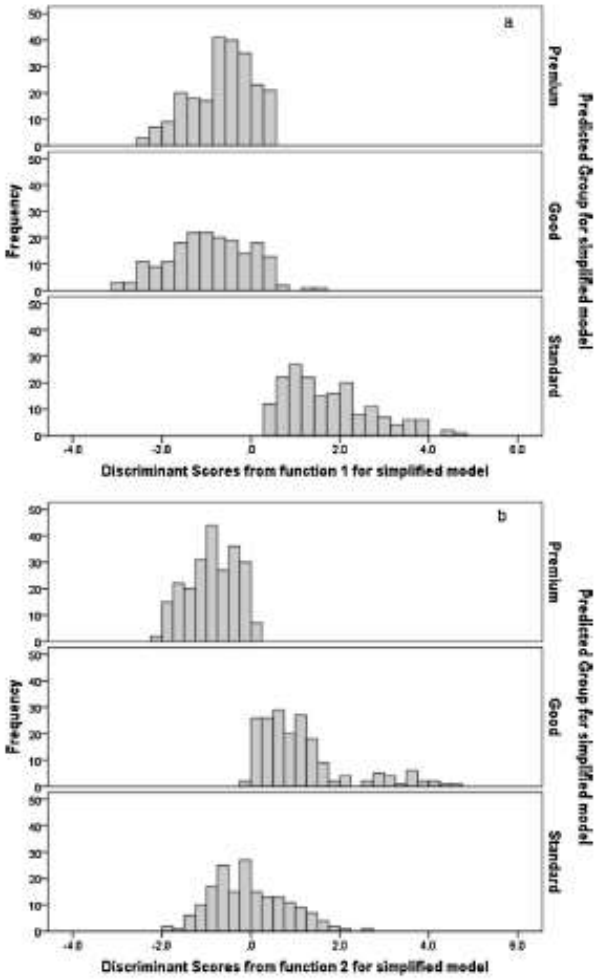

Fig. 3 – Histograms showing the distribution of discriminant scores for each predicted cork stoppers quality class by the simplified model: (a) function 1 and (b) function 2.

perform classification the three functions are computed and an individual is assigned to the group with the highest score.

The classification results for the modeling set reveal that 76.2% of the cork stoppers were classified correctly into quality classes. Like the previous models, the good quality class had the lowest accuracy of 68.6%. It is important to highlight the accuracy of 70.6% obtained with the validation set (Table 3).

When comparing to a simplistic model with the porosity coefficient as the only variable, the inclusion of color-type variables increased the overall accuracy in more than 10%. The misclassification corresponded, on average, to 13% of the totality of the cork stoppers, with higher values for the good quality class. It is noteworthy that 14.3% of the cork stoppers originally classified as standard quality were predicted by the model as premium class stoppers.

4. Discussion

4.1. *Characterization of stoppers quality classes*

As expected, the surface of the cork stoppers is not homogeneous when comparing the transverse, tangential and radial sections. The lenticular channels appear with a different

aspect in the three sections: in the radial and transverse sections they look like elongated rectangular channels and in the tangential section they have a circular to elliptical form (Figs. 1 and 2).

Several porosity features such as porosity coefficient or total number of pores presented an increasing trend from premium to standard quality class, for all sections in accordance with the published data (Costa and Pereira, 2007).

The tangential section had the highest porosity coefficients (Fig. 2a) due to the high number of pores even if the average pore area was smaller (Fig. 2b). Pereira et al. (1996) had already stated that the average pore area was higher in the transverse/radial section than in the tangential section. Lopes and Pereira (2000) reported an average pore area of 0.25 mm^2 for cork discs corresponding to the tangential section of cork. Pores in the transverse section had a higher aspect ratio than in the radial and tangential sections, and therefore were more elongated or thinner.

The shape variables presented identical values between quality classes, as previously reported by Gonzalez-Adrados and Pereira (1996), and Costa and Pereira (2009). On the other hand, the color-type variables showed differences between classes although without a trend.

4.2. *Quality classification models*

Several predictive classification models of stoppers into quality classes were built based on the presented surface characteristics using stepwise discriminant analysis (SDA) for selection of a specific set of variables (Table 2).

All the five classification models presented, on average, accuracy superior to 69.5% for the modeling set or superior to 68.3% for the validation set. The results achieved with the validation set are much better than those presented by Costa and Pereira (2006) for seven quality classes with the application of the established decisions rules for classification stopper by stopper, on an individual basis.

It is empirically known that the quality classification of stoppers is subjective to some extent and therefore varying between individual experts as demonstrated by Barros and Pereira (1987) who reported classification match values of 31% for two operators and higher classification difficulty in the mid-quality classes. This lack of objective criteria for visual classification contributes to the higher mismatch found for the mid-quality range; indeed it was in the good class of stoppers that the lowest accuracy was obtained (from 60.0% in model 1 to 78.6% for model 4).

In the analysis of models 1 and 2 it is important to notice that the unique variable considered by SDA with significant power from tops was the porosity coefficient. Gonzalez-Adrados et al. (2000) reported that the first variable to be entered into classification models of cork planks was the porosity coefficient in the transverse section. However, this variable does not have the same discriminant power in cork stoppers classification probably because the transverse area (of the tops) is smaller and visually less relevant when compared with that in cork planks.

The accuracy achieved with these models is comparable with the 65% and 72% of overall accuracy achieved by Costa and Pereira (2006) when tested a simplified classification using three quality classes and considering the significant variables selected by SDA. The evaluation of models 1 and 2 suggests that the observation of cork stoppers tops is irrelevant for the construction and accuracy of the classification model, and therefore for the classification of cork stoppers in quality classes.

In models 3 and 4 the color variables were selected for the discriminating functions and lead to a higher accuracy in the classification when compared with models 1 and 2. The accuracy obtained for the validation set (72.8% and 73.3% for, respectively, models 3 and 4), despite being smaller than those obtained when building the model (modeling set), improve those published to date by Costa and Pereira (2006). The color variation of pores represents the color heterogeneity of the filling tissues of pores and allows a better separation of the quality classes. In general "darker" pores will lead to the allocation of the corresponding stoppers to worse quality classes.

In model 5 the different selection of discriminating variables that occurred for both sections reflects the anisotropy of porosity features shown by cork stoppers.

Overall the porosity coefficient is the most important variable with discriminant power for separation of cork stoppers quality classes and was selected in all the models.

Comparing the three "new" models (3, 4 and 5) that included the color type-variables with the "traditional" models represented by models 1 and 2, it seems that color has an important discriminating power conferring a better accuracy. The classification based on colored vision systems can therefore ensure improved quality class uniformity and a higher transparency in trade.

4.3. *Quality classification algorithm*

A simplified model using the main discriminant features, i.e. porosity coefficient and the RGB color-type variables calculated for the body lateral surface were therefore proposed here. This model minimizes the processing of data by reducing the dimensionality of the problem and suppressing information redundancy. Moreover, the classification results were slightly better than the ones found for "traditional" models. Most published studies, like Paniagua et al. (2011), assume that the classification made by human experts is optimal/perfect and the aim is to obtain the most similar classification results. However the stoppers that were considered as misclassified should be analyzed, because of the human inspection subjectivity already referred. A blind belief in the accuracy of the present in-use classification is therefore an exaggeration. The 30% of "misclassification" should therefore be considered only as indicative, and the model classification probably translates more exactly the features and quantified appearance of the external surface of the stoppers.

The most common criteria considered in automated grading include variables like total area and number of pores, area of the largest pores and concentration level of pores, i.e. dimension and concentration variables. The inclusion of color-variables improves the classification and probably approximates more the model to the presently used classification related to visual appearance of cork stopper as perceived by the operator, thereby approximating the results from manual and automated grading. The proposed quality classification algorithm can be applied in the industry to ensure improved uniformity within each stoppers' quality class. By using measurable and quantified features of the external surface of the natural stoppers, this classification algorithm will allow a higher transparency in trade. Moreover, the highlight on key features of cork can be used in research, development and enhancement of new products that have cork as raw material.

Acknowledgments

This work was supported by FEDER funds through the Operational Programme for Competitiveness Factors – COMPETE and by National Funds under the project FCOMP-01-0124-FEDER-005421. Centro de Estudos Florestais (Forest Research Center) is a research unit supported by the National Research funding of Fundação para a Ciência e Tecnologia (PEst-OE/AGR/UI0239/2011). Funding from FCT is acknowledged by Vanda Oliveira as a doctoral student (SFRH/BD/77550/2011), and Sofia Knapic as a post-doctoral researcher (SFRH/BPD/76101/2011). The authors acknowledge the collaboration of Amorim & Irmãos, S.A. in materials supply and the assistance of our colleague Lídia Silva in the image analysis.

References

Barber, N.A., Taylor, C.D., Dodd, T.H., 2009. Twisting tradition: consumers' behavior toward alternative closures. J. Food Prod. Market. 15, 80–103.

Barros, L., Pereira, H., 1987. Influência do operador na classificação manual da cortiça por classes de qualidade. Cortiça 582, 103–105.

Benkirane, H., Benslimane, R., Hachmi, M., Sesbou, A., 2001. Possibilité de contrôle automatique de la qualité du liège par vision artificielle. Ann. For. Sci. 58, 455–465.

Brunetti, A., Cesareo, R., Golosio, B., Luciano, P., Ruggero, A., 2002. Cork quality estimation by using Compton tomography. Nucl. Instrum. Methods Phys. Res. Sect. B Beam Interact. Mater. Atoms 196, 161–168.

Chang, J., Han, G., Valverde, J.M., Griswold, N.C., Duque-Carrillo, J.-F., Sanchez-Sinencio, E., 1997. Cork quality classification system using a unified image processing and fuzzy-neural network methodology. IEEE Trans. Neural Netw. 8, 964–974.

Costa, A., Pereira, H., 2009. Computer vision applied to cork stoppers inspection. In: Zapata, S. (Ed.), Cork Oak Woodlands and Cork Industry: Present, Past and Future. Museu del Suro de Palafrugell Publications, Barcelona, pp. 394–405.

Costa, A., Pereira, H., 2007. Influence of vision systems, black and white, colored and visual digitalization, in natural cork stopper quality estimation. J. Sci. Food Agric. 87, 2222–2228.

Costa, A., Pereira, H., 2006. Decision rules for computer-vision quality classification of wine natural cork stoppers. Am. J. Enol. Viticult. 57, 210–219.

Costa, A., Pereira, H., 2005. Quality characterization of wine cork stoppers using computer vision. J. Int. Sci. Vigne Vin 39, 209–218.

Fortes, M.A., Rosa, M.E., Pereira, H., 2004. A Cortiça, first ed. IST Press, Lisbon.

Gómez-Sánchez, I., Ceca, J.L., García-Olmo, J., Lara-Buil, L., López-Luque, R., Prades, C., 2013. Application of image analysis and NIRS technology to the evaluation of the porosity of planks, sheets and cork stoppers, and its relation with the industrial quality. Maderas Ciencia Tecnol. 15, 293–309.

Gonzalez-Adrados, J., Pereira, H., 1996. Classification of defects in cork planks using image analysis. Wood Sci. Technol. 30, 207–215.

Gonzalez-Adrados, J., Lopes, F., Pereira, H., 2000. Quality grading of cork planks with classification models based on defect characterisation. Holz Roh Werkst. 58, 39–45.

Hor, Y.L., Federici, J.F., Wample, R.L., 2008. Nondestructive evaluation of cork enclosures using terahertz/millimeter wave spectroscopy and imaging. Appl. Opt. 47, 72–78.

Jordanov, I., Georgieva, A., 2009. Neural network classification: a cork industry case. In: IEEE International Symposium on Industrial Electronics, Seoul. IEEE Computer Society, pp. 232–237.

Lima, J., Costa, P., 2006. Real-time cork classification method: a colour image processing approach. Int. J. Fact. Autom. Rob. Soft Comput. 2, 1–10.

Lopes, F., Pereira, H., 2000. Definition of quality classes for champagne cork stoppers in the high quality range. Wood Sci. Technol. 34, 3–10.

Lopes, P., Saucier, C., Glories, Y., 2005. Nondestructive colorimetric method to determine the oxygen diffusion rate through closures used in winemaking. J. Agric. Food Chem. 53, 6967–6973.

Oliveira, V., Knapic, S., Pereira, H., 2012. Natural variability of surface porosity of wine cork stoppers of different commercial classes. J. Int. Sci. Vigne Vin 46, 331–340.

Paniagua, B., Vega-Rodríguez, M.A., Gómez-Pulido, J.A., Sánchez-Pérez, J.M., 2011. Automatic texture characterization using Gabor filters and neurofuzzy computing. Int. J. Adv. Manuf. Technol. 52, 15–32.

Pereira, H., Rosa, M.E., Fortes, M.A., 1987. The cellular structure of cork from *Quercus suber* L. IAWA Bull. 8, 213–218.

Pereira, H., Melo, B., Pinto, R., 1994. Yield and quality in the production of cork stoppers. Holz Roh Werkst. 52, 211–214.

Pereira, H., Lopes, F., Graça, J., 1996. The evaluation of the quality of cork planks by image analysis. Holzforschung 50, 111–115.

Pereira, H., 2007. Cork: Biology, Production and Uses. Elsevier, Amsterdam.

Radeva, P., Bressan, M., Tovar, A., Vitrià, J., 2002. Bayesian classification for inspection of industrial products. In: Escrig, M.T., et al. (Eds.), Proceedings of 5th Catalonian Conference Artificial Intelligence. Springer-Verlag, Heidelberg, pp. 399–407.

Sharma, S., 1996. Applied Multivariated Techniques. John Wiley & Sons, Inc.

Vega-Rodríguez, M.A., Sánchez-Pérez, J.M., Gómez-Pulido, J.A., 2001. Cork stopper classification using FPGAs and digital image processing techniques. In: Proceedings of the Euromicro Symposium on Digital Systems Design, Washington, DC. IEEE Computer Society, pp. 270–275.

Vitrià, J., Bressan, M., Radeva, P., 2007. Bayesian classification of cork stoppers using class-conditional independent component analysis. IEEE Trans. Syst. Man Cybern. Part C Appl. Rev. 37, 32–38.

PUBLICATION III.
KINETICS OF OXYGEN INGRESS INTO WINE BOTTLES CLOSED WITH NATURAL CORK STOPPERS OF DIFFERENT QUALITIES

Research Note

Kinetics of Oxygen Ingress into Wine Bottles Closed with Natural Cork Stoppers of Different Qualities

Vanda Oliveira,[1]* Paulo Lopes,[2] Miguel Cabral,[2] and Helena Pereira[1]

Abstract: The kinetics of oxygen ingress into bottles closed with natural cork stoppers was investigated by a nondestructive colorimetric measurement method using the oxidation of an indigo carmine solution. In order to encompass the natural variability of cork regarding its oxygen ingress into the bottle, 600 natural cork stoppers from different quality classes and produced from cork planks of different calipers were analyzed. The kinetics of oxygen transfer was similar in all cases and could be adjusted to logarithmic models. A significant variability was found for oxygen ingress into the bottles closed with natural cork stoppers: ingress at 12 months ranged from 0.3 to 4.8 mg; 21% of the stoppers reached the limit of oxygen quantification along the experiment. The results suggest that the variation of oxygen ingress is a consequence of the natural differing features in the cell dimensions and air volume within the stopper's structure.

Key words: oxygen ingress rate, colorimetric oxygen measurement, natural cork stoppers, cork permeability

The contact between wine and oxygen is of critical importance for wine conservation and bottle aging processes, during which wine characteristics evolve toward the appearance of developed characters (Godden et al. 2005). Wine postbottling development is complex: red wines benefit from a small degree of oxygenation as it contributes to color stabilization, astringency reduction, and aroma improvement (Lopes et al. 2005, Silva et al. 2011); white wines are less resistant to oxygen, leading to oxidative off-flavors and browning that reduce wine quality (Escudero et al. 2002, Karbowiak et al. 2010). However, a tight sealing and lack of oxygen can also lead to negative sensory attributes (Karbowiak et al. 2010).

The closure is the most obvious factor that influences in-bottle wine development. The main function of a closure is to ensure an appropriate seal, preventing liquid leakage and sensory deterioration during storage. The sealing performance of closures is strictly related to their permeability properties that are commonly used for evaluating their barrier efficiency (Godden et al. 2005, Karbowiak et al. 2010). Exposure to oxygen of bottled wines is usually low but can be variable depending, primarily, on the amount of oxygen in the headspace at bottling, the oxygen permeability of the bottle closure, and the storage conditions (Caillé et al. 2010, Mas et al. 2002, Lopes et al. 2005, 2006, Kontoudakis et al. 2008, Silva et al. 2011).

Cork is a cellular material with chemical inertia and a set of physical and mechanical properties that allow its use as a sealant (Fortes et al. 2004, Pereira 2007). Several studies have compared the oxygen permeability performance of different closure systems. The permeability to oxygen of natural cork stoppers decreased along time during a 36-month wine storage experiment, totaling 2.43 and 3.29 mg of oxygen for cork stoppers of two visual quality grades (Lopes et al. 2006). Technical cork stoppers (agglomerated cork topped by two discs of natural cork) allowed ingress of 1.0 to 1.2 mg of oxygen over 36 months, with low and constant rates 0.003 mg O_2/month (2 to 36 months). After 36 months postbottling, natural cork stoppers reached a mean permeation of 9.33 mg O_2/stopper/year and Altec technical closures reached 0.52 mg O_2/stopper/year (Godden et al. 2005). Screwcaps were the closures least permeable to oxygen (Godden et al. 2005). Synthetic stoppers were the least successful barriers to oxygen, reaching a mean oxygen ingress of 1.60 mg O_2 in the first month (Lopes et al. 2005). Despite their lower permeability to oxygen, chemical and sensory analyses showed that oxidation developed faster with plastic stoppers and metal screwcaps (Mas et al. 2002).

Several studies have focused on the mechanisms and main routes of oxygen ingress through closures. Lopes et al. (2007) found no significant differences in the oxygen ingress rates of cork-stopped bottles when comparing uncovered, interface-covered, and fully covered natural cork stoppers, suggesting that oxygen diffuses mainly out of the cork into the wine due to the high pressure in the cork cells. The high internal pressure (from 0.6 to 0.9 MPa) created when natural cork

[1]Centro de Estudos Florestais, Instituto Superior de Agronomia, Universidade Técnica de Lisboa, Tapada da Ajuda, P-1349-017 Lisboa, Portugal; and [2]Amorim & Irmãos, R&D Department, Rua de Meladas 380, P.O. Box 20, Mozelos, 4536-902, Portugal.

*Corresponding author (email: vandaoliveira@isa.utl.pt; tel: +351 213653491; fax: +351 213645000)

Acknowledgments: This work was supported by FEDER funds through the Operational Programme for Competitiveness Factors–COMPETE and by National Funds under the project FCOMP-01-0124-FEDER-005421. Centro de Estudos Florestais is a research unit supported by national funding from Fundação para a Ciência e Tecnologia (PEst-OE/AGR/UI0239/2011). The first author acknowledges a scholarship from FCT.

Publication costs for this article defrayed in part by page fees.

Manuscript submitted Jan 2013, revised Apr 2013, accepted May 2013

doi: 10.5344/ajev.2013.13009

stoppers are compressed into the bottleneck could force air out of the cork structure, preferentially during the first 12 months (Fortes et al. 2004, Lopes et al. 2007). In a recent study, Faria et al. (2011) investigated the permeability of gases through uncompressed cork and suggested that the gas transport mechanism occurs through minute channels present in the cork cell walls, the plasmodesmata that cross the wall and have a diameter of ~0.1 µm (Teixeira and Pereira 2009). The transfer of oxygen in raw cork may be essentially controlled by a mechanism of diffusion through the cork cell walls (Lequin et al. 2012).

The studies related to oxygen permeability in natural cork stoppers were primarily designed to compare different closure systems or storage positions and the samplings were limited in the number of replicates tested for each type of closure. For example, one study had a design with only four replicates of each natural cork commercial quality (Lopes et al. 2006) and another had 12 cork stoppers per reference class (Godden et al. 2005).

The natural variability of cork in terms of oxygen permeability has therefore not been adequately measured. Here we studied the kinetics of oxygen ingress into bottles closed with natural cork stoppers over 12 months using a large sample of stoppers encompassing the natural variability and a non-destructive colorimetric method (as described in Lopes et al. 2005). We analyzed natural cork stoppers from different quality classes and originating from cork planks of different calipers. The experimental set-up and measurement conditions were rigorously maintained to allow a broad confidence in the results.

Materials and Methods

Chemicals. Deionized water was purified with a Milli-Q water system (Millipore, Bedford, MA) prior to use. Indigo carmine was purchased from Merck (Darmstadt, Germany). Sodium dithionite and sodium benzoate were obtained from Merck and Sigma Aldrich (St Louis, MO), respectively.

Closures. A total of 600 natural cork stoppers (24 mm diameter x 45 mm length; supplied by Amorim & Irmãos, S.A., Santa Maria de Lamas, Portugal) were selected: 300 stoppers were punched out from cork planks of 27–32 mm caliper and 300 stoppers from cork planks of 45–54 mm caliper. The stoppers were randomly sampled from the production line after grading by an automated vision system, subsequently inspected by skilled operators and graded into three final reference quality classes: premium, good, and standard. From each class, 100 stoppers were taken before washing and surface treatment. The stoppers were used for the closure of bottles for oxygen ingress measurements. During the process seven bottles were lost and therefore measurements were taken from 593 bottles.

Bottles. Extra-white (colorless) bordelaise classic bottles (375 mL) were used for cylindrical closures. The bottleneck dimensions complied with the CETIE specifications: 18–19 mm diameter at a depth of 3 mm and 19–21 mm diameter at a depth of 45 mm from the bottle entrance. All bottles were supplied by Saint-Gobain Glass Packaging (Cognac, France). A calibration bottle (without bottleneck) was developed to allow the calibration procedure. This bottle had exactly the same dimensions, volume capacity, and glass thickness as the extra-white bordelaise classic bottles (375 mL). The bottle used for calibration was purchased from Atelier Jean Prémon (Bordeaux, France).

Method calibration procedure. The procedure for reduction and oxidation of indigo carmine solution in the calibration bottle is described in Lopes et al. (2005). In the current study, the procedure was adapted by adding sodium dithionate in a controlled excess in order to reduce the indigo carmine and consume some amount of oxygen (which led to a color change from blue indigo to yellow). This excess of sodium dithionate was predetermined to correspond to the necessary amount to consume the oxygen that enters into bottle due to the bottling operation (1.4 to 1.9 mg). For calibration, controlled amounts of oxygen were injected 28 different times into the reduced indigo carmine bottled solution. Until 1.9 mg of oxygen, the color solution did not change since the oxygen was being consumed by the excess of dithionate. Once the excess of sodium dithionate was consumed, the reduced indigo carmine began to consume the oxygen, resulting in a color change to the original indigo blue of the carmine. Color changes were measured with a colorimeter apparatus. Each point of the calibration curve was obtained by calculating the mean of five replicates. The calibration curve is valid up to a maximal limit of oxygen quantification of 5.7 mg, the amount necessary to fully oxidize the excess of sodium dithionate and to reduce the indigo carmine.

Bottling and storage. For the bottling trials, 600 sterilized commercial bottles with 375 mL were used. These bottles were filled with indigo carmine solution that was reduced with 20 mL sodium dithionite solution (2.9 g/L). Bottles were then sealed with different closures using a single-head corker (Bertolaso Epsilon R/S, Zimella, Italy). All closures were compressed to 16 mm diameter before insertion under vacuum into bottles. At 2 hours after bottling, the internal pressure values were 0 bar. These measurements were carried out in 30 bottles especially prepared for this purpose using a pressure gauge. The final filling level for each bottle was 65 ± 3 mm from the top of the bottle. The temperature of the indigo carmine solution ranged from 17.2 to 21.1°C. All bottles were left upright for 24 hr after bottling and then stored horizontally over 12 months. All bottles were stored under room conditions where temperature varied from 13.6 to 27.8°C.

Bottle colorimetric measurements. The CIELab measurements of the parameters L*, a*, b* were performed by directly scanning the bottled solutions with a Minolta series CM-508i spectrocolorimeter equipped with a transmittance accessory CM-A76 (Osaka, Japan). These measurements were obtained using illuminant D65 and a 10° observer according to CIELab 76 (McLaren 1980). A clean Pyrex bottle filled with water was used to carry out autozero calibration (blank). All bottles were cleaned with ethanol and dried before CIELab measurements. These measurements were carried out in the upright position at 5 cm from the base of the

bottle. Four body measurements were collected by rotating each bottle 90° on its vertical axis. All positions were marked on the bottleneck to allow consistent measurement over time. All measurements were made in the dark at room temperature (18 ± 4°C).

Calculation of oxygen ingress. The calculation of the oxygen ingress into the bottle after closure with the cork stopper was made by deducting the oxygen that was already present in the bottle headspace to the values obtained by the colorimetric measurement. This means that the value of 1.50 mg of oxygen (present in the bottle headspace due to the bottling process) was withdrawn from all measurements, corresponding to the assumption of the rapid and total consumption of this oxygen by the indigo carmine (the bottles were shaken immediately after bottling and before each color measurement). Therefore the oxygen ingress was set at zero at time 0. The limit of oxygen measurement by the method was reached at 4.2 mg of oxygen. This value corresponds to the amount of oxygen that the method had the capacity to consume after the oxygen introduced due to bottling. Oxygen ingress rates were calculated on a daily (µg/day) and monthly (mg/month) basis.

For data analysis the natural cork stoppers were clustered into five oxygen ingress classes in function of the total oxygen measured at 12 months: class 1 comprised the stoppers for which the total oxygen measured in the bottle at 12 months was <1.4 mg; classes 2 and 3 comprised the stoppers with total oxygen at 12 months between 1.4 and 2.9 mg and between 2.9 and 4.2 mg, respectively; class 4 comprised the stoppers for which the limit of oxygen quantification (4.2 mg) was reached after the fourth month and class 5 comprised those that reached that limit before the fourth month. The clustering was done following the authors' choice without statistical procedures but ensuring that the distribution of the number of stoppers was approximately the same in the different oxygen ingress classes.

Data analysis. Microsoft Excel 2000 software was used for data analysis. All statistical analyses, namely, the analysis of variance (two-way ANOVA) were performed using SPSS statistical software (ver. 19.0; SPSS Inc., Chicago, IL).

Results

As noted above, the natural cork stoppers were clustered into five oxygen ingress classes in terms of the total oxygen measured at 12 months in order to simplify the data analysis. Twenty-one percent of the total cork stoppers reached the limit of oxygen quantification along the experiment and were assigned to oxygen classes 4 (11%) and 5 (10%). Classes 1, 2, and 3 included 23%, 32%, and 24%, respectively, of the total sample of cork stoppers.

The kinetics of oxygen ingress during the 12 months of storage clustered by cork plank caliper and oxygen class (1, 2, and 3 oxygen classes) of stoppers was determined (Figure 1). Despite the wide variability between stoppers (the coefficient of variation of the mean was 67% and 49% for the oxygen ingress measured at 5 and 360 days, respectively), a common behavior along time was found corresponding to a logarithmic kinetics of oxygen ingress with time. There was rapid and high oxygen ingress in the first days after bottling, with an initial high ingress rate, followed by decreasing ingress rates until the first month and further on, until stabilizing a low and rather constant ingress rate from the third to twelfth months. On average, 35% of the overall ingress of oxygen occurred in the first five days, 59% in the first month, and 78% in the first three months.

The kinetics models were all similar corresponding to logarithmic curves and differing mainly on their position on the y axis. For instance, on average, the oxygen ingress after 90 days was 0.77 mg, 1.50 mg, and 2.66 mg for classes 1, 2, and 3, respectively, and at the end of the 360 days, it was 0.99 mg, 1.92 mg, and 3.44 mg, respectively. Differences in bottle oxygen ingress were found for the three oxygen classes between the cork stoppers punched out from cork planks of different calipers. On average, the cork stoppers from the thicker caliper had a higher oxygen ingress of 3% (for class 1) and 8% (for classes 2 and 3) than the corks from the thinner caliper.

The evolution over time of the total oxygen ingress into the bottle averaged for the stoppers obtained from cork planks of the two calipers and the three reference quality classes is shown (Table 1). In these calculations, we only considered the stoppers that did not reach the limit of oxygen quantification within the 12 months. The two-way ANOVA of oxygen ingress indicated significant differences between cork stoppers of the two caliper thicknesses ($p = 0.00$) but no interaction between cork plank caliper and stopper quality class. For each cork plank caliper, the differences between quality classes had a low statistical significance ($p = 0.04$) and no between-class trend was found.

There were cork stoppers that reached the limit of oxygen quantification for the colorimetric method within 12 months (Figure 2). Within the 360 days of storage, 25% of the cork stoppers from the thicker caliper and 17% of the stoppers from the thinner caliper had reached the limit of oxygen quantification (6% and 15% of the stoppers, respectively, within 120 days).

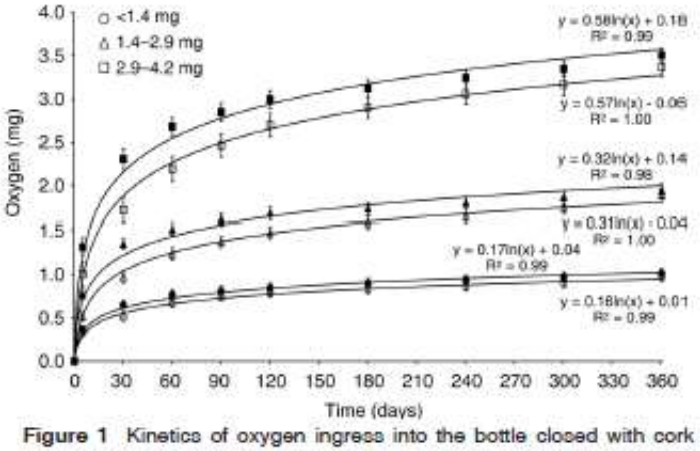

Figure 1 Kinetics of oxygen ingress into the bottle closed with cork stoppers of three oxygen classes divided into cork plank calipers (open symbols represent stoppers from 27–32 mm cork planks and filled symbols represent stoppers from 45–54 mm cork planks). Error bars represent the 95% confidence interval for the mean.

Table 1 Evolution in time of total oxygen ingress (mg) into the bottle closed with the natural cork stoppers grouped by cork plank caliper (27–32 mm and 45–54 mm) and reference quality classes (premium, good, and standard) after different periods of time (5 days, 1, 3, 6, and 12 months) and considering the oxygen classes 1 to 3 (n = 467). Parentheses enclose standard deviations.

	5 days	1 month	3 months	6 months	12 months
27–32 mm caliper	0.56 (0.41)	0.97 (0.60)	1.39 (0.76)	1.60 (0.87)	1.88 (0.99)
Premium	0.63 (0.44)	1.03 (0.59)	1.52 (0.76)	1.74 (0.87)	2.04 (0.95)
Good	0.49 (0.38)	0.90 (0.54)	1.32 (0.70)	1.53 (0.82)	1.76 (0.94)
Standard	0.55 (0.39)	0.97 (0.65)	1.32 (0.79)	1.55 (0.91)	1.85 (1.07)
45–54 mm caliper	0.90 (0.50)	1.58 (0.74)	1.92 (0.86)	2.10 (0.93)	2.35 (1.02)
Premium	0.92 (0.53)	1.72 (0.71)	2.06 (0.81)	2.26 (0.89)	2.46 (0.94)
Good	0.92 (0.53)	1.50 (0.77)	1.71 (0.85)	1.89 (0.92)	2.17 (1.06)
Standard	0.87 (0.46)	1.53 (0.72)	2.03 (0.88)	2.16 (0.94)	2.43 (1.04)

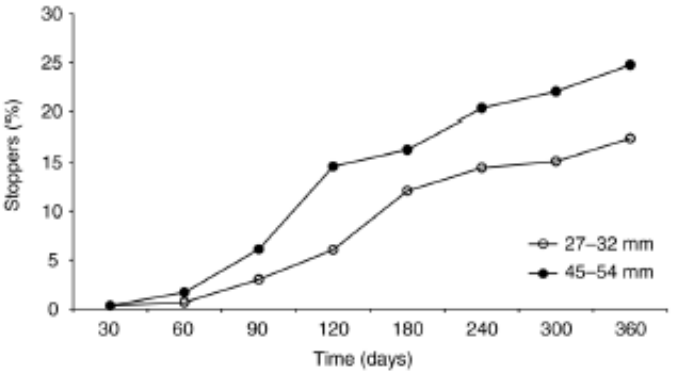

Figure 2 Percentage of natural cork stoppers from the two cork plank calipers that reached the limit of oxygen quantification.

Table 2 Oxygen ingress rates (µg/day) into the bottle closed with cork stoppers of each oxygen class (1 to 5) during 12 months.

	Oxygen class					
Time	**1**	**2**	**3**	**4**	**5**	**Total**
0–5 days	68.02	130.25	236.61	287.39	420.96	188.19
5–30 days	8.19	20.70	35.29	41.26	57.04	27.25
Month 1	18.16	38.96	68.84	82.28	117.70	54.07
Month 2	5.05	7.07	13.76	20.57	13.19	10.29
Month 3	2.18	4.06	7.00	11.65	10.43	5.75
Month 4	1.39	2.77	6.12	8.85	12.84	4.57
Months 4–12	0.76	1.38	2.41	5.48	–	2.51

Results confirmed that the oxygen ingress rate of natural cork stoppers depends on time (Table 2), as stated previously by Lopes et al. (2006). The rates of oxygen ingress in the first month of storage were statistically different (p = 0.00) than the rates from the second until the twelfth month, independently of the oxygen class considered. The oxygen ingress rates in the first month were 18.16 and 68.84 µg/day for classes 1 and 3, respectively. The average oxygen ingress rates after the fourth month of storage were 0.76, 1.38, and 2.41 µg/day, respectively, for classes 1, 2, and 3.

Discussion

In order to understand and explain the variability found in oxygen ingress into the bottle, it is necessary to analyze the cork cell structure and the amount of oxygen contained therein, as oxygen ingress occurs mainly out of the cork due to the high internal pressure in the cork cells created when the cork stoppers are compressed into the bottleneck (Ribéreau-Gayon 1933). Natural cork stoppers with 24 mm diameter x 45 mm length have a volume of 20.4 mL, of which 80 to 85% is air contained in the cell lumen, implying 4.9 to 5.2 mg (3.4–3.6 mL) of oxygen within their structure (Fortes et al. 2004). Therefore, the average oxygen ingress into the wine bottles (Figure 1), in relation to the theoretically estimated total oxygen within the stoppers, represented 27 to 29% (1.0 mL, or 1.43 mg) in the first month of storage, and 42 to 45% (1.5 mL, or 2.15 mg) at the end of the 12-month storage.

There are no published data relating the thickness of the cork planks and the quality and permeability to oxygen of cork stoppers produced from them. Cork planks with thicker calipers have larger growth rings than thinner cork planks, and they also differ in the proportion of the earlycork and latecork cells, since the number of latecork cells in a radial row is independent of the cork ring width (Pereira et al. 1992). Earlycork cells are larger than latecork cells and have thinner cell walls, and consequently they differ in their lumen empty (air-filled) volume: approximately 91 to 92% in the earlycork region and 78 to 85% in the latecork region (Pereira 2007). The average cell prism height (radial direction) was 22% higher in the cells of larger growth rings (Pereira et al. 1992). Therefore, cork planks with thinner caliper have a higher proportion of smaller cells with thicker cell walls, and less air-filled empty volume which increases the barrier to the diffusion of gases, explaining the significant differences found in oxygen ingress of the stoppers produced from the thinner and thicker calipers (Table 1, Figure 1). Our results show that, on average, 1.88 mg and 2.35 mg of oxygen diffuses from natural cork stoppers from 27–32 mm and 45–54 mm calipers, respectively (Table 1), representing 36 to 38% and 47 to 50% of the theoretically total oxygen in the cell structure. These results are in agreement with others (Faria et al. 2011), who noted that samples from thinner planks on average permeate less than those from thicker planks.

The results showed no significant correlations between the reference quality classes and the oxygen ingress (Table 1). These results are in accordance with others (Lopes et al.

2005), who found no significant differences in the overall oxygen diffusion of stoppers of different quality.

The occurrences of structural discontinuities, like lenticular channels or woody inclusions, which may cause variation in the mechanical properties of cork, eventually explain this higher oxygen ingress. The cork stoppers from thicker caliper reached the limit of oxygen quantification in higher number and earlier than the cork stoppers from thinner caliper (Figure 2). The thickness of the cork plank is also a factor of mechanical behavior variation, with larger caliper planks showing lower strength in compression for all strains (Pereira et al. 1992).

Independently of the oxygen class of the stoppers, the oxygen ingress rates were higher in the first month of storage, and particularly high in the first days after bottling, decreased thereafter, and stabilized at rather constant values after 3 months (Figure 1), suggesting a decrease in the permeability of the cork closure over time (Karbowiak et al. 2010). The higher air pressure within the cells due to the compression of the stopper in the bottleneck certainly will increase ingress rates immediately after bottling as oxygen ingress progresses, the pressure decreases and so the ingress rates, until reaching a rather constant value.

The rates of oxygen ingress found for the cork stoppers of oxygen classes 1, 2, and 3 (Table 2) are within the range and exhibit similar trends to those reported by Lopes et al. (2006), who published values of 35.8 to 64.6 µg/day (25 to 45 µL/day) in the first month and ranging from 2.43 to 8.73 µg/day (1.7 to 6.1 µL/day) from the second to twelfth months for the bottles stored horizontally. For natural cork stoppers, Godden et al. (2005) reported a mean oxygen permeation of 25.6 µg/day (17.9 µL/day), with a range from 0.1 to 175.7 µg/day (0.1 to 122.7 µL/day), tested after ~36 months postbottling.

Conclusion

The variability of oxygen ingress into the bottle closed with the cork stoppers led us to classify the stoppers in oxygen ingress classes. The kinetics of oxygen ingress was similar regardless of the oxygen class and could be adjusted to similar logarithmic models with high statistical significance. The results suggest that this variation of oxygen ingress is a consequence of the natural differing features in the cell dimensions and air volume within the stopper's structure.

Literature Cited

Caillé, S., A. Samson, J. Wirth, J.B. Diéval, S. Vidal, and V. Cheynier. 2010. Sensory characteristics changes of red Grenache wines submitted to different oxygen exposures pre and post bottling. Anal. Chim. Acta. 660:35-42.

Escudero, A., E. Asensio, J. Cacho, and V. Ferreira. 2002. Sensory and chemical changes of young white wines stored under oxygen. An assessment of the role played by aldehydes and some other important odorants. Food Chem. 77:325-331.

Faria, D.P., A.L. Fonseca, H. Pereira, and O.M.N.D. Teodoro. 2011. Permeability of cork to gases. J. Agric. Food Chem. 59:3590-3597.

Fortes, M.A., M.E. Rosa, and H. Pereira. 2004. A Cortiça. IST Press, Lisbon, Portugal.

Godden, P., et al. 2005. Towards offering wine to the consumer in optimal condition–The wine, the closures and other packaging variables. A review of AWRI research examining the changes that occur in wine after bottling. Wine Ind. J. 20:20-30.

Karbowiak, T., R.D. Gougeon, J.B. Alinc, L. Brachais, F. Debeaufort, A. Voilley, and D. Chassagne. 2010. Wine oxidation and the role of cork. CRC Crit. Rev. Food Sci. Nutr. 50:20-52.

Kontoudakis, K., P. Biosca, R. Canals, F. Fort, J.M. Canals, and F. Zamora. 2008. Impact of stopper type on oxygen ingress during wine bottling when using an inert gas cover. Aust. J. Grape Wine Res.14:116-122.

Lequin, S., D. Chassagne, T. Karbowiak, J.M. Simon, C. Paulin, and J.P. Bellat. 2012. Diffusion of oxygen in cork. J. Agric. Food Chem. 60:3348-3356.

Lopes, P., C. Saucier, and Y. Glories. 2005. Nondestructive colorimetric method to determine the oxygen diffusion rate through closures used in winemaking. J. Agric. Food Chem. 53:6967-6973.

Lopes, P., C. Saucier, P.L. Teissedre, and Y. Glories. 2006. Impact of storage position on oxygen ingress through different closures into wine bottles. J. Agric. Food Chem. 54:6741-6746.

Lopes, P., C. Saucier, P.L. Teissedre, and Y. Glories. 2007. Main routes of oxygen ingress through different closures into wine bottles. J. Agric. Food Chem. 55:5167-5170.

Mas, A., J. Puig, N. Lladó, and F. Zamora. 2002. Sealing and storage position effects on wine evolution. J. Food Sci. 67:1374-1378.

McLaren, K. 1980. Food colorimetry. *In* Developments in Food Colors. J. Walford (ed.), pp. 27-45. Applied Science Publishers, London.

Pereira, H. 2007. Cork: Biology, Production and Uses. Elsevier, Amsterdam.

Pereira, H., J. Graça, and C. Baptista. 1992. The effect of growth rate on the structure and compressive properties of cork. IAWA Bull. 13:389-396.

Ribéreau-Gayon, J. 1933. Dissolution d'oxygène dans les vins. *In* Contribution à l'étude des oxidations et réductions dans les vins. Application à l'étude de vieillissement et des cases. Delmas, Bordeaux.

Silva, M.A., M. Julien, M. Jourdes, and P.L. Teissedre. 2011. Impact of closures on wine post-bottling development: A review. Eur. Food Res. Technol. 233:905-914.

Teixeira, R.T., and H. Pereira. 2009. Ultrastructural observations reveal the presence of channels between cork cells. Microsc. Microanal. 15:1-6.

PUBLICATION IV.
CORK STRUCTURAL DISCONTINUITIES STUDIED WITH X-RAY MICROTOMOGRAPHY

Vanda Oliveira*, Jan Van den Bulcke, Joris Van Acker, Thomas de Schryver and Helena Pereira

Cork structural discontinuities studied with X-ray microtomography

Abstract: Cork is a natural cellular material with a rather unique set of properties, and its best known application is as stopper for wine bottles. The cork tissue contains structural discontinuities, for example, lenticular channels (LCh), that influence the in-use performance of cork products. X-ray microtomography, in combination with image analysis, has been used for cork characterisation and provided new insights into the three-dimensional location of discontinuities, which are hidden for a visual inspection. It was demonstrated that the presence of LCh is positively correlated with cork density, and the void fraction of LCh in the lower part of a cork stopper is strongly related to the oxygen ingress in the bottle during the first month after bottling. The results contribute to better understanding the natural variation of cork properties.

Keywords: cork, image processing, lenticular channels, natural cork stoppers, structural discontinuities, X-ray microtomography

DOI 10.1515/hf-2014-0245
Received September 9, 2014; accepted December 12, 2014; previously published online xx

Introduction

Cork is produced from the bark of *Quercus suber* L. Its properties as a lightweight material are unique. For example, it is viscoelastic and allows large deformation under compression without fracture, largely impermeable to water and other liquids and gases, a thermal and electric insulator, and an acoustic and vibration absorber (Fortes et al. 2004; Pereira 2007). Cork is best known as a successful bottle closure since ancient times (Pereira 2007) and is still the most popular closure, especially for long-term aging of red wines (Phillips 2014).

The cork tissue has a honeycomb structure with a considerable regularity in the cellular arrangement: the cells are closed and noncommunicating, with thin walls that surround an air-filled lumen; the cell volume is, on average, 1.7×10^{-5} mm^3, and its solid content is around 13.5%. However, the tissue contains discontinuities that influence the in-use performance of cork products and are thereby closely associated with the commercial value of raw cork and of cork products (Pereira 2007). Lenticular channels (LChs) are the most important features in this context: they cross the cork layers from the outside to the inner tissue and are loosely filled with a dark brown, unsuberified material, usually conspicuous to visual observation (Pereira et al. 1996; Oliveira et al. 2012). Other discontinuities can have an accidental occurrence, such as the galleries made by the larva of *Coroebus undatus* or by the ant *Crematogaster scutellaris* (Gonzalez-Adrados and Pereira 1996; Pereira 2007).

X-ray imaging in its two-dimensional (2D) form is widely used in wood science for microdensitometry studies (Ikonen et al. 2008; Boden et al. 2010; Helama et al. 2012; Knapic et al. 2014). X-ray tomography is a nondestructive 3D imaging technique that allows the study of interior structures of an object (Landis and Keane 2010). Industrial X-ray tomography scanners are successful for determination of wood properties in terms of internal log features such as pith, growth rings, heartwood and sapwood, knots, and decay (Wei et al. 2011; Longuetaud et al. 2012).

X-ray microtomography (XRMT) has a higher spatial resolution and has been proved to be of value in different fields such as biomedicine (Kim et al. 2014), geoscience (Cnudde and Boone 2013), and material science (Dewanckele et al. 2012; Česen et al. 2013). In wood science, 3D XRMT was employed to study the shrinkage behaviour of cells (Taylor et al. 2013), the analysis of coatings (Van den Bulcke et al. 2010; Bessières et al. 2013), the compressive

*Corresponding author: Vanda Oliveira, Universidade de Lisboa, Instituto Superior de Agronomia, Centro de Estudos Florestais (CEF), Tapada da Ajuda, P-1349-017 Lisboa, Portugal,
e-mail: vandaoliveira@isa.ulisboa.pt.
http://orcid.org/0000-0003-3461-7028
Jan Van den Bulcke and Joris Van Acker: UGCT-Woodlab-UGent, Faculty of Bioscience Engineering, Department of Forest and Water Management, Ghent University, Coupure Links 653, 9000 Ghent, Belgium
Thomas de Schryver: UGCT, Centre for X-ray Tomography, Department of Physics and Astronomy, University Ghent, Proeftuinstraat 86, 9000 Ghent, Belgium
Helena Pereira: Universidade de Lisboa, Instituto Superior de Agronomia, Centro de Estudos Florestais (CEF), Tapada da Ajuda, P-1349-017 Lisboa, Portugal. http://orcid.org/0000-0002-5393-4443

behaviour of low-density fibreboard (Tran et al. 2013), wood anatomical details (Van den Bulcke et al. 2009), the pore structure of paper (Axelsson and Svensson 2010), wood composites (Wieland et al. 2013), and dendrochronology (Van den Bulcke et al. 2013).

XRMT was not yet applied for cork characterisation, which is usually performed by image analysis of the surface, in the course of which the internal discontinuities remain concealed (Pereira et al. 1996). Brunetti et al. (2002) applied Compton tomography in the study of cork stopper density to refine the visual classification. Hor et al. (2008) evaluated and imaged natural cork by means of terahertz spectroscopy. Donepudi et al. (2010) visualised images of cork stoppers with a novel imaging technology, called diffraction-enhanced imaging.

The present work explores XRMT for the visualisation and quantification of cork structural discontinuities. These discontinuities are decisive for the commercial value of raw cork and of cork products as they are a possible pathway for air, impregnation liquids and microbial penetration. The expectation is that XRMT may contribute to a better understanding of the natural variation in cork (Oliveira et al. 2013) and that it can contribute to the development of an improved monitoring of its key features in terms of an increased quality of existing cork products as well as to the design of new products.

Materials and methods

Ten natural cork stoppers (24 mm diameter×45 mm length) were selected, produced in one major Portuguese cork producer before washing and surface treatment. The stoppers were punched out from cork planks and classified in three visual quality classes (premium, good, and standard). Their surface (lateral and top surface) was imaged with photographic equipment and subsequently processed by image analysis according to the procedure of Oliveira et al. (2012). The objects that can be visualised with adequate thresholding (in general, called cork pores) can be individually characterised quantitatively. The porosity coefficient (%), defined as the proportion of the area occupied by pores, was calculated (Oliveira et al. 2012).

Then, bottles were closed by the stoppers and oxygen ingress measurements were performed using a nondestructive colorimetric method, by which oxidation was detected by means of an indigo carmine solution (Oliveira et al. 2013). The total amount of oxygen that had reached the interior of the bottle 30 days after closure was taken as a key feature, as it is an indicator for the quick and high oxygen ingress in the first days after bottling.

An XRMT instrument built at the Centre for X-ray Computed Tomography (UGCT, Ghent University, Belgium; www.ugct.ugent.be) was applied. The scanner used at Woodlab-UGent, further referred to as Nanowood, is specifically designed to obtain very high resolution scans as well as scans of larger objects. The instrument is equipped with a generic in-house developed computed tomography scanner control software platform (Dierick et al. 2010) that allows full control of the scanner hardware (see Dierick et al. 2014). For all stoppers, a total of 900 projections were acquired over an angle of 360°. All stoppers were reconstructed using Octopus 8.6, a server/client tomography reconstruction package for parallel and cone beam geometry (Vlassenbroeck et al. 2007), resulting in a voxel size of 50 µm for a scan covering the entire stopper.

Image processing and analysis were performed using the Fiji image processing package (Schindelin et al. 2012) and Morpho+ (Vlassenbroeck et al. 2007; Brabant et al. 2011), aiming at noise removal, image enhancement, and feature extraction. Morpho+ was used in combination with a bilateral filter (nonlinear, edge-preserving, and noise-reducing smoothing filter) to perform histogram equalisation for contrast improvement.

A circular region of interest was manually selected within each stack, which is representative for the transverse (Tv) cork stopper section. Segmentation was performed by means of an automated thresholding based on the isodata algorithm (Ridler and Calvard 1978). A single threshold level was selected for pores and another one for high-density regions (HDRs) through the entire volume. When focusing on the void fraction, every data point was assigned to either background (solid material) or foreground (voids), and the closing mathematical morphology operator was applied to the binary images to fill misclassified pixels inside the pores as well as to maintain pore connections.

The void volume was calculated using the "3D Object Counter" plugin (Bolte and Cordelières 2006). The 3D void fraction coefficient was calculated by dividing the total volume of voids by the volume of interest. The same analysis was done for the 3D characterisation of HDR.

Data analysis was performed using Microsoft Excel 2010. The results from the analysis of the X-ray volumes were compared with data from previous measurements of surface image analysis, density, and oxygen ingress. All statistical correlation and regression analyses were performed by means of the SPSS statistical software (version 22.0; SPSS Inc., Chicago, IL).

Results and discussion

Visual observation of cork structural discontinuities

Different materials can be distinguished by XRMT based on their differences in X-ray absorption coefficient at each point and due to the relationship of these data to material density. The 3D internal structure of cork can also be inferred, which is typically displayed as a series of 2D "slices," and LChs can be visualised in different sections. Figure 1A illustrates different sections in the three orthogonal planes, i.e., in tangential (Tg), radial (R), and Tv directions. The anisotropy of LCh is clearly observable, which is closely related to their biological development within the corkboard and the orientation

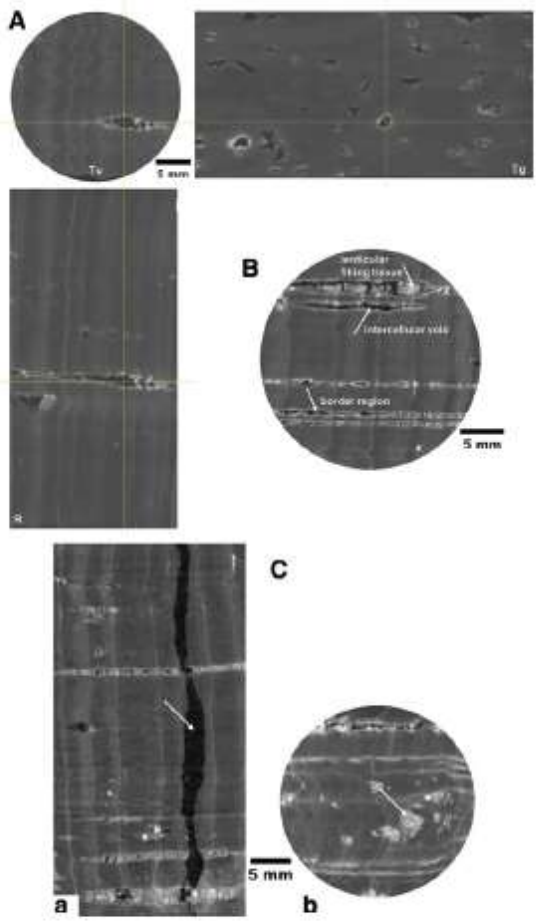

Figure 1 (A) Typical 2D "slices" from a 3D greyscale image of a cork stopper scanned at 50 µm resolution.
Different sections through the cork stopper in three orthogonal planes: Tv, R, and Tg. Crossing lines represent the same point in the three images. (B) Tv greyscale image with identification of lenticular filling tissue, intracellular voids and the border region of the LChs. And (C) Defects in the cork structure: (a) empty ant gallery and (b) "nail" lignocellulosic inclusion.

of the cutting process during stopper production (Pereira 2007). LChs have a tubular form, and in Tv and R planes, they appear as linear strands. In each slice, only parts of the channels are observed (Figure 1A) because the Tv plane does not coincide with the LCh development axis. However, the full development of the LCh can be well observed in the orthogonal R plane, while in the Tg slices, the LChs are sectioned perpendicularly to their axis and look rounded. These observations can be compared with the surface seen by image analysis of the main sections of cork planks (Pereira et al. 1996; Gonzalez-Adrados et al. 2000) and of cork stoppers (Oliveira et al. 2012).

The observed geometry of the LCh certainly impacts the cork properties for applications where bending properties are of importance (Anjos et al. 2011a). Figure 1B corroborates that LChs are loosely filled with a tissue of rigid unsuberified cells with thick walls, showing ruptures and intercellular voids in a great extent (Pereira 2007). It is also visible that the region bordering the LCh has higher density than the surrounding material does due to the presence of lignified and thick-walled cells at their borders (Figure 1B).

Additionally, cork may also contain features of biological or external origin that are classified as defects in practical application. Such features could also be observed by XRMT. As mentioned in the Introduction, *C. undatus* F. larvae and several species of ants that excavate galleries that run through the cork plank may be the origin of such defects. The larvae galleries are filled with residual material, while the ant galleries are usually empty and have a random direction. They can appear at the cork stopper surface only as a small hole, which may go unnoticed even to expert operators but cause wine leakage. Figure 1Ca shows the development from top-to-top of one of these empty ant galleries in a premium classified cork stopper.

Another possible defect is the inclusion of small portions of lignified cells within the cork tissue, referred to in the cork jargon as "nail". These cells have thick walls and a lignocellulosic chemical composition, and therefore, their density is well above the density of the surrounding cork tissue (Pereira 2007). Figure 1Cb shows these nail inclusions as HDRs. The above-mentioned defects can be scanned with an approximate voxel pitch of maximally 0.1 mm.

Quantitative analysis and 3D characterisation

Table 1 summarises the main features of the stoppers in focus. The stoppers (St) were selected to cover a wide range of properties: the lateral surface porosity coefficient ranged from 1.1% (St 2 and 4) to 8.6% (St 7); top surface porosity coefficient ranged from 0.7% (St 1) to 4.7% (St 7); density ranged from 152.0 kg m^{-3} (St 8) to 262.7 kg m^{-3} (St 7); total amount of oxygen ingress at 30 days ranged from 1.4 mg (Sts 1 and 7) to 4.0 mg (St 9).

Figure 2 illustrates the structure of internal cork discontinuities. By thresholding the voids and HDRs, the internal LCh network becomes observable. Figure 2a shows the surface of the cork St comparable to what image analysis could reveal by photography. Figure 2b shows the void fraction consisting mainly of intracellular voids, and

Table 1 Characterization of the natural cork stoppers: lateral and top surface porosity coefficient, density, and oxygen ingress at 30 days after bottling.

Stopper	Visual class	Porosity coeff. (lateral) (%)	Porosity coeff. (top) (%)	Density (kg m^{-3})	Oxygen ingress at 30 days (mg)
1	Premium	1.8	0.7	182.8	1.4
2	Premium	1.1	1.3	166.9	3.6
3	Premium	1.4	1.3	185.5	3.5
4	Premium	1.1	1.3	161.9	1.6
5	Good	3.9	3.1	227.8	2.5
6	Good	2.2	3.4	205.4	3.4
7	Standard	8.6	4.7	262.7	1.4
8	Standard	6.3	1.7	152.0	3.3
9	Standard	4.5	1.3	224.8	4.0
10	Standard	3.4	4.0	196.8	2.6

Figure 2c shows the void fraction (green) and the HDRs (red). It is noticeable that these HDRs preferably appear bordering the void fraction.

The quantification of 3D structural discontinuities is summarised in Table 2. For each St the following are presented: the void and HDR volume; the void fraction and the HDR fraction, defined as the proportion of the volume occupied by the void or HDR regions; the maximum void or HDR volume, defined as the largest single connected structure; and the porosity coefficient, calculated as the sum of the void and the HDR fractions. This XRMT porosity coefficient was calculated to establish the relation with image analysis measurements. In fact, image analysis of the cork St surface distinguishes the LCh by adequate thresholding but does not discriminate between voids and HDRs.

The void fraction ranged from 0.7% (St 4) to 2.3% (St 9), while the maximum single void volume ranged from 7.9 mm^3 (St 6) to 104.9 mm^3 (St 9). The total HDR volume ranged from 231 mm^3 (St 4) to 2747 mm^3 (St 7), corresponding to a HDR fraction of 1.3% and 19.2%, respectively. The high HDR volume of St 7 corresponds to a single connected structure measuring 2468 mm^3. The cork St 3 that was classified as a premium St (i.e., low porosity coefficient by image analysis and high visual quality) had one of the highest total void volume (404 mm^3).

Relating surface image analysis and XRMT

Quality classes of natural cork Sts depend on the apparent homogeneity of their external surface, as seen by human eye or machine vision (Fortes et al. 2004; Pereira 2007). The heterogeneity of the cork surface is given by the presence of LCh, woody inclusions, small fractures, or other defects that can be identified by image analysis and are referred to as the porosity of cork (Gonzalez-Adrados and Pereira 1996; Pereira et al. 1996). Figure 3a shows the correlation between the lateral surface porosity coefficient calculated by image analysis (Oliveira et al. 2012) and the interior porosity coefficient calculated using XRMT.

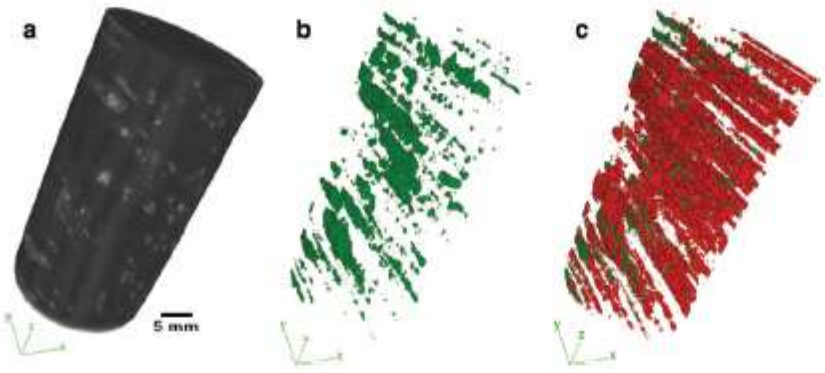

Figure 2 3D overview: (a) rendered volume of a cork stopper, (b) the void fraction of cork stopper structural discontinuities, and (c) cork stopper structural discontinuities colour coded: in red, the high density regions; and in green, the void fraction.

Table 2 Characterisation of 3D structural discontinuities of natural cork stoppers: voids and HDRs.

Stopper	Void volume (mm^3)	Void fraction (%)	Maximal void (mm^3)	HDR volume (mm^3)	HDR fraction (%)	Maximal HDR (mm^3)	Porosity coeff. (%)
1	159.9	0.9	62.6	512.9	3.0	208.8	3.9
2	176.8	0.8	22.1	328.1	1.6	39.0	2.4
3	403.8	1.8	86.9	829.6	3.7	48.6	5.5
4	127.4	0.7	21.2	231.0	1.3	20.3	2.0
5	217.7	1.1	23.5	1247.1	6.1	480.9	7.2
6	163.6	1.0	7.9	853.2	5.0	221.1	5.9
7	184.4	1.3	17.4	2747.0	19.2	2467.8	20.5
8	399.3	1.9	64.7	609.7	2.9	292.4	4.8
9	486.1	2.3	104.9	2406.7	11.5	1065.2	13.8
10	329.9	2.0	52.0	90.7	0.6	6.4	2.6

Because these two variables quantify porosity (LCh and other defects), a linear fit was used for data evaluation. Pearson's correlation analysis shows a positive linear relationship between the two data sets (r=0.78, R^2=0.61, and R_{adj}=0.56) (P<0.008). St 7 significantly influences this linear fit, which is an example for a high-porosity material due to woody inclusions. Nevertheless, the variability between the samples is evident in Figure 3a. For instance,

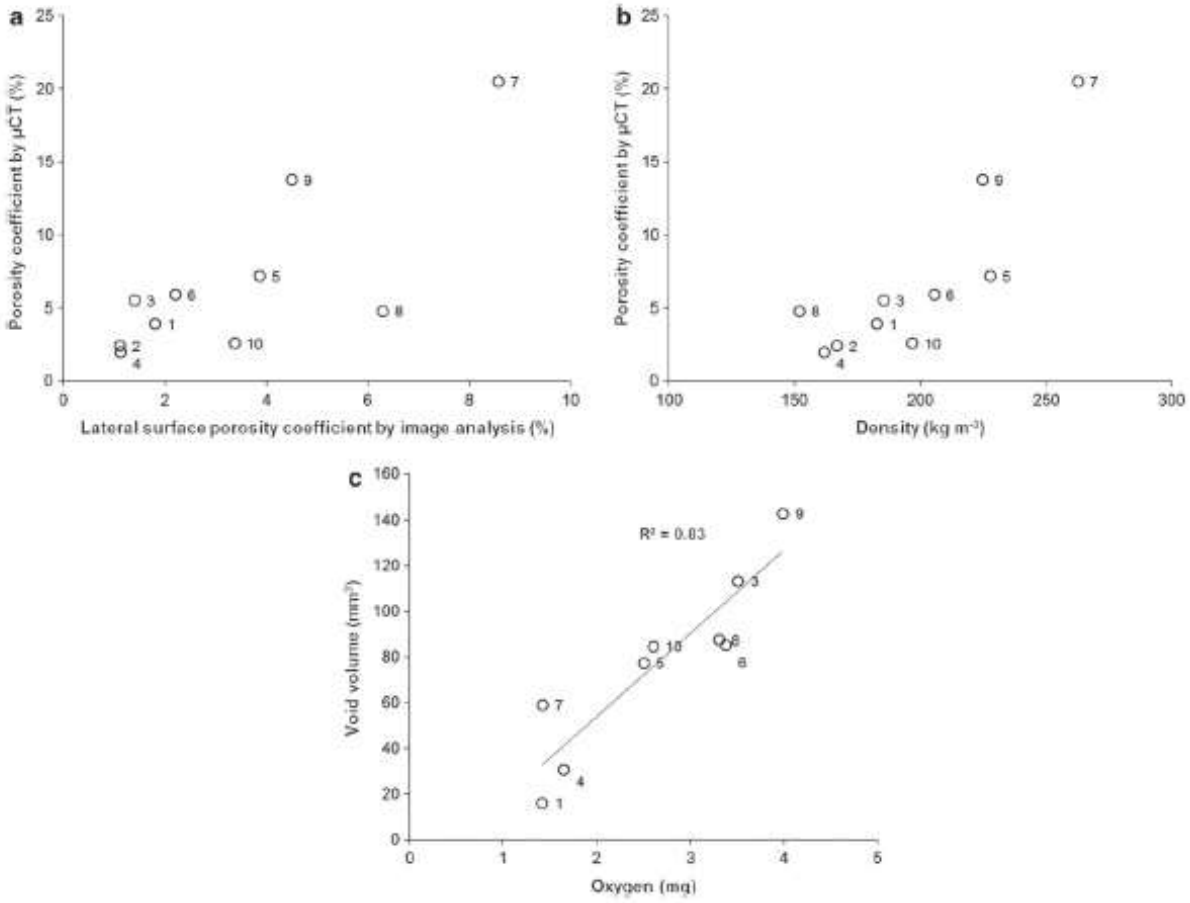

Figure 3 (a) Relation between the porosity coefficient calculated by image analysis and XRMT; (b) Relation between air-dried cork density and the porosity coefficient calculated by XRMT; and (c) Relation between the void volume in the bottom third part of the cork stopper and the oxygen ingress 30 days after bottling.

Sts 8 and 10, both classified as standard and with lateral surface porosity coefficient of 6.3% and 3.4%, respectively, have a smaller porosity coefficient calculated with XRMT (4.8% and 2.6% respectively), meaning that the interior of these cork Sts has less discontinuities than predicted by visual analysis of the surface. On the other hand, Sts 7 and 9, also classified as standard with lateral surface porosity coefficient of 8.6% and 4.5%, have 20.3% and 13.8% porosity coefficient calculated with XRMT due to the presence of nail regions. Accordingly, surface imaging and XRMT may give deviating results concerning LCh. Moreover, when considering the porosity coefficient calculated for the Tv section (top) by image analysis, the Pearson's correlation (r) is only 0.47 (R^2=0.22 and R_{adj}=0.12) (P<0.173).

Calculating the porosity coefficient by XRMT for all Tv slices of each St separately (to assess internal heterogeneity) resulted in an averaged coefficient of variation of 74%. This very high value corroborates the existence of an important axial variation in the tree (coincident with the St axis) and, therefore, a probable occurrence of large between-top differences in a St since they correspond to two different axial positions in the tree. Oliveira et al. (2012) obtained a median value of 2.1 for a porosity ratio calculated between tops, with extreme between-top differences (15.3% and 0.2% in the two tops of the same St).

This indicates that the Tv porosity coefficient that serves for quality grading of cork Sts, and which is derived from the cutting of the cork planks into parallel strips, does not give reliable information about the internal structure of LCh.

Density and porosity relationship

The density of air-dried cork tissue is low (150–160 kg m^{-3}), but there are also extremes around 120 to over 200 kg m^{-3} (Pereira 2007). In the first instance, it is conceivable that the numerous voids could reduce the density of cork, but this is not the case, and a relation between density and the void fraction was not found. This means that porosity in cork is not equivalent to voids. The reason is that the LChs are filled with nonsuberous material and, in some cases, delineated by thick-walled lignified cells (Anjos et al. 2008).

Against the expectation, the extent of LCh is positively related to cork density, with an r of 0.85 (R^2=0.72 and R_{adj}=0.69) (P<0.0001), as seen in Figure 3b. González-Hernández et al. (2014) also applied a linear fit to relate porosity and density and found a moderate positive correlation (r=0.58, P<0.0001). The higher r value in the present study can be related to the sample size and the presence of Sts 7 and 9 that have a high porosity and density due to the presence of woody inclusions. Anjos et al. (2014) reported that porosity increased from the lower to the higher density class of cork Sts and presented scanning electron microscope (SEM) cork images showing the concentration of sclerenchymatic cells in the region surrounding the LCh.

The lignocellulosic inclusions (nail) observed in cork Sts 5, 7, and 9 increase the density of cork to values above 200 kg m^{-3}. Nail inclusions influence fracture propagation under tensile stress (Anjos et al. 2011b).

Oxygen ingress and porosity relationship

The contact between wine and oxygen is of critical importance for wine conservation and the in-bottle aging process (Godden et al. 2005), and thus, the oxygen ingress through cork Sts was also investigated. Despite the large variability between cork Sts, there is a common logarithmic behaviour of oxygen ingress as a function of time (Oliveira et al. 2013). There is quick and high oxygen ingress in the first days after bottling, with an initial high ingress rate, followed by a decreasing ingress rate until the first month, and further on stabilizing at a low and rather constant ingress rate from the 3rd to the 12th month. Ribéreau-Gayon (1933) suggested that the initial high oxygen ingress is due to the high internal pressure in the cork cells created when the cork Sts are compressed into the bottleneck (see also Lopes et al. 2007). Therefore the initial high ingress rate of oxygen into the bottle should be related to the cork structural discontinuities, i.e., more specifically to the void fraction and the air located there. Apart of the first period, gas transport through the cork cells occurs with very low diffusion rates through small channels (i.e., through the plasmodesmata) present in the cork cells walls (Faria et al. 2011).

The void volume in the lower part of the St was calculated by taking only the 1/3 of the St, i.e., the part in contact to the bottled liquid. The relationship between the void volume of this 1/3 St and the amount of oxygen diffused during 30 days after bottling is presented in Figure 3c.

The linear regression established between these data has a coefficient of determination (R^2) of 0.83 and adjusted R^2 of 0.81. These results suggest that the high oxygen ingress rates immediately after bottling are due to the transfer of the air trapped in the voids in the bottom part of the cork St. This knowledge is relevant for the cork industry, which means that the orientation of the St must be carefully attended, i.e., the question which top of the St should be in contact with the wine.

Conclusions

XRMT was successfully applied for visualisation and quantification of cork structural discontinuities, which are decisive for the commercial value of raw cork and of cork products. The results demonstrated that image analysis of cork stoppers surface as used for quality grading has a poor relation with the internal structure quantification. The presence of LChs is positively correlated with cork density. The void fraction of LCh in the innermost part of the cork stopper inserted in the bottle is strongly related to the oxygen ingress in the first month after bottling. The results can be interpreted that XRMT scanning as quality control for stopper production may improve essentially the quality control. In view of the availability of rapid XRMT scanning set-ups, this kind of approach seems to be feasible.

Acknowledgments: Financial support by the Transnational Access to Research Infrastructures activity in the 7th Framework Programme of the EC under the Trees4Future project (no. 284181) for conducting the research is gratefully acknowledged. This work was partially supported by FEDER funds through the Operational Programme for Competitiveness Factors – COMPETE – and by National Funds under the project FCOMP-01-0124-FEDER-005421.

The research was carried out under the framework of Centro de Estudos Florestais, a research unit funded by Fundação para a Ciência e Tecnologia, Portugal (PEst OE/AGR/UI0239/2014). Funding from FCT is acknowledged by the first author as a doctoral student (SFRH/BD/77550/2011). The authors acknowledge the collaboration of Amorim & Irmãos, S. A. in materials supply.

References

Anjos, O., Pereira, H., Rosa, M.E. (2008) Effect of quality, porosity and density on the compression properties of cork. Holz Roh Werkst. 66:295–301.

Anjos, O., Pereira, H., Rosa, M.E. (2011a) Characterization of radial bending properties of cork. Eur. J. Wood Prod. 69:557–563.

Anjos, O., Pereira, H., Rosa, M.E. (2011b) Tensile properties of cork in axial stress and influence of porosity, density, quality and radial position in plank. Eur. J. Wood Prod. 69:85–91.

Anjos, O., Rodrigues, C., Morais, J., Pereira, H. (2014) Effect of density on the compression behaviour of cork. Mater. Des. 53:1089–1096.

Axelsson, M., Svensson, S. (2010) 3D pore structure characterization of paper. Pattern Anal. Appl. 13:159–172.

Bessières, J., Maurin, V., George, B., Molina, S., Masson, E., Merlin, A. (2013) Wood-coating layer studies by X-ray imaging. Wood Sci. Technol. 47:853–867.

Boden, S., Schinker, M.G., Duncker, P., Spiecker, H. (2010) Resolution abilities and measuring depth of high-frequency densitometry on wood samples. Measurement 45:1913–1921.

Bolte, S., Cordelières, F.P. (2006) A guided tour into subcellular colocalization analysis in light microscopy. J. Microsc. 224:213–232.

Brabant, L., Vlassenbroeck, J., De Witte, Y., Cnudde, V., Boone, M.N., Dewanckele, J., Van Hoorebeke, L. (2011) Three-dimensional analysis of high-resolution X-ray computed tomography data with Morpho+. Microsc. Microanal. 17:252–263.

Brunetti, A., Cesareo, R., Golosio, B., Luciano, P., Ruggero, A. (2002) Cork quality estimation by using Compton tomography. Nucl. Instrum. Methods Phys. Res., Sect. B 196:161–168.

Česen, A., Korat, L., Mauko, A., Legat, A. (2013) Microtomography in building materials. Mater. Technol. 47:661–664.

Cnudde, V., Boone, M.N. (2013) High-resolution X-ray computed tomography in geosciences: a review of the current technology and applications. Earth Sci. Rev. 123:1–17.

Dewanckele, J., De Kock, T., Boone, M.A., Cnudde, V., Brabant, L., Boone, M.N., Fronteau, G., Van Hoorebeke, L., Jacobs, P. (2012) 4D imaging and quantification of pore structure modifications inside natural building stones by means of high resolution X-ray CT. Sci. Total Environ. 416:436–448.

Dierick, M., Van Loo, D., Masschaele, B., Boone, M.N., Van Hoorebeke, L. (2010) A LabVIEW (R) based generic CT scanner control software platform. J. X-Ray Sci. Technol. 18:451–461.

Dierick, M., Van Loo, D., Masschaele, B., Van den Bulcke, J., Van Acker, J., Cnudde, L., Van Hoorebeke, L. (2014) Recent micro-CT scanner developments at UGCT. Nucl. Instrum. Methods Phys. Res. Sect. B 324:35–40.

Donepudi, V.R., Cesareo, R., Brunetti, A., Zhong, Z., Yuasa, T., Akatsuka, T., Takeda, T., Gigante, G.E. (2010) Cork embedded internal features and contrast mechanisms with DEI using 18, 20, 30, 36, and 40 keV synchrotron X-rays. Res. Nondestr. Eval. 21:171–183.

Faria, D.P., Fonseca, A.L., Pereira, H., Teodoro, O.M.N.D. (2011) Permeability of cork to gases. J. Agric. Food Chem. 59:3590–3597.

Fortes, M.A., Rosa, M.E., Pereira, H. A Cortiça. IST Press, Lisbon, 2004.

Godden, P., Lattey, K., Francis, L., Gishen, M., Cowey, G., Holdstock, M., Robinson, E., Waters, E., Skouroumounis, G., Sefton, M., Capone, D., Kwiatkowski, M., Field, J., Coulter, A., D'Costa, N., Bramley, B. (2005) Towards offering wine to the consumer in optimal condition – the wine, the closures and other packaging variables: a review of AWRI research examining the changes that occur in wine after bottling. Wine Ind. J. 20:20–30.

Gonzalez-Adrados, J., Pereira, H. (1996) Classification of defects in cork planks using image analysis. Wood Sci. Technol. 30:207–215.

Gonzalez-Adrados, J., Lopes, F., Pereira, H. (2000) Quality grading of cork planks with classification models based on defect characterisation. Holz Roh Werkst. 58:39–45.

González-Hernández, F., González-Adrados, J.R., Gracia de Ceca, J.L., Sánchez-González, M. (2014) Quality grading of cork stoppers based on porosity, density and elasticity. Eur. J. Wood Prod. 72:149–156.

Helama, S., Begin, Y., Vartiainen, M., Peltola, H., Kolström, T., Meriläinen, J. (2012) Quantifications of dendrochronological information from contrasting microdensitometric measuring circumstances of experimental wood samples. Appl. Radiat. Isot. 70:1014–1023.

Hor, Y.L., Federici, J.F., Wample, R.L. (2008) Nondestructive evaluation of cork enclosures using terahertz/millimetre wave spectroscopy and imaging. Appl. Optics 47:72–78.

Ikonen, V.-P., Peltola, H., Wilhelmsson, L., Kilpeläinen, A., Väisänen, H., Nuutinen, T., Kellomäki, S. (2008) Modelling the distribution of wood properties along the stems of Scots pine (*Pinus sylvestris* L.) and Norway spruce (*Picea abies* (L.) Karst.) as affected by silvicultural management. For. Ecol. Manage. 256:1356–1371.

Kim, K., Yoon, H., Diez-Silva, M., Dao, M., Dasari, R., Park, Y. (2014) High-resolution three-dimensional imaging of red blood cells parasitized by *Plasmodium falciparum* and in situ hemozoin crystals using optical diffraction tomography. J. Biomed. Opt. 19: Article 011005.

Knapic, S., Pirralho, M., Louzada, J.L., Pereira, H. (2014) Early assessment of density features for 19 *Eucalyptus* species using X-ray microdensitometry in a perspective of potential biomass production. Wood Sci. Technol. 48:37–49.

Landis, E.N., Keane, D.T. (2010) X-ray microtomography. Mater. Charact. 61:1305–1316.

Longuetaud, F., Mothe, F., Kerautret, B., Krähenbühl, A., Hory, L., Leban, J.M., Debled-Rennesson, I. (2012) Automatic knot detection and measurements from X-ray CT images of wood: a review and validation of an improved algorithm on softwood samples. Comput. Electron. Agric. 85:77–89.

Lopes, P., Saucier, C., Teissedre, P.-L., Glories, Y. (2007) Main routes of oxygen ingress through different closures into wine bottles. J. Agric. Food Chem. 55:5167–5170.

Oliveira, V., Knapic, S., Pereira, H. (2012) Natural variability of surface porosity of wine cork stoppers of different commercial classes. J. Int. Sci. Vigne Vin 46:331–340.

Oliveira, V., Lopes, P., Cabral, M., Pereira, H. (2013) Kinetics of oxygen ingress into wine bottles closed with natural cork stoppers of different qualities. Am. J. Enol. Viticult. 64:3. doi:10.5344/ajev.2013.13009.

Pereira, H. Cork: Biology, Production and Uses. Elsevier, Amsterdam, 2007.

Pereira, H., Lopes, F., Graça, J. (1996) The evaluation of the quality of cork planks by image analysis. Holzforschung 50:111–115.

Phillips, C. (2014) Closure survey report: consistency key in selecting closures. Wine Business Monthly. XXI:18–28.

Ribéreau-Gayon, J. (1933) Dissolution d'oxygène dans les vins. In: Contribution à l'étude des oxidations et réductions dans les vins. Application à l'étude de vieillissement et des cases. Ed. Libraire Delmas. Bordeaux, France. pp. 35.

Ridler, T.W., Calvard, S. (1978) Picture thresholding using an iterative selection method. IEEE Trans. Syst. Man Cybern. SMC-8:630–632.

Schindelin, J., Arganda-Carreras, I., Frise, E., Kaynig, V., Longair, M., Pietzsch, T., Preibisch, S., Rueden, C., Saalfeld, S., Schmid, B., Tinevez, J.-Y., White, D.J., Hartenstein, V., Eliceiri, K., Tomancak, P., Cardona, A. (2012) Fiji: an open-source platform for biological-image analysis. Nat. Methods 9:676–682.

Taylor, A., Plank, B., Standfest, G., Petutschnigg, A. (2013) Beech wood shrinkage observed at the micro-scale by a time series of X-ray computed tomographs (μXCT). Holzforschung 67:201–205.

Tran, H., Doumalin, P., Delisee, C., Dupre, J.C., Malvestio, J., Germaneau, A. (2013) 3D mechanical analysis of low-density wood-based fiberboards by X-ray microcomputed tomography and digital volume correlation. J. Mater. Sci. 48:3198–3212.

Van den Bulcke, J., Boone, M., Van Acker, J., Stevens, M., Van Hoorebeke, L. (2009) X-ray tomography as a tool for detailed anatomical analysis. Ann. For. Sci. 66:508.

Van den Bulcke, J., Boone, M., Van Acker, J., Van Hoorebeke, L. (2010) High-resolution X-ray imaging and analysis of coatings on and in wood. J. Coat. Technol. Res. 7:271–277.

Van den Bulcke, J., Wernersson, E.L.G., Dierick, M., Van Loo, D., Masschaele, B., Brabant, L., Boone, M.N., Van Hoorebeke, L., Haneca, K., Brun, A., Hendriks, C.L.L., Van Acker, J. (2013) 3D tree-ring analysis using helical X-ray tomography. Dendrochronologia 32:39–46.

Vlassenbroeck, J., Dierick, M., Masschaele, B., Cnudde, V., Van Hoorebeke, L., Jacobs, P. (2007) Software tools for quantification of X-ray microtomography at the UGCT. Nucl. Instrum. Meth. Phys. Res. A 580:442–445.

Wei, Q., Leblon, B., La Rocque, A. (2011) On the use of X-ray computed tomography for determining wood properties: a review. Can. J. For. Res. 41:2120–2140.

Wieland, S., Grünewald, T., Ostrowski, S., Plank, B., Standfest, G., Mies, B., Petutschnigg, A. (2013) Assessment of mechanical properties of wood-leather panels and the differences in the panel structure by means of X-ray computed tomography. BioResources 8:818–832.

PUBLICATION V.

INFLUENCE OF CORK DEFECTS IN THE OXYGEN INGRESS THROUGH WINE STOPPERS: INSIGHTS WITH X-RAY TOMOGRAPHY

Journal of Food Engineering 165 (2015) 66–73

Contents lists available at ScienceDirect

Journal of Food Engineering

journal homepage: www.elsevier.com/locate/jfoodeng

Influence of cork defects in the oxygen ingress through wine stoppers: Insights with X-ray tomography

Vanda Oliveira [a,*], Paulo Lopes [b], Miguel Cabral [b], Helena Pereira [a]

[a] Universidade de Lisboa, Instituto Superior de Agronomia, Centro de Estudos Florestais (CEF), Tapada da Ajuda, P-1349-017 Lisboa, Portugal
[b] Amorim & Irmãos, R&D Department, Rua de Meladas 380, P.O. Box 20, Mozelos 4536-902, Portugal

ARTICLE INFO

Article history:
Received 4 February 2015
Received in revised form 27 April 2015
Accepted 12 May 2015
Available online 13 May 2015

Keywords:
Cork
X-ray tomography
Oxygen ingress rate
Image analysis
Insect galleries
Wetcork

ABSTRACT

Cork may sporadically include defects of biological or external origin that will influence the adequacy of cork to specific uses and the performance of cork products, namely of wine stoppers.

The present work evaluates cork defects in relation to the oxygen ingress to the bottle through wine stoppers. The characterization of defects is made by image analysis of the cork stopper's surface. Non-destructive observation by X-ray tomography allowed the observation and identification of the internal defects. The performance was followed by studying the kinetics of oxygen ingress into the bottles during 12 months using a non-destructive colorimetric method. There is a common logarithmic behaviour of oxygen ingress with time. Insect galleries have a major influence on the oxygen ingress rate.

The results may be applied to selection of quality key features and contribute to value enhancement of natural cork stoppers and to their qualified use in wine ageing.

1. Introduction

Cork is a natural cellular material with an interesting and unusual set of properties that became world known as closure for wine bottles (Fortes et al., 2004; Pereira, 2007).

Cork is the external layer of the bark of the cork oak (*Quercus suber*) from which it is removed periodically in a sustainable exploitation along the tree's lifetime (Pereira, 2007). Cork is a homogeneous tissue made up of the same type of cells, arranged in a regularly ordered and compact structure, forming a honeycomb of small closed cells with thin cell walls (Pereira et al., 1987). Heterogeneity is given by one natural feature related with the tree's physiology: the presence of lenticular channels crossing the cork layers from the outside to the inside, that are loosely filled with a dark brown unsuberified material, usually conspicuous to the visual observation (Oliveira et al., 2012; Pereira et al., 1996). This distinctive feature, usually referred to as the porosity of cork, is the basis for the commercial classification of natural cork stoppers by quality grades (Costa and Pereira, 2006; Oliveira et al., 2015a). Automated image-based inspection systems allow an identification of surface defects and quantification of porosity features (Chang et al., 1997; Jordanov and Georgieva, 2009; Pereira et al., 1994; Radeva et al., 2002).

However, cork may sporadically include defects of biological or external origin that will influence the performance of cork products, namely of wine stoppers. If present in a natural cork stopper, some defects will disqualify it from its wine sealant functions, e.g. the presence of wetcork spots, insect galleries or microbial stains.

Cork planks with stains (yellow and marble stain) that result from microbial attacks are discarded for the production of cork stoppers to avoid eventual contamination with off-flavours and taints (Pereira, 2007).

Galleries can be excavated in cork by the larva of the coleopteron *Coroebus undatus* F. or the ant *Crematogaster scutellaris* (Gonzalez-Adrados et al., 2000; Pereira, 2007). If detected in the cork planks at initial processing steps, the areas with insect attacks are not used for the production of cork stoppers.

In early summer, the *C. undatus* females hide and lay their eggs on cork, favouring deep fissures. In this case, the neonate larvae gain faster access to the cork-generating layer (i.e. the phellogen), where they feed and excavate long and elliptical galleries filled with residual material (Gallardo et al., 2012). With the subsequent cork growth, the galleries become embedded in the cork tissue where they develop in vertical and tangential directions in the growth rings (Pereira, 2007). Larval development lasts from two to three years (larvae can reach 3.5–4 cm of length), after which follows emergence of the adults from their host (Jiménez et al., 2012; Sallé et al., 2014).

* Corresponding author.
E-mail address: vandaoliveira@isa.ulisboa.pt (V. Oliveira).

http://dx.doi.org/10.1016/j.jfoodeng.2015.05.019
0260-8774/

C. scutellaris is the most widespread and common ant species in oak habitats with preference for *Quercus ilex* and *Q. suber* (Cammell et al., 1996; Gallardo et al., 2012; Ruiz et al., 2006). The density of nests is related to tree density, age and a minimum cork thickness necessary to build the nest (Suñer and Abós, 1992). Each nest may reach 2–3 m of length along the stem, consisting of galleries usually empty and running in random direction.

Wetcork designates cork that has regions with high water content (400–500%) in comparison to the 25% average moisture content of cork planks (Pereira, 2007) or the 40% in cork planks immediately after harvesting (Costa and Pereira, 2013).

The wetcork regions will take more time to dry than the usual plank processing time; if detected in the post-harvest period, wetcork planks will undergo kiln drying (Carpintero et al., 2014), after which they integrate the normal processing line. If undetected, wetcork spots will shrink by approximately 30% during drying, and the cells wrinkle and collapse in some cases, appearing as concave areas at the stopper's surface (Pereira, 2007).

A natural cork stopper should ensure an appropriate seal without liquid leakage and allowing wine aging in the bottle without organoleptic deterioration. The sealing performance of closures is related to their permeability properties, namely to oxygen. Several studies compared the oxygen permeability of different closures (Godden et al., 2005; Karbowiak et al., 2010; Lopes et al., 2006). Lopes et al. (2007) showed that the main route of oxygen ingress into wine bottles closed with natural cork stoppers is from the cork structure itself during the first 12 months of storage, although some permeation through the cork-glass interface is possible after that time but at very residual levels.

The present work evaluates the influence of cork defects (insect galleries and wetcork) in the sealing performance of natural cork stoppers regarding oxygen ingress into the bottle. First we characterized the defects as they appear in the surface of the stoppers as well as their internal identification and development using a non-destructive observation by X-ray tomography. Then their performance was followed by studying the kinetics of oxygen ingress into the bottles during 12 months using a non-destructive colorimetric method as described in Oliveira et al. (2013).

It is the objective to ascertain the impact of the above mentioned defects in the performance of the natural cork stoppers in the bottle as regards oxygen ingress. The results may be applied to selection of quality key features of natural cork stoppers and contribute to their value enhancement and qualified use in wine ageing.

2. Materials and methods

2.1. Materials

A total of 150 natural cork stoppers (24 mm diameter × 45 mm length) with defects were selected: 50 stoppers with the presence of ant (*C. scutellaris*) galleries, 50 stoppers with *C. undatus* larvae galleries and 50 stoppers with wetcork spots. From each type of defect, 30 stoppers were used for the closure of bottles and oxygen ingress measurements. The cork stoppers were supplied by Amorim & Irmãos, S.A. (Santa Maria de Lamas, Portugal).

2.2. Image analysis of cork stoppers surface

The lateral surface and the tops of the cork stoppers were imaged using eight successive rectangular frames and two circular frames, respectively, with an image analysis system that included a digital 7 mega pixels in macro stand solution set on an acquisition Kaiser RS1 Board with a controlled illumination apparatus, connected to a computer using AnalySIS® image processing software (Analysis Soft Imaging System GmbH, Münster, Germany, version 3.1) and subsequently processed by image analysis according to the procedure described in Oliveira et al. (2012).

Briefly, the visualization of all the stoppers was made using the same calibration and light intensity. The object extraction was carried out inside two predefined regions of interest, one rectangular, with an area of 423.9 mm^2, for the lateral surface, and another circular for the tops with an area of 433.9 mm^2. The image threshold was adjusted individually for each image. A set of dimension- and shape-type variables was collected automatically for each object (pore), filtered (only pores with area equal or superior to 0.1 mm^2 were considered for the analysis), averaged and transformed into cork stopper body variables. The pixel size was 0.05 mm and therefore the lowest pore area that could be resolved was 0.04 mm^2. One of the most relevant variables is the porosity coefficient (%) defined as the proportion of the area occupied by pores (all objects identified as not cork tissue). Other calculated variables included: average pore area (mm^2), calculated as the arithmetic mean of the area of all objects, area of the largest pore (mm^2), selected as the maximum area of all objects, average aspect ratio, calculated as the arithmetic mean of all maximum ratio between width and length of a bounding rectangle of the object, largest pore aspect ratio, selected as the aspect ratio of the pore with maximum area, and average elongation and largest pore elongation, that results from sphericity and can be considered as lack of roundness.

2.3. X-ray tomography

X-ray tomography is a radiographic imaging technique in which X-rays from a source pass through the sample and are detected by film or CCD-based detector for radiography in the opposite side of the sample. The resulting image is a projection of a volume in a 2D plane with contrast resulting from differential attenuation of X-rays. To get 3D information X-ray tomography combines information from a series of those radiographs recorded while rotating the sample about a single axis or, in the case of medical scanners, by holding the sample stationary while the X-ray source and detector are rotated around the object. The filtered back-projection algorithm (mathematical principles of tomography) can then be used to reconstruct the volume of the sample from these radiographs (Webb, 2003).

The cork stoppers were scanned using a medical X-ray CT scanner Philips Tomoscan AV, with an X-ray source of 130 kV high voltage generators and a current of 140 mA. The greyscale images (512 × 512 pixels) are composed of a set of consecutive 2D slices, spaced by 2 mm, and the grey levels correspond to density computed in Hounsfield units (HU). On this scale, typical densities are 0 HU for water and −1000 HU for air. The spatial resolution of 2 mm/voxel allows the visualization of structures larger than 4 mm^2 when seen in 2D or 8 mm^3 in 3D. As insect galleries have on average 122.5 mm^2 (Gonzalez-Adrados et al., 2000) the spatial resolution achieved seems appropriate for the visualization.

In the resulting grey images the voids will appear as dark regions while the high density areas will appear as brighter regions. Segmentation was performed by means of an automated thresholding base on the modified isodata algorithm implemented in Fiji image processing package (Schindelin et al., 2012). The resulting binary images were used for 3D reconstruction, performed using the 3D viewer plugin for ImageJ (Schmid et al., 2010).

2.4. Oxygen ingress

The kinetics of oxygen ingress into bottles closed with the selected cork stoppers was studied by a non-destructive colorimetric method (Oliveira et al., 2013). The procedure for reduction and

oxidation of an indigo carmine solution in the calibration bottle was described in Lopes et al. (2005).

Concisely, the calibration procedure consists in using an aqueous indigo carmine solution that is totally reduced by adding sodium dithionite in a controlled excess (the excess corresponds to the quantity necessary to consume the oxygen that enters into the bottle in the bottling operation) leading to a colour change from indigo blue to yellow. Once the excess of sodium dithionite was consumed, the reduced indigo carmine starts to consume the oxygen that is introduced into the bottle in known amounts, resulting in a colour change that was measured with a colorimeter apparatus. Each point of the calibration curve was obtained by calculating the mean of five replicates. The calibration curve is valid up to a maximal limit of oxygen quantification of 5.7 mg, which is the amount necessary to fully oxidize the excess of sodium dithionite and the indigo carmine in the bottle.

Sterilized commercial bottles (375 mL) were used, filled with the reduced indigo carmine solution and closed using a single headed corker Bertolazo Epsilon R/S. The stoppers were compressed to 16 mm diameter before insertion into the bottles under vacuum. The final filling level for each bottle was 65 ± 3 mm below the top of the bottle. All bottles were left upright for 24 h after bottling and then stored horizontally under room conditions (temperature from 27.8 °C to 13.6 °C) over 12 months.

Measurements of the CIELAB parameters L^*, a^*, b^* were performed by directly scanning the bottled solutions with a Minolta series CM-508i spectrocolorimeter equipped with a transmittance accessory CM-A76 (Osaka, Japan).

3. Results and discussion

3.1. Characterization of cork stoppers

Fig. 1 shows images from the lateral surface of cork stoppers with the presence and identification of the three types of defects.

The lateral surface of the cork stoppers is characterized in Tables 1 and 2.

The average lateral surface porosity coefficient was 3.7%, 4.4% and 1.8%, respectively, for cork stoppers with ant and C. larvae galleries, and wetcork. The cork stoppers with insect galleries had a porosity that would be in the range of stoppers classified as standard that present an average porosity coefficient of 5.5% with 1.9% of standard deviation (Oliveira et al., 2012).

Table 1
Characterization of the porosity of the lateral surface of cork stoppers by type of defect. Mean (n = 50) and standard deviation (in brackets).

	Defect type		
	Ant's galleries	C. larvae galleries	Wetcork
Porosity coefficient (%)	3.7 (1.5)	4.4 (2.2)	1.8 (0.6)
Number of pores	162 (49)	186 (58)	93 (32)
Average area (mm^2)	0.9 (0.4)	0.9 (0.3)	0.7 (0.2)
Average aspect ratio	2.1 (0.2)	2.1 (0.2)	2.1 (0.3)
Average elongation	2.3 (0.2)	2.5 (0.4)	2.4 (0.4)
Area of largest pore (mm^2)	42.1	99.1	12.6
Largest pore aspect ratio	1.1	3.8	2.9
Largest pore elongation	1.1	7.0	3.9

The wetcork stoppers had a porosity coefficient of the lateral surface from 1.7% to 2.0% that is below the 2.4% average value published by Oliveira et al. (2012) for the premium stoppers and close to the 1.4% reported by Costa and Pereira (2009) for extra cork stoppers.

The stoppers with C. larvae galleries present the largest pore (99.1 mm^2) characterized by an aspect ratio of 3.8 and elongation of 7.0 which is indicative of the gallery extension. Gonzalez-Adrados et al. (2000) found that these galleries have on average 122.5 mm^2 and a length of 36.2 mm in the tangential section.

Overall, the average aspect ratio of pores presented identical value between the different types of defects. This is identical to the performance of shape variables in natural cork stoppers without defects (Costa and Pereira, 2009; González-Adrados and Pereira, 1996; Oliveira et al., 2012).

Table 2 presents the porosity characterization discriminated by pore dimension class. The number of pores per cork stopper is comparatively higher for pores with small dimensions (less than 5 mm^2) and should correspond to lenticular channels. At this level the pore features were similar for the three types of stoppers. Differentiation between the stoppers with insect galleries and wet cork occurred however for the larger pores.

Each stopper with insect galleries contained, in average, 2 to 3 pores with dimension superior to 10 mm^2 corresponding probably to the insect galleries and showing an elongated form e.g. pores larger than 20 mm^2 presented average elongation of 4.2 and 8.8 for ant and C. larvae galleries, respectively. On the contrary, the pores in wetcork retained their shape features regardless of

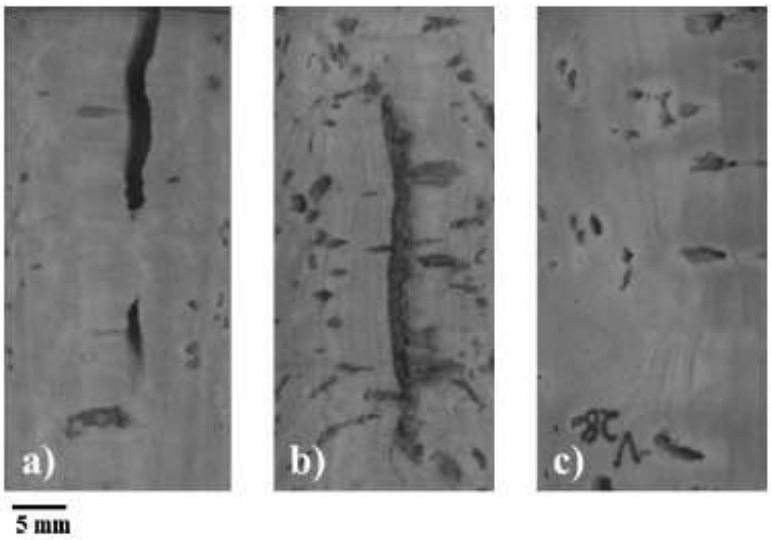

Fig. 1. Image of the lateral body surface of cork stoppers showing defects in the cork structure: (a) empty ant gallery; (b) *Coroebus undatus* F. larvae gallery; and (c) wetcork.

Table 2
Characterization of the porosity of the lateral surface of cork stoppers by pore dimension class and type of defect. Mean and standard deviation (in brackets).

	Defect type		
	Ant's galleries	C. larvae galleries	Wetcork
Pore dimension class <1 mm²			
Average number of pores by stopper	134 (43)	152 (52)	75 (28)
Average pore area (mm²)	0.3 (0.04)	0.3 (0.04)	0.3 (0.04)
Average porosity coefficient (%)	1.2 (0.4)	1.4 (0.4)	0.7 (0.3)
Average pore aspect ratio	2.0 (0.2)	2.0 (0.2)	2.1 (0.2)
Average pore elongation	2.2 (0.2)	2.3 (0.3)	2.3 (0.3)
Pore dimension class [1–5] mm²			
Average number of pores by stopper	25 (12)	30 (15)	16 (7)
Average pore area (mm²)	1.9 (0.2)	1.9 (0.2)	1.9 (0.3)
Average porosity coefficient (%)	1.4 (0.7)	1.7 (0.9)	0.9 (0.4)
Average pore aspect ratio	2.2 (0.3)	2.2 (0.4)	2.1 (0.3)
Average pore elongation	2.5 (0.5)	2.5 (0.6)	2.3 (0.4)
Pore dimension class [5–10] mm²			
Average number of pores by stopper	3 (2)	3 (2)	1 (0)
Average pore area (mm²)	6.8 (1.1)	6.4 (0.8)	6.4 (1.1)
Average porosity coefficient (%)	0.6 (0.5)	0.5 (0.5)	0.3 (0.1)
Average pore aspect ratio	2.4 (0.9)	3.0 (1.3)	2.5 (1.2)
Average pore elongation	2.8 (1.3)	3.7 (1.8)	3.0 (1.9)
Pore dimension class [10–20] mm²			
Average number of pores by stopper	1 (1)	2 (1)	1 (0)
Average pore area (mm²)	13.1 (3.1)	14.7 (2.7)	11.1 (0.9)
Average porosity coefficient (%)	0.5 (0.5)	0.8 (0.4)	0.3 (0.0)
Average pore aspect ratio	2.7 (1.4)	5.0 (3.3)	2.5 (1.2)
Average pore elongation	3.4 (2.1)	7.0 (5.1)	3.0 (1.6)
Pore dimension class ⩾ 20 mm²			
Average number of pores by stopper	1 (0)	1 (1)	–
Average pore area (mm²)	28.0 (6.1)	46.5 (21.5)	–
Average porosity coefficient (%)	1.0 (0.5)	1.6 (0.8)	–
Average pore aspect ratio	3.1 (1.7)	5.7 (2.4)	–
Average pore elongation	4.2 (2.4)	8.8 (4.2)	–

dimension. Similar shape features were already reported and used to differentiate such defects by image analysis (González-Adrados and Pereira, 1996; Gonzalez-Adrados et al., 2000). Therefore the cork with insect defects will be differentiated mostly by the features of the larger pore structures.

The visualization and identification of some defects within the cork stopper was possible with X-ray tomography due to the non-destructive nature of the X-ray tomography analysis and the relationship between X-ray absorption and material density. The analysis used a spatial resolution of 2 mm/voxel, therefore allowing the visualization of larger structures. With this spatial resolution it is possible to individualize and identify structures with dimension higher than 5 mm² that correspond, as referred previously, to insect galleries (Table 2). Due to their small dimensions lenticular channels are not visible with the spatial resolution achieved with the medical X-ray CT scanner. Nevertheless, even for the largest structures and for quantification purposes it will be preferable to have a better spatial resolution. Examples of the resulting greyscale images from inside of the stoppers are shown in Fig. 2.

The ant galleries are typically empty and run through the cork plank in random directions as shown in Fig. 2a; they can appear at the cork stopper surface as small holes that may go unnoticed even to expert's operators. Fig. 2a includes an example of the development from top-to-top of one of these empty ant galleries in a cork stopper. In such a case, the gallery would constitute a free path through the stopper leading to wine leakage.

The *C. larvae* galleries are filled with residual material that has a density well above (white region) that from the surrounding cork tissue, as shown in Fig. 2b. The filling tissue is not fully compacted and empty spaces occur occasionally as shown in the image. The

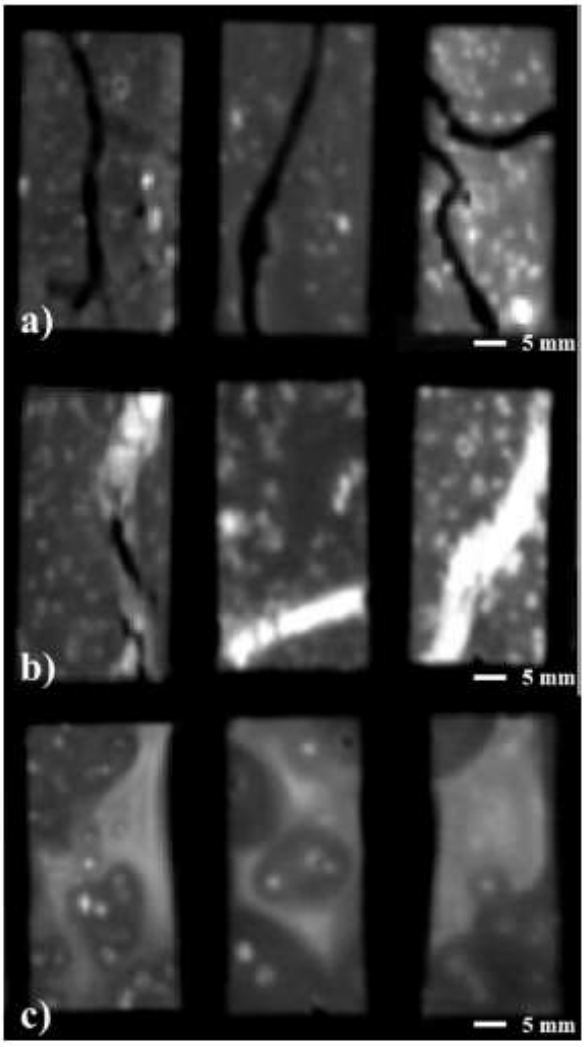

Fig. 2. X-ray tomography greyscale images (stopper center slice) with 2 mm resolution, showing the defects in the cork structure: (a) empty ant gallery; (b) *Coroebus undatus* F. larvae gallery; and (c) wetcork. For each type of defect the stopper corresponding to the right image was used for 3D reconstruction in Fig. 3.

galleries are embedded in the cork tissue with a spatial development in vertical and tangential directions in the growth rings.

Fig. 2c displays cork stoppers with wetcork regions. The wetcork area is distinguished as brighter due to the higher density resulting from cells shrinkage and collapse during the drying process as shown by scanning electron microscope (Pereira, 2007). With X-ray tomography, the wetcork regions are clearly visible and distinguished contrary to what happens in classical surface image analysis.

Fig. 3 presents examples of 3D defect reconstruction obtained from the greyscale images using an automated thresholding (considering dark background when selecting the brighter areas) and representing the defect in grey. The development of the ant's galleries (a low density area in the tomography images) as well as those of *Coroebus* (a high density area) is clearly seen crossing the stopper. In the case of the wetcork regions, which correspond to higher density zones, it is noteworthy that they may extend to a substantial part of the stopper.

To the best of our knowledge, this is the first time that X-ray tomography was applied for visualization and identification of this type of defects in cork. In a recent study X-ray microtomography

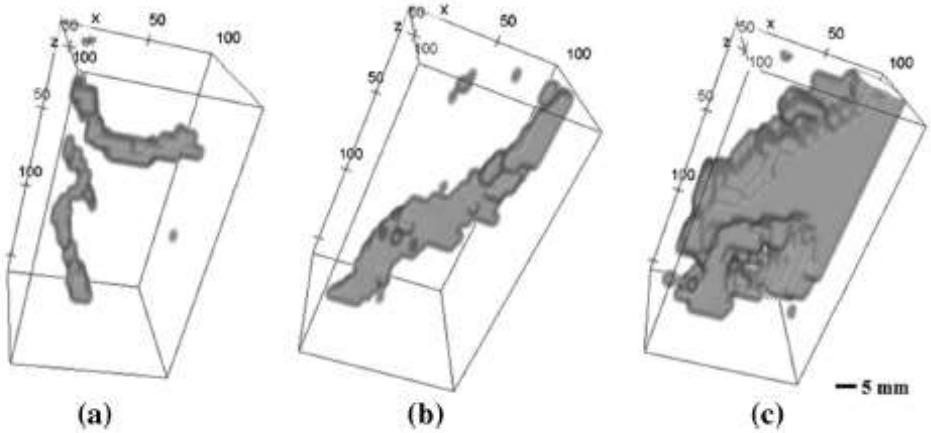

Fig. 3. 3D overview showing examples of the defects in the cork structure: (a) empty ant gallery; (b) *Coroebus undatus* F. larvae gallery; and (c) wetcork. The images corresponds to right images of Fig. 2.

with higher resolution (50 μm) was successively applied to the study of cork with focus on the lenticular channels quantification and their three-dimensional structure showing the importance of their internal development in the stopper (Oliveira et al., 2015b). The spatial resolution of 50 μm/voxel used allows the identification of structures and the quantification of the void and dense fractions of lenticular channels. However the number of projections (900 images per stopper) and the time needed to process that information are much higher when compared with the present study (22 images per stopper).

Another recent study compares two techniques: digital photography and neutron imaging (radiography and tomography) to identify and quantify the lenticular channels present in different classes of cork stoppers (Lagorce-Tachon et al., 2015). In this study, the pixel size used was 63 μm with a total of 625 projections taken around the samples (360° rotation). Moreover, other technics such as Synchrotron, Compton and Terahertz tomography were recently applied for a non-destructive evaluation of natural cork leading to a better understanding of their inner structure but without identification and classification of defects (Brunetti et al., 2002; Donepudi et al., 2010; Hor et al., 2008; Mukherjee and Federici, 2011).

3.2. Oxygen ingress

In this study, the method's limit for oxygen measurement was reached before the end of the experiment for some of the bottles: 27% with stoppers with ant galleries, 23% with *C. larvae* galleries and 13% with wetcork spots. In cork stoppers without identified defects, Oliveira et al. (2013) found that 21% of the total cork stoppers reached the limit of oxygen quantification within 12 months of storage.

Fig. 4 shows the variability found for the oxygen ingress in the first two months of storage. For comparison, the average behaviour of cork stoppers without defects was calculated with the data given by Oliveira et al. (2013). It is noteworthy that wetcork stoppers behave very similarly to defect-free stoppers while the stoppers with insect galleries showed a higher ingress of oxygen especially in the first 5 days after bottling.

In order to study the kinetics of oxygen ingress along the 12 months of storage, these bottles were removed from the experiment. Fig. 5 shows the kinetics of oxygen ingress along the 12 months of storage clustered by type of defect. As previous, for comparison, the average behaviour of cork stoppers without defects was calculated with the data presented by Oliveira et al. (2013). The data encompass all the reference quality classes (premium, good, and standard) and average data for oxygen classes 1, 2 and 3.

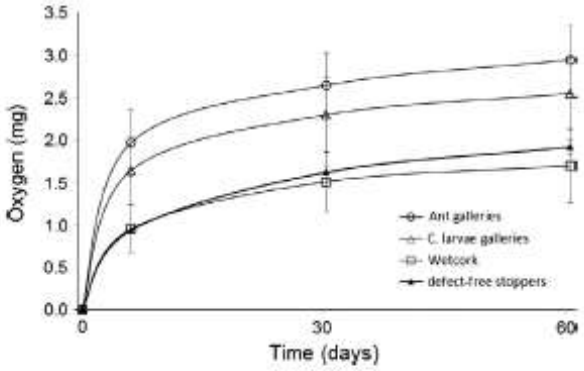

Fig. 4. Variability of oxygen ingress in the first two months of storage by defect type. In bold is the average kinetic of oxygen ingress into bottles closed with cork stoppers without defects (Oliveira et al., 2013). Error bars represent the 95% confidence interval for the mean.

There is a common logarithmic behaviour of oxygen ingress with time. There is a quick and high oxygen ingress during the first month after bottling, which is particularly high in the first days, decreasing thereafter until stabilizing at low and constant rate after the 3rd month. This behaviour of oxygen ingress into the bottle closed with cork stoppers was first shown by Lopes et al. (2005, 2006, 2007) and was validated with a large number of stoppers by Oliveira et al. (2013).

Table 3 shows the oxygen ingress rates (μg/day) into the bottle for the cork stoppers with each defect type during the 12 months of the experiment.

Independently of the stoppers and of the type of defect existent, the oxygen ingress rates were higher in the first month of storage, and particularly high in the first days after bottling, decreased thereafter and stabilized at rather constant values after 3 months (Fig. 4 and Table 3).

The results show that the oxygen ingress from stoppers with insect galleries is higher than the average reported for stoppers without defects, while the contrary applies for wetcork (Fig. 5). There is a clear difference in oxygen ingress rates in the first month between stoppers with insect galleries (66.5 and 63.1 μg/day) and wetcork (39.9 μg/day). The one-way analysis of variance (Table 4)

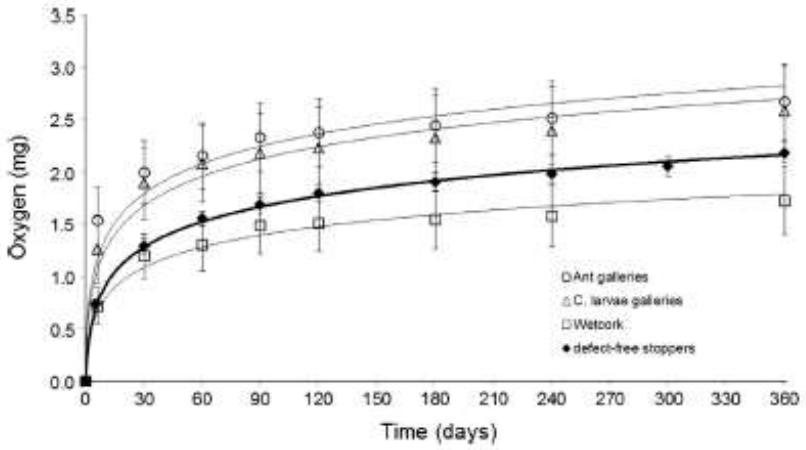

Fig. 5. Kinetics of oxygen ingress into bottles closed with cork stoppers by defect type. In bold is the average kinetic of oxygen ingress into bottles closed with cork stoppers without defects (Oliveira et al., 2013). Error bars represent the 95% confidence interval for the mean.

Table 3
Oxygen ingress rates (μg/day) into the bottle closed with cork stoppers of each defect type during 12 months. Mean and standard deviation (in brackets).

Period of time	Defect type			Without apparent defects[a]
	Ant's galleries	*C. larvae* galleries	Wetcork	
0–5 days	255.8 (129.6)	210.6 (130.8)	119.8 (75.8)	145.2
5–30 days	19.2 (11.9)	26.2 (17.6)	19.9 (10.5)	21.4
First month	66.5 (27.9)	63.1 (32.8)	39.9 (20.1)	42.0
Second month	5.2 (3.3)	6.3 (5.8)	3.6 (4.7)	8.6
Third month	6.0 (4.1)	3.2 (3.2)	6.2 (5.2)	4.4
Fourth month	1.5 (1.4)	1.7 (2.4)	0.8 (0.9)	3.4
4th to 12th month	1.2 (0.8)	1.5 (1.3)	0.9 (0.8)	1.5

[a] Average data for oxygen classes 1, 2 and 3 presented by Oliveira et al. (2013).

Table 4
One-way analysis of variance (ANOVA) of oxygen ingress rates at different periods.

Period of time		df	Mean square	*F*	Sig.
0–5 days	Between Groups	2	116492.134	9.075	.000
	Within Groups	68	12837.050		
5–30 days	Between Groups	2	347.510	1.883	.160
	Within Groups	68	184.533		
Second month	Between Groups	2	44.860	1.983	.146
	Within Groups	68	22.627		
Third month	Between Groups	2	64.650	3.492	.036
	Within Groups	68	18.516		
Fourth month	Between Groups	2	5.814	2.162	.123
	Within Groups	68	2.690		
4th to 12th month	Between Groups	2	2.070	2.170	.122
	Within Groups	68	.954		

showed that significant differences in the oxygen ingress rate only occur for the first 5 days, due to the lower average oxygen ingress rate of stoppers with wetcork (119.8 μg/day).

This result corroborates the assumption that the high oxygen ingress rate observed during the first month after bottling is due to the air forced out of the cork structure when stoppers are compressed into the bottleneck, as suggested in previous studies (Brotto et al., 2010; Karbowiak et al., 2010; Lopes et al., 2007; Oliveira et al., 2013; Ribéreau-Gayon, 1933).

Theoretically, natural cork stoppers with 24 mm diameter × 45 mm length have a volume of 20.4 mL of which 80–85% is air contained in the cell lumen, implying the existence of 4.9–5.2 mg (3.4–3.6 mL) of oxygen within their structure (Fortes et al., 2004). Cork stoppers with insect galleries, as seen previously, have higher porosity coefficient and comparatively a higher empty fraction and accordingly more oxygen that can be transferred to the wine. Oliveira et al. (2015b) found a positive correlation between the oxygen ingress rates immediately after bottling and the voids in the bottom part of the cork stopper i.e. innermost part in the bottle.

On the contrary, in stoppers with wetcork spots the cells have shrunk and collapsed during the drying process leading to a lower percentage of air contained in the cell lumen. This is similar to the effect of having smaller cells as derived from thinner cork rings. In fact, Oliveira et al. (2013) found significant differences between oxygen ingress of stoppers produced from thin and thick calliper planks, and explained the differences by the higher proportion of smaller cells with thicker cell walls in the thin calliper planks, therefore with less air filling the empty volume and an increased barrier to the diffusion of gases. Moreover, stoppers with wetcork have a lower porosity coefficient (Tables 1 and 2) meaningless voids and consequently less air trapped in their structure, registering lower oxygen ingress immediately after bottling.

The average oxygen ingress rates after the fourth month of storage were 1.2 μg/day, 1.5 μg/day and 0.9 μg/day, respectively, for stoppers with ants and *C. larvae* galleries and wetcork (Table 3). Oliveira et al. (2013) reported average oxygen ingress rates after the fourth month of 1.5 μg/day. The similarity of the values found suggests that the galleries were present only near the cork stopper surface and therefore only impacted on the short-term oxygen ingress (the first 3 months).

The results indicate that the presence of galleries inside the stopper has a major influence on the oxygen ingress rate in the first month of storage but after that period the stoppers have a similar behaviour with oxygen ingress stabilizing at low and constant rate. On the contrary, stoppers with wetcork regions allow mean oxygen ingress rates comparable to defect-free stoppers.

Despite the need for further studies, in this sense X-ray tomography may be considered as a future methodological approach for improvement of cork stoppers quality control through the detection of the hidden defects inside a stopper.

4. Conclusion

The image analysis of the cork stoppers' surface revealed that stoppers with insect galleries have an average porosity coefficient comparable to the worst commercial quality classes, while the stoppers with wetcork are comparable to the best quality classes.

X-ray tomography demonstrated to be useful as a non-destructive technique for the visualization and identification of cork internal defects and can be used in future for quality control, namely, to prevent wine leakage.

Regardless of the presence and type of defect, the kinetics of oxygen ingress into the bottle has a common logarithmic behaviour with time with higher rates in the first days after bottling that stabilize at small and approximately constant ingress rates after three months. The results demonstrated that stoppers with wetcork spots have generally a better sealing performance regarding oxygen ingress into the bottle, corroborating previous suggestions that the variation of oxygen ingress is a consequence of the natural differing features in the cell dimensions and air volume within the stopper's structure.

Acknowledgements

This work was supported by FEDER funds through the Operational Programme for Competitiveness Factors – COMPETE and by National Funds under the project FCOMP-01-0124-FEDER-005421. The research was carried out under the framework of Centro de Estudos Florestais, a research unit funded by Fundação para a Ciência e Tecnologia, Portugal (PEst OE/AGR/UI0239/2014). Funding from FCT is acknowledged by Vanda Oliveira as a doctoral student (SFRH/BD/77550/2011). The authors acknowledge the collaboration of UAVISION in X-ray tomography image acquisition.

References

Brotto, L., Battistutta, F., Tat, L., Comuzzo, P., Zironi, R., 2010. Modified nondestructive colorimetric method to evaluate the variability of oxygen diffusion rate through wine bottle closures. J. Agric. Food Chem. 58 (6), 3567–3572. http://dx.doi.org/10.1021/jf903846h.

Brunetti, A., Cesareo, R., Golosio, B., Luciano, P., Ruggero, A., 2002. Cork quality estimation by using Compton tomography. Nucl. Instrum. Methods Phys. Res., Sect. B 189 (1–2), 161–168. http://dx.doi.org/10.1016/S0168-583X(02)01289-2.

Cammell, M.E., Way, M.J., Paiva, M.R., 1996. Diversity and structure of ant communities associated with oak, pine, eucalyptus and arable habitats in Portugal. Insectes Soc. 43 (1), 37–46. http://dx.doi.org/10.1007/BF01253954.

Carpintero, E., Jurado, M., Prades, C., 2014. Application of a kiln drying technique to *Quercus suber* L. cork planks. Food Bioprod. Process. 93, 176–185. http://dx.doi.org/10.1016/j.fbp.2013.12.010.

Chang, J., Han, G., Valverde, J.M., Griswold, N.C., Duque-Carrillo, J.-F., Sanchez-Sinencio, E., 1997. Cork quality classification system using a unified image processing and fuzzy-neural network methodology. IEEE Trans. Neural Networks 8 (4), 964–974. http://dx.doi.org/10.1109/72.595897.

Costa, A., Pereira, H., 2006. Decision rules for computer-vision quality classification of wine natural cork stoppers. Am. J. Enol. Viticult. 57 (2), 210–219.

Costa, A., Pereira, H., 2009. Computer vision applied to cork stoppers inspection. In: Zapata, Santiago (Ed.), Cork Oak Woodlands and Cork Industry: Present, Past and Future. Museu del Suro de Palafrugell, Barcelona, pp. 394–405.

Costa, A., Pereira, H., 2013. Drying kinetics of cork planks in a cork pile in the field. Food Bioprod. Process. 91 (1), 14–22. http://dx.doi.org/10.1016/j.fbp.2012.08.002.

Donepudi, V.R., Cesareo, R., Brunetti, A., Zhong, Z., Yuasa, T., Akatsuka, T., Takeda, T., Gigante, G.E., 2010. Cork embedded internal features and contrast mechanisms with Dei using 18, 20, 30, 36, and 40 keV Synchrotron X-rays. Res. Nondestr. Eval. 21 (3), 171–183. http://dx.doi.org/10.1080/09349847.2010.493990.

Fortes, M.A., Rosa, M.E., Pereira, H., 2004. A Cortiça. IST Press, Lisbon.

Gallardo, A., Jiménez, A., Antonietty, C.A., Villagrán, M., Ocete, M.E., Soria, F.J., 2012. Forecasting infestation by *Coraebus undatus* (Coleoptera, Buprestidae) in cork oak forests. Int. J. Pest Manage. 58 (3), 275–280. http://dx.doi.org/10.1080/09670874.2012.698765.

Godden, P., Lattey, K., Francis, L., Gishen, M., Cowey, G., Holdstock, M., Robinson, E., Waters, E., Skouroumounis, G., Sefton, M., Capone, D., Kwiatkowski, M., Field, J., Coulter, A., D'Costa, N., Bramley, B., 2005. Towards offering wine to the consumer in optimal condition - the wine, the closures and other packaging variables. A review of AWRI research examining the changes that occur in wine after bottling. Aust. NZ Wine Ind. J. 20 (4), 20–30.

González-Adrados, J., Pereira, H., 1996. Classification of defects in cork planks using image analysis. Wood Sci. Technol. 30 (3), 207–215. http://dx.doi.org/10.1007/BF00231634.

Gonzalez-Adrados, J., Lopes, F., Pereira, H., 2000. Quality grading of cork planks with classification models based on defect characterisation. Holz als Roh- und Werkstoff 58 (1–2), 39–45. http://dx.doi.org/10.1007/s001070050383.

Hor, Y.L., Federici, J.F., Wample, R.L., 2008. Nondestructive evaluation of cork enclosures using terahertz/millimetre wave spectroscopy and imaging. Appl. Opt. 47 (1), 72–78. http://dx.doi.org/10.1364/AO.47.000072.

Jiménez, A., Gallardo, A., Antonietty, C.A., Villagrán, M., Ocete, M.E., Soria, F.J., 2012. Distribution of *Coraebus undatus* (Coleoptera: Buprestidae) in cork oak forests of southern Spain. Int. J. Pest Manage. 58 (3), 281–288. http://dx.doi.org/10.1080/09670874.2012.700493.

Jordanov, I., Georgieva, A., 2009. Neural network classification: a cork industry case. In: Proceedings of the IEEE International Symposium on Industrial Electronics, Seoul. http://dx.doi.org/10.1109/ISIE.2009.5213287.

Karbowiak, T., Gougeon, R.D., Alinc, J.-B., Brachais, L., Debeaufort, F., Voilley, A., Chassagne, D., 2010. Wine oxidation and the role of cork. Crit. Rev. Food Sci. Nutr. 50 (1), 20–52. http://dx.doi.org/10.1080/10408398.2010.526854.

Lagorce-Tachon, A., Karbowiak, T., Loupiac, C., Gaudry, A., Ott, F., Alba-Simionesco, C., Gougeon, R.D., Alcantara, V., Mannes, D., Kaestner, A., Lehmann, E., Bellat, J.-P., 2015. The cork viewed from the inside. J. Food Eng. 149, 214–221. http://dx.doi.org/10.1016/j.jfoodeng.2014.10.023.

Lopes, P., Saucier, C., Glories, Y., 2005. Nondestructive colorimetric method to determine the oxygen diffusion rate through closures used in winemaking. J. Agric. Food Chem. 53 (18), 6967–6973. http://dx.doi.org/10.1021/jf0404849.

Lopes, P., Saucier, C., Teissedre, P.-L., Glories, Y., 2006. Impact of storage position on oxygen ingress through different closures into wine bottles. J. Agric. Food Chem. 54 (18), 6741–6746. http://dx.doi.org/10.1021/jf0614239.

Lopes, P., Saucier, C., Teissedre, P.-L., Glories, Y., 2007. Main routes of oxygen ingress through different closures into wine bottles. J. Agric. Food Chem. 55 (13), 5167–5170. http://dx.doi.org/10.1021/jf0706023.

Mukherjee, S., Federici, J., 2011. Study of structural defects inside natural cork by pulsed terahertz tomography. In: Proceedings of 36th International Conference on Infrared, Millimeter and Terahertz Waves (IRMMW-THz), Houston, USA. http://dx.doi.org/10.1109/irmmw-THz.2011.6104965.

Oliveira, V., Knapic, S., Pereira, H., 2012. Natural variability of surface porosity of wine cork stoppers of different commercial classes. J. Int. des Sci. de la Vigne et du Vin 46 (4), 331–340.

Oliveira, V., Lopes, P., Cabral, M., Pereira, H., 2013. Kinetics of oxygen ingress into wine bottles closed with natural cork stoppers of different qualities. Am. J. Enol. Viticult. 64 (3), 395–399. http://dx.doi.org/10.5344/ajev.2013.13009.

Oliveira, V., Knapic, S., Pereira, H., 2015a. Classification modelling based on surface porosity for the grading of natural cork stoppers for quality wines. Food Bioprod. Process. 93, 69–76. http://dx.doi.org/10.1016/j.fbp.2013.11.004.

Oliveira, V., Van den Bulcke, J., Van Acker, J., de Schryver, T., Pereira, H., 2015b. Cork structural discontinuities studied with X-ray microtomography. Holzforschung. http://dx.doi.org/10.1515/hf-2014-0245.

Pereira, H., 2007. Cork: Biology, Production and Uses. Elsevier, Amsterdam.

Pereira, H., Rosa, M.E., Fortes, M.A., 1987. The cellular structure of cork from *Quercus suber* L. IAWA J. 8 (3), 213–218. http://dx.doi.org/10.1163/22941932-90001048.

Pereira, H., Melo, B., Pinto, R., 1994. Yield and quality in the production of cork stoppers. Holz als Roh- und Werkstoff 52 (4), 211–214. http://dx.doi.org/10.1007/BF02619093.

Pereira, H., Lopes, F., Graça, J., 1996. The evaluation of the quality of cork planks by image analysis. Holzforschung 50 (2), 111–115. http://dx.doi.org/10.1515/hfsg.1996.50.2.111.

Radeva, P., Bressan, M., Tovar, A., Vitrià, J., 2002. Bayesian classification for inspection of industrial products. In: Topics in Artificial Intelligence. Proceedings of 5th Catalonian Conference on AI, 2504, pp. 399–407. http://dx.doi.org/10.1007/3-540-36079-4_35.

Ribéreau-Gayon, J., 1933. Dissolution d'oxygène dans les vins. In Contribution à l'étude des oxidations et réductions dans les vins. Application à l'étude d. vieillissement et des cases. Delmas, Bordeaux, France, pp. 35.

Ruiz, E., Martínez, M.H., Martínez, M.D., Hernández, J.M., 2006. Morphological study of the stridulatory organ in two species of Crematogaster genus: *Crematogaster scutellaris* (Olivier 1792) and *Crematogaster auberti* (Emery 1869)

(Hymenoptera: Formicidae). Annales de la Société Entomologique de France (N.S.), vol. 42(1). Springer, pp. 99–105. http://dx.doi.org/10.1080/00379271.2006.10697454.

Sallé, A., Nageleisen, L.-M., Lieutier, F., 2014. Bark and wood boring insects involved in oak declines in Europe: current knowledge and future prospects in a context of climate change. For. Ecol. Manage. 328, 79–93. http://dx.doi.org/10.1016/j.foreco.2014.05.027.

Schindelin, J., Arganda-Carreras, I., Frise, E., Kaynig, V., Longair, M., Pietzsch, T., Preibisch, S., Rueden, C., Saalfeld, S., Schmid, B., Tinevez, J.-Y., White, D.J., Hartenstein, V., Eliceiri, K., Tomancak, P., Cardona, A., 2012. Fiji: an open-source platform for biological-image analysis. Nat. Methods 9 (7), 676-682. http://dx.doi.org/10.1038/nmeth.2019.

Schmid, B., Schindelin, J., Cardona, A., Longair, M., Heisenberg, M., 2010. A high-level 3D visualization API for Java and ImageJ. BMC Bioinformatics 11, 274. http://dx.doi.org/10.1186/1471-2105-11-274.

Sañer, D., Abós, L., 1992. Determinación de la incidencia de Crematogaster scutellaris (Olivier, 1791), en los alcornocales del nordeste de la Península Ibérica. Scientia Gerundensis 18, 223–233.

Webb, A., 2003. Introduction to Biomedical Imaging. John Wiley & Sons Inc, Hoboken, New Jersey.

INTEGRATIVE DISCUSSION

In this work we analysed the cork structural characteristics and their influence on the oxygen ingress through wine stoppers aiming to contribute to an increased added-value of the natural cork stoppers.

Cork is the closure material preferred by wine consumers. It is an outstanding material when in-bottle wine aging is wanted, by combining the required minute oxygen transfer with mechanical sealing of the bottle, durability and chemical stability (Lopes et al. 2005, Pereira 2007, 2015). However, the natural variability of cork brings some performance heterogeneity that producers and consumers would like to circumvent. Among the performance properties, the oxygen transmission rate (OTR) into the closed bottle is one important parameter for the wine cellars given its relation to the quality development of the wines (Caillé et al. 2010, Mas et al. 2002, Lopes et al. 2005, 2006, Kontoudakis et al. 2008, Silva et al. 2011). Therefore the OTR properties of cork stoppers will define its ability as quality sealant, also in comparison with other types of wine closures (Escudero et al. 2002, Lopes et al. 2006, Karbowiak et al. 2010). The path of oxygen ingress in the bottle was experimentally studied and it was shown that the oxygen coming into the bottle and the wine during the storage period comes from the cork stopper itself, namely from its cellular structure (Lopes et al. 2007). In fact the cells of cork contain air-filled lumens while lenticular channels or other tissue voids may provide additional air-filled pockets (Pereira et al. 1987). The cork itself has very low permeability to oxygen (Faria et al. 2011, Lequin et al. 2012) and correspondingly the cork stoppers are essentially impermeable to atmospheric oxygen (Lopes et al. 2007).

Nowadays, the natural cork stoppers are graded into commercial quality classes in function of the visual homogeneity of their external surface mostly regarding the extent of the lenticular porosity or the presence of defects, as seen by human or machine vision (Costa and Pereira 2005, 2007, Pereira 2007). However, the stoppers within each quality class present a considerable heterogeneity in oxygen transmission rate (Lopes et al. 2006).

These results seem to indicate that the explanation for the heterogeneity of the natural cork stoppers within each quality class should lie in the specific features of their internal structure. It was in this context that the research project INCORK (FCOMP-01-0124-FEDER-005421), framework for this study, was developed with the participation of Amorim & Irmãos, Centro de Estudos Florestais, and New Jersey Institute of Technology. The study encompassed a detailed characterization of the natural cork stoppers using non-destructive methods including a surface analysis using image analysis and the use of X-ray tomography for material internal characterization, before the determination of the oxygen transmission rate after bottling.

The commercial quality classes of cork stoppers can be differentiated in general by the mean values of the main porosity features of their surface, namely dimension and concentration variables, considering either the lateral surface or tops. These features showed an increasing trend from the premium to standard quality class (Table 1, pages 49 and 60). On the contrary, shape variables (shape factor, sphericity, convexity, aspect ratio) present identical values between quality classes (Table 1, pages 49 and 60), as previously reported by Gonzalez-Adrados and Pereira (1996) and Costa and Pereira (2009), and the colour-type variables showed differences between classes although without a trend with an average RGB of pores of 74.4, 61.5 and 65.8 for good, and 61.5, 46.0 and 51.3 for standard stoppers (Table 1, page 49).

The porosity features shown by the external surface of cork stoppers differentiate the three main commercial classes used nowadays (Table 1, page 49). The premium class is characterized by an average porosity coefficient of 2.4% and 2.1% in their body and tops, respectively, with pores smaller than 5.7 mm^2 and with approximate 69% of the porosity resulting from pores smaller than 2 mm^2. The good quality class will have, on average, a porosity coefficient of 4.0% and 3.1% in the lateral surface and tops, respectively, with pores up to 10.6 mm^2 and 9.0 mm^2. Stoppers belonging to the standard class will have a porosity coefficient of 5.5% and 3.7% in the lateral surface and tops, respectively, with pores smaller than 16.1 mm^2 and nearly 40% of the porosity resulting from pores smaller than 2 mm^2. The large sampling that was used in the present study (600 cork stoppers) allows a strong confidence in the results, well above the results obtained previously with much smaller sampling (Costa and Pereira 2005, 2006, 2007, 2009).

The image analysis of cork stoppers also distinguishes defects in the cork structure that are important for their performance: empty ant gallery; *Coroebus undatus* F. larvae gallery; and wetcork. The cork with insect defects will be differentiated mostly by the features of the larger pore structures: each stopper with insect galleries contained, in average, 2 to 3 pores with dimension superior to 10 mm^2 corresponding probably to the insect galleries and showing an elongated form e.g. pores larger than 20 mm^2 presented average elongation of 4.2 and 8.8 for ant and *C.* larvae galleries, respectively (Table 2, page 84). On the contrary, the pores in wetcork retain their shape features regardless of dimension. Similar shape features were already reported and used to differentiate such defects by image analysis (Gonzalez-Adrados and Pereira, 1996; Gonzalez-Adrados et al., 2000).

The detailed study of the surface porosity of the stoppers gave also insight in aspects related to cork formation. The comparison of porosity between the two tops confirmed the existence

of axial variation in the tree e.g. one top may have significantly lower porosity than the other top. This can be used in practical terms in the production of cork stoppers that have one of the tops covered with a covering cap, such as those designed for bottling fortified wines and spirits, i.e., by selecting the top with the lowest porosity as the apparent top. On other hand, the surface of the cork stoppers is not homogeneous when comparing the transverse, tangential and radial sections around the lateral cylindrical body (Figures 6 to 9, pages 52 and 53). The anisotropy of porosity features shown by cork stoppers is a consequence of the biological development of cork and of their production method. The lenticular channels appear with a different aspect in the three sections: in the radial and transverse sections they look like elongated rectangular channels and in the tangential section they have a circular to elliptical form.

The results obtained in this work can be used to set better and quantified requirements for the quality classification of the stoppers. It is empirically known that the quality classification of stoppers is subjective to some extent and therefore varies between individual experts, as demonstrated by Barros and Pereira (1987) who reported classification match values of 31% for two operators and higher classification difficulty in the mid-quality classes. For that reason and using the results from cork stoppers surface characterization, several predictive classification models of stoppers into quality classes were built based on the presented surface characteristics using stepwise discriminant analysis (SDA) in order to select a specific set of variables (Table 2, page 61). The evaluation of those models suggests that: i) the observation of cork stoppers tops is irrelevant for the classification of cork stoppers in quality classes; ii) overall the porosity coefficient is the most important variable with discriminant power for separation of cork stoppers quality classes; iii) it seems that colour has an important discriminating power conferring a better accuracy to the models. A simplified model using the main discriminant features i.e. porosity coefficient and the RGB colour-type variables calculated for the body lateral surface can minimize the processing of data while keeping the model accuracy. The inclusion of colour-variables improves the classification and probably approximates more the model to the presently used classification related to visual appearance of cork stopper as perceived by the operator, thereby approximating the results from manual and automated grading.

X-ray tomography was used as a non-destructive technique to acquire knowledge on the internal structure of natural cork stoppers since previous studies suggested that oxygen diffuses mainly out of the cork itself into the wine and that oxygen permeability is not related with commercial quality classes (Lopes et al. 2007).The totality of the cork stoppers were

scanned using a medical X-ray CT scanner with a spatial resolution of 2 mm/voxel that allows the visualization of structures larger than 4 mm^2 when seen in 2D or 8 mm^3 in 3D. The results allowed an understanding of the inner structure of the cork stoppers (Figure 2, page 84) but, due to the low resolution of the images obtained, porosity quantification by determination of volume was not possible. However, the visualization and identification of some defects within the cork stopper was possible due to the non-destructive nature of the X-ray tomography analysis and the relationship between X-ray absorption and material density. For instance the ant galleries are typically empty and run through the cork plank in random directions, they can appear at the cork stopper surface as small holes that may go unnoticed even to expert's operators and can constitute a free path through the stopper leading to wine leakage (Figure 2, page 84). On other hand, *C.* larvae galleries are filled with residual material that has a density well above that from the surrounding cork tissue; the galleries are embedded in the cork tissue with a spatial development in vertical and tangential directions in the growth rings (Figure 2, page 84). With X-ray tomography, and contrary to what happens with surface image analysis, the wetcork regions are clearly visible and distinguished as brighter areas due to the higher density resulting from cells shrinkage and collapse during the drying process (Figure 2, page 84).

Following the X-ray scanning, the natural cork stoppers were used for the closure of bottles and oxygen diffusion measurements were made along time. The kinetics of oxygen transfer was similar i.e. including stoppers of the three quality classes and with defects, and could be adjusted to logarithmic models (Figure 1, page 68). There is quick and high oxygen ingress in the first days after bottling, with an initial high ingress rate, followed by a decreasing ingress rates until the 1st month and further on, until stabilizing a low and rather constant ingress rate from the 3rd to the 12th month and thereafter. In fact, it was observed that on average 35% of the overall ingress of oxygen occurred in the first 5 days, 59% in the 1st month and 78% in the first 3 months (Table 2, page 69). However, a considerable variability was found: the oxygen ingress at 12 months ranged between 0.3 mg and 4.8 mg and 21% of the stoppers reached 4.2 mg (the limit of oxygen quantification allowed by the method used) along the experiment. No influence of the quality class of the stoppers was found in the oxygen transfer to the bottle (Table 1, page 69), as a previous study of Lopes et al. (2005) already reported.

In order to understand and explain this variability, we should analyse the cork cell structure and the amount of oxygen contained therein. As primarily suggested by Ribéreau-Gayon (1933), oxygen ingress into bottles occurs mainly out of the cork structure due to the high internal pressure in the cork cells created when the cork stoppers are compressed into the

bottleneck. Natural cork stoppers with 24 mm diameter and 45 mm length have a volume of 20.4 mL of which 80-85% is air contained in the cell lumen, implying the existence of 4.9-5.2 mg of oxygen within their structure (Fortes et al. 2004). Our results show that, in average, 1.88 mg and 2.35 mg of oxygen diffuse from the natural cork stoppers that were bored out of cork planks with 27-32 mm and 45-54 mm callipers, respectively, representing 36-38% and 47-50% of the theoretically total oxygen present in the cell structure.

Moreover, the results from stoppers with defects (Figure 4, page 85) show that the oxygen ingress from stoppers with insect galleries is higher (66.5 and 63.1 μg/day in the first month) than the average found for stoppers without defects (42.0 μg/day), while the contrary applies for wetcork (39.9 μg/day). The limit of oxygen quantification was reached before the end of the experiment for 27% of stoppers with ant galleries, 23% with *C.* larvae galleries and 13% with wetcork spots.

These results corroborate the assumption that the high oxygen ingress rate observed during the first month after bottling is due to the air forced out of the cork structure when stoppers are compressed into the bottleneck and suggest that the variation of oxygen ingress is mainly a consequence of the natural differing features in the cell dimensions and air volume within the stopper's structure.

Considering that a correlation between surface porosity features and oxygen transmission rate was not found, and that oxygen results emphasized the need of quantification for the internal porosity features, led us to the search for the acquisition of X-ray images with higher resolution. With financial support of the Trees4Future project, the porosity quantification was possible for a selected sample of 10 cork stoppers scanned using a high resolution prototype X-ray equipment built at the Centre for X-ray Computed Tomography (UGCT, Ghent University, Belgium; www.ugct.ugent.be). The stoppers were selected to cover a wide range of properties: the lateral surface porosity coefficient ranged from 1.1% to 8.6%, the top surface porosity coefficient ranged from 0.7% to 4.7%, density ranged from 152.0 kg m^{-3} to 262.7 kg m^{-3}, and the total amount of oxygen ingress after 30 days ranged from 1.4 mg to 4.0 mg (Table 1, page 75).

The image resolution achieved with this equipment (voxel size of 50 μm) allowed the observation of lenticular channels development and geometry (Figure 1, page 74). The channels are loosely filled with a tissue of rigid unsuberified cells with thick walls, showing ruptures and intercellular voids in a great extent (Pereira 2007). The region bordering the lenticular channels showed higher density than the surrounding material due to the presence

of lignified and thick-walled cells at their borders (Figure 1, page 74). With this resolution it was possible to quantify the extracellular void and high density regions (HDR) fractions. The void fraction ranged from 0.7% to 2.3% while the maximum single void volume ranged from 7.9 mm^3 to 104.9 mm^3. The total HDR volume ranged from 231 mm^3 to 2747 mm^3, corresponding to a HDR fraction of 1.3% and 19.2% respectively (Table 2, page 76).

Considering the hypothesis that the initial high ingress rate of oxygen into the bottle should be related to the cork structural discontinuities, i.e. more specifically to the void fraction and the air located there, a first approach was made to relate the total extracellular void volume of the cork stoppers with the oxygen ingress rate at 30 days after bottling. The linear relation calculated had a coefficient of determination (R^2) of 0.41. It was then considered that probably only the air present in the lower part of the cork stopper could ingress into the bottle during this period and the void volume was calculated by taking only the innermost 1/3 of the stopper, i.e. the part in contact to the bottled liquid. The linear regression established between these data had a coefficient of determination (R^2) of 0.83 and adjusted R^2 of 0.81. These results suggest that the high oxygen ingress rates immediately after bottling are due to the transfer of the air trapped in the voids in the bottom part of the cork stopper. After this first period, gas transport through the cork cells occurs with very low diffusion rates through small channels (i.e. through the plasmodesmata) present in the cork cells walls (Faria et al. 2011).

Despite the positive relationship found between the porosity coefficient calculated by surface image analysis and the microtomography (Figure 3a, page 76), the surface image analysis seems to be a poor predictor of the cork stoppers internal void fraction. In the same way, even if, in a first approach, it is conceivable that numerous voids could reduce the density of cork, making therefore density a good predictor of the void fraction, this was not the case, and a relation between density and the void fraction was not found. This means that porosity in cork is not equivalent to voids namely because the lenticular channels are filled with non-suberous material and often bordered by thick walled lignified cells.

The evidence that the void fraction of lenticular channels in the innermost part of the cork stopper inserted in the bottle was strongly related to the oxygen ingress in the first month after bottling can be used for quality enhancement of natural cork stoppers with incorporation of performance requirements.

In view of the results and of the availability of rapid microtomography scanning set-ups, this kind of approach to improve the quality control of natural cork stoppers seems to be feasible.

CONCLUSIONS AND FUTURE WORK

The research carried out in this PhD work allowed gathering knowledge on the oxygen transfer performance of natural cork stoppers and on its relation with porosity and structural features. This was possible with a detailed characterization of the surface porosity and the determination of oxygen transmission rate after bottling in a large sample of natural cork stoppers. Using tomography, it was possible to elucidate the internal porosity spatial distribution and to identify critical parameters of the internal structure of natural cork stoppers that could be responsible the heterogeneity found across the visual quality classes of the oxygen transmission rate.

Consequently, the results achieved contribute to a valorisation enhancement of the natural cork stoppers and the knowledge can be used for accomplishing higher levels of quality and consistency in performance.

Considering the specific objectives of the work, the conclusions can be summarized as follows:

1. X-ray microtomography can be successfully applied for visualization and quantification of cork structural discontinuities, which are decisive for the commercial value of raw cork and of cork products. The image resolution achieved (voxel size of 50 µm) allowed the observation of lenticular channels development and geometry and it was possible to quantify the void and high density regions (HDR) fractions within each cork stopper.
2. The variation of oxygen transmission rate is a consequence of the natural differing features in the cell dimensions and air volume within the stopper's structure, namely the void fraction (lenticular channels and possible defects) in the innermost part of the cork stopper.
3. The oxygen transmission rate of natural corks stoppers is independent of the parameters presently used for quality evaluation such as visual quality grades or density. Moreover, such parameters cannot be used to infer about internal structural features of the natural cork stopper that are related to the oxygen transmission rate.

Despite the need for further studies, the results suggest that microtomography scanning can be used for the development of a new integrated system for non-destructive evaluation and quality control of natural cork stoppers. It is expected that such integrated system should include the visual quality of the cork surface as well as the performance requirements regarding oxygen transmission quality classes. Considering that nowadays there are very fast CT scanning set-ups, this non-destructive technique may be used for in-line cork stoppers quality control.

The results found in the studies contained in this thesis and the conclusions presented here suggest that further research is needed:

- Further microtomography scanning of a larger sample of natural cork stoppers is required to corroborate the evidence that the void fraction in the innermost part of the cork stopper is related to the oxygen ingress in the first month after bottling. The microtomography scanning should be applied in cork stoppers prior to the insertion into the bottleneck and the measures of oxygen transmission rate.
- Microporosimetry analysis could be used for determination of accessible porosity and pore size distribution, corroborating and complementing the results from microtomography. This technique could reveal features with dimension smaller than the microtomography resolution limit and explain some of the variability found in oxygen transmission rate.
- In a future work it is important to have a characterization of cork permeability in relation to compression, and both related to the cellular features. The effect of compression in the internal structure of lenticular channels and other features is also an important aspect.
- A further aspect that was not approached here but that could have importance in the performance of the cork stoppers regarding oxygen transfer and compression behaviour is the chemical composition of cork itself e.g. regarding extractives, suberin and lignin content.

REFERENCES

Anjos O, Pereira H, Rosa ME (2008) Effect of quality, porosity and density on the compression properties of cork. Holz Roh Werkst 66:295-301. DOI: 10.1007/s00107-008-0248-2

APCOR (2015) Cork Yearbook 2015. Portuguese Cork Association, Santa Maria de Lamas, Portugal

Axelsson M, Svensson S (2010) 3D pore structure characterization of paper. Pattern Anal Applic 13:159-172. DOI: 10.1007/s10044-009-0146-1

Barber NA, Taylor CD, Dodd TH (2008) Twisting tradition: Consumers' behavior toward alternative closures. J Food Prod Market 15:80-103. DOI: 10.1080/10454440802470615

Benkirane H, Benslimane R, Hachmi M, Sesbou A (2001) Possibilité de contrôle automatique de la qualité du liège par vision artificielle. Ann For Sci 58:455-465. DOI: 10.1051/forest:2001139

Bessières J, Maurin V, George B, Molina S, Masson E, Merlin A (2013) Wood-coating layer studies by X-ray imaging. Wood Sci Technol 47:853-867. DOI: 10.1007/s00226-013-0546-7

Besson CK, Lobo-do-Vale R, Rodrigues ML, Almeida P, Herd A, Grant OM, David TS, Schmidt M, Otieno D, Keenan TF, Gouveia C, Mériaux C, Chaves MM, JS (2014) Cork oak physiological responses to manipulated water availability in a Mediterranean woodland. Agr Forest Meteorol 184: 230-242. DOI: 10.1016/j.agrformet.2013.10.004

Bleibaum RN (2013) Wine Closures - Research Update 2013. Is cork experiencing a renaissance? Tragon Corporation

Boden S, Schinker MG, Duncker P, Spiecker H (2012) Resolution abilities and measuring depth of high-frequency densitometry on wood samples. Measurement 45:1913-1921.DOI: 10.1016/j.measurement.2012.03.013

Bolte S, Cordelières FP (2006) A guided tour into subcellular colocalization analysis in light microscopy. J Microsc 224:213-232.

Brabant L, Vlassenbroeck J, De Witte Y, Cnudde V, Boone MN, Dewanckele J, Van Hoorebeke L (2011) Three-dimensional analysis of high-resolution X-ray computed tomography data with Morpho+. Microsc Microanal 17:252-263. DOI: 10.1017/S1431927610094389

Brazinha C, Fonseca AP, Pereira H, Teodoro OM, Crespo JG (2013) Gas transport through cork: Modelling gas permeation based on the morphology of a natural polymer material. J Membrane Sci 428:52-62. DOI: 10.1016/j.memsci.2012.10.019

Brunetti A, Cesareo R, Golosio B, Luciano P, Ruggero A (2002) Cork quality estimation by using Compton tomography. Nucl Instrum Methods Phys Res Sect B-Beam Interact Mater Atoms 196:161-168.DOI: 10.1016/S0168-583X(02)01289-2

Caillé S, Samson A, Wirth J, Diéval J-B, Vidal S, Cheynier V (2010) Sensory characteristics changes of red Grenache wines submitted to different oxygen exposures pre and post bottling. Anal Chim Acta 660:35-42.DOI: 10.1016/j.aca.2009.11.049

Caritat A, Gutiérrez E, Molinas M (2000) Influence of weather on cork-ring width. Tree Physiol 20:893-900.

Catry FX, Moreira F, Cardillo E, Pausas, JG (2012) Post-Fire Management of Cork Oak Forests. In: Moreira F, Arianoutsou M, Corona P, De las Heras J (eds) Post-Fire Management and Restoration of Southern European Forests. Springer Netherlands, Dordrecht, pp 195-222. DOI: 10.1007/978-94-007-2208-8_9

Celiège (2013) International Code of Cork Stopper Manufacturing Practice – Edition 6.05. European Cork Federation, Paris, France

Česen A, Korat L, Mauko A, Legat A (2013) Microtomography in Building Materials. Mater Technol 47:661-664.

Chang J, Han G, Valverde JM, Griswold NC, Duque-Carrillo J-F, Sanchez-Sinencio E (1997) Cork quality classification system using a unified image processing and fuzzy-neural network methodology. IEEE Trans Neural Netw 8:964-974. DOI: 10.1109/72.595897

Cnudde V, Boone MN (2013) High-resolution X-ray computed tomography in geosciences: A review of the current technology and applications. Earth-Sci Rev 123:1-17. DOI: 10.1016/j.earscirev.2013.04.003

Costa A, Pereira H, Oliveira A (2002) Influence of climate on the seasonality of radial growth of cork oak during a cork production cycle. Ann For Sci 59:429-437. DOI: 10.1051/forest:2002017

Costa A, Pereira H (2004) Caracterização e análise de rendimento da operação de traçamento na preparação de pranchas de cortiça para a produção de rolhas. Silva Lusitana 12:51-66

Costa A, Pereira H (2005) Quality characterization of wine cork stoppers using computer vision. J Int Sci Vigne Vin 9:209-218

Costa A, Pereira H (2006) Decision rules for computer-vision quality classification of wine natural cork stoppers. Am J Enol Vitic 57:210-219

Costa A, Pereira H (2007) Influence of vision systems, black and white, colored and visual digitalization, in natural cork stopper quality estimation. J Sci Food Agric 87:2222-2228. DOI: 10.1002/jsfa.2947

Costa A, Madeira M, Oliveira AC (2008) The relationship between cork oak growth patterns and soil, slope and drainage in cork oak woodland in Southern Portugal. Forest Ecol Manag 255: 1525-1535. DOI: 10.1016/j.foreco.2007.11.008

Costa A, Pereira H (2009) Computer vision applied to cork stoppers inspection. In: Santiago Zapata (eds), Cork oak woodlands and cork industry: present, past and future. Barcelona, pp 394-405

Costa A, Pereira H, Madeira M (2009) Landscape dynamics in endangered cork oak woodlands in Southwestern Portugal (1958–2005). Agroforest Syst 77: 83-96. DOI: 10.1007/s10457-009-9212-3

Costa A, Pereira H (2010) Influence of cutting direction of cork planks on the quality and porosity characteristics of natural cork stoppers. Forest Systems 19:51-60

Cumbre F, Lopes F, Pereira H (2000) The effect of water boiling on annual ring width and porosity of cork. Wood Fiber Sci 32:125-133.

David TS, Henriques MO, Kurz-Besson C, Nunes J, Valente F, Vaz M, Pereira JS, Siegwolf R, Chaves MM, Gazarini LC, David JS (2007) Water-use strategies in two co-occuring Mediterranean evergreen oaks: surviving the summer drought. Tree Physiol 27: 793-803.

David TS, Pinto CA, Nadezhdina N, Kurz-Besson C, Henriques MO, Quilhó T, Cermak J, Chaves MM, Pereira JS, David JS (2013) Root functioning, tree water use and hydraulic redistribution in Quercus suber trees: A modeling approach based on root sap flow. Forest Ecol Manag 307:136-146. DOI: 10.1016/j.foreco.2013.07.012

Demertzi M, Silva RP, Neto B, Dias AC, Arroja L (2016) Cork stoppers supply chain: potential scenarios for environmental impact reduction. J Cleaner Production 113: 1985-1994. DOI: 10.1016/j.jclepro.2015.02.072

Dewanckele J, De Kock T, Boone MA, Cnudde V, Brabant L, Boone MN, Fronteau G, Van Hoorebeke L, Jacobs P (2012) 4D imaging and quantification of pore structure modifications inside natural building stones by means of high resolution X-ray CT. Sci Total Environ 416: 436-448. DOI: 10.1016/j.scitotenv.2011.11.018

Dierick M, Van Loo D, Masschaele B, Boone MN, Van Hoorebeke L (2010) A LabVIEW (R) based generic CT scanner control software platform. J X-Ray Sci Technol 18:451-461. DOI: 10.3233/XST-2010-0268

Dierick M, Van Loo D, Masschaele B, Van den Bulcke J, Van Acker J, Cnudde L, Van Hoorebeke L (2014) Recent micro-CT scanner developments at UGCT. Nucl Instrum Methods Phys Res Sect B-Beam Interact Mater Atoms 324: 35-40. DOI: 10.1016/j.nimb.2013.10.051

Donepudi VR, Cesareo R, Brunetti A, Zhong Z, Yuasa T, Akatsuka T, Takeda T, Gigante GE (2010) Cork embedded internal features and contrast mechanisms with Dei using 18, 20, 30, 36, and 40 keV Synchrotron X-rays. Res Nondestruct Eval 21:171-183. DOI: 10.1080/09349847.2010.493990

Escudero A, Asensio E, Cacho J, Ferreira V (2002) Sensory and chemical changes of young white wines stored under oxygen. An assessment of the role played by aldehydes and some other important odorants. Food Chem 77:325-331. DOI: 10.1016/S0308-8146(01)00355-7

Faria DP, Fonseca AL, Pereira H, Teodoro OMND (2011) Permeability of cork to gases. J Agric Food Chem 59:3590-3597. DOI: 10.1021/jf200491t

Ferreira A, Lopes F, Pereira H (2000) Caractérisation de la croissance et de la qualité du liège dans une région de production. Ann For Sci 57:187-193. DOI: 0.1051/forest:2000169

Fortes MA, Rosa ME (1992) Growth stresses and strains in cork. Wood Sci Technol 26:241-58. DOI: 10.1007/BF00200160

Fortes MA, Rosa ME, Pereira H (2004) A Cortiça. IST Press, Lisbon

Gea-Izquierdo G, Fernández-de-Uñu L, Cañellas I (2013) Growth projections reveal local vulnerability of Mediterranean oaks with rising temperatures. For Ecol Manag 305:282–293. DOI:10.1016/j.foreco.2013.05.058

Godden P, Lattey K, Francis L, Gishen M, Cowey G, Holdstock M, Robinson E, Waters E, Skouroumounis G, Sefton M, Capone D, Kwiatkowski M, Field J, Coulter A, D'Costa N, Bramley B (2005) Towards offering wine to the consumer in optimal condition - the wine, the closures and other packaging variables. A review of AWRI research examining the changes that occur in wine after bottling. Wine Ind J 20:20-30.

Gómez-Plaza E, Cano-López M (2011) A review on micro-oxygenation of red wines: Claims, benefits and the underlying chemistry. Food Chem 125:1131-1140. DOI: 10.1016/j.foodchem.2010.10.034

Gonzalez-Adrados J, Pereira H (1996) Classification of defects in cork planks using image analysis. Wood Sci Technol 30:207-215. DOI: 10.1007/BF00231634

Gonzalez-Adrados J, Lopes F, Pereira H (2000) Quality grading of cork planks with classification models based on defect characterisation. Holz Roh Werkst 58:39-45. DOI: 10.1007/s001070050383

Gonzalez-Adrados JR, Garcia-Vallejo MC, Caceres-Esteban MJ, de Ceca JL, Gonzalez-Hernandez F, Calvo-Haro R (2012) Control by ATR-FTIR of surface treatment of cork stoppers and its effect on their mechanical performance. Wood Sci Technol 46:349-60. DOI: 10.1080/02773813.2011.599697

Graça J, Pereira H (2004) The periderm development in Quercus suber. IAWA Bull 25:325-336. DOI: 10.1163/22941932-90000369

Granda E, Camarero JJ, Gimeno TE, Martínez-Fernández J, Valladares F (2013) Intensity and timing of warming and drought differentially affect growth patterns of co-occuring Mediterranean tree species. Eur J For Res 132:469‑480. DOI:10.1007/s10342-013-0687-0

Han G, Ugliano M, Currie B, Vidal S, Diéval J-B, Waterhouse AL (2015) Influence of closure, phenolic levels and microoxygenation on Cabernet Sauvignon wine composition after 5 years' bottle storage. J Sci Food Agric 95: 36-43. DOI: 10.1002/jsfa.6694

Helama S, Bégin Y, Vartiainen M, Peltola H, Kolström T, Meriläinen J (2012) Quantifications of dendrochronological information from contrasting microdensitometric measuring circumstances of experimental wood samples. Appl Radiat Isot 70:1014-1023.DOI: 10.1016/j.apradiso.2012.03.025

Hor YL, Federici JF, Wample RL (2008) Nondestructive evaluation of cork enclosures using terahertz/millimetre wave spectroscopy and imaging. Appl Optics 47:72-78. DOI: 10.1364/AO.47.000072

Ikonen V-P, Peltola H, Wilhelmsson L, Kilpeläinen A, Väisänen H, Nuutinen T, Kellomäki S (2008) Modelling the distribution of wood properties along the stems of Scots pine (Pinus sylvestris L.) and Norway spruce (Picea abies (L.) Karst.) as affected by silvicultural management. For Ecol Manage 256:1356-1371. DOI: 10.1016/j.foreco.2008.06.039

Jordanov I, Georgieva A (2009) Neural network classification: a cork industry case. In: IEEE Computer Society (ed.), IEEE International Symposium on Industrial Electronics. Seoul, pp 232-237

Karbowiak T, Gougeon RD, Alinc J-B, Brachais L, Debeaufort F, Voilley A, Chassagne D (2010) Wine oxidation and the role of cork. CRC Crit Rev Food Sci Nutr 50:20-52. DOI: 10.1080/10408398.2010.526854

Kim K, Yoon H, Diez-Silva M, Dao M, Dasari R, Park Y (2014) High-resolution three-dimensional imaging of red blood cells parasitized by Plasmodium falciparum and in situ hemozoin crystals using optical diffraction tomography. J Biomed Opt 19:011005. DOI: 10.1117/1.JBO.19.1.011005

Knapic S, Pirralho M, Louzada JL, Pereira H (2014) Early assessment of density features for 19 Eucalyptus species using X-ray microdensitometry in a perspective of potential biomass production. Wood Sci Technol 48:37-49. DOI: 10.1007/s00226-013-0579-y

Kontoudakis K, Biosca P, Canals R, Fort F, Canals JM, Zamora F (2008) Impact of stopper type on oxygen ingress during wine bottling when using an inert gas cover. Aust J Grape Wine Res 14:116-122. DOI: 10.1111/j.1755-0238.2008.00013.x

Lagorce-Tachon A, Karbowiak T, Simon J-M, Gougeon R, Bellat J-P (2014) Diffusion of oxygen through cork stopper: Is it a Knudsen or a Fickian mechanism? J Agric Food Chem 62:9180-9185. DOI: 10.1021/jf501918n

Lagorce-Tachon A, Karbowiak T, Loupiac C, Gaudry A, Ott F, Alba-Simionesco C, Gougeon RD, Alcantara V, Mannes D, Kaestner A, Lehmann E, Bellat J-P (2015) The cork viewed from the inside. J Food Eng 149:214-221. DOI: 10.1016/j.jfoodeng.2014.10.023

Landis EN, Keane DT (2010) X-ray microtomography. Mater Charact 61:1305-1316. DOI: 10.1016/j.matchar.2010.09.012

Lauw, A., Oliveira, V., Lopes, F., Pereira, H. (submitted). Variation of cork quality for wine stoppers across the production regions in Portugal. Eur J Wood Wood Prod. Manuscript ID: HARW-D-15-00372

Lequin S, Chassagne D, Karbowiak T, Simon J-M, Paulin C, Bellat J-P (2012) Diffusion of oxygen in cork. J Agric Food Chem 60:3348-3356. DOI: 10.1021/jf204655c

Lima J, Costa P (2006) Real-Time Cork Classification Method: A Colour Image Processing Approach. Int J Fact Automation, Robotics and Soft Comput 2:1-10

Longuetaud F, Mothe F, Kerautret B, Krähenbühl A, Hory L, Leban JM, Debled-Rennesson I (2012) Automatic knot detection and measurements from X-ray CT images of wood: A review and validation of an improved algorithm on softwood samples. Comput Electron Agric 85:77-89. DOI: 10.1016/j.compag.2012.03.013

Lopes F, Pereira H (2000) Definition of quality classes for champagne cork stoppers in the high quality range. Wood Sci Technol 34:3-10. DOI: 10.1007/s002260050002

Lopes P, Saucier C, Glories Y (2005) Nondestructive colorimetric method to determine the oxygen diffusion rate through closures used in winemaking. J Agric Food Chem 53:6967-6973.DOI: 10.1021/jf0404849

Lopes P, Saucier C, Teissedre P-L, Glories Y (2006) Impact of storage position on oxygen ingress through different closures into wine bottles. J Agric Food Chem 54:6741-6746.DOI: 10.1021/jf0614239

Lopes P, Saucier C, Teissedre P-L, Glories Y (2007) Main routes of oxygen ingress through different closures into wine bottles. J Agric Food Chem 55:5167-5170. DOI: 10.1021/jf0706023

Lopes P, Marques J, Lopes T, Lino J, Coelho J, Alves C, Roseira I, Mendes A, Cabral M (2011) Permeation of d5-2, 4, 6-Trichloroanisole via Vapor Phase through Different Closures into Wine Bottles. Am J Enol Viticult 62:245-249. DOI: 10.5344/ajev.2010.10098

Mas A, Puig J, Lladó N, Zamora F (2002) Sealing and storage position effects on wine evolution. J Food Sci 67:1374-1378. DOI: 10.1111/j.1365-2621.2002.tb10292.x

McLaren K (1980) Food colorimetry. In: Developments in Food Colors. Walford J (eds), pp. 27-45. Applied Science Publishers, London, U.K.

Melo B, Pinto R (1989) Análise de diferenças nos critérios de classificação qualitativa das rolhas. Cortiça 601:293-302

Miranda PMA, Valente MA, Tomé AR, Trigo R, Coelho MFES, Aguiar A, Azevedo EB (2006) O clima de Portugal nos séculos XX e XXI. In: Santos FD, Miranda PMA (eds) Alterações climáticas em Portugal Cenários, impactos e medidas de adaptação, 1st ed. Gradiva, Lisbon, pp. 45-113

Mukherjee S, Federici J (2011) Study of structural defects inside natural cork by pulsed terahertz tomography. In: Proceedings of 36th International Conference on Infrared, Millimeter and Terahertz Waves (IRMMW-THz), Houston, USA. DOI: 10.1109/irmmw-THz.2011.6104965

Oliveira V, Rosa ME, Pereira H (2014) Variability of the compression properties of cork. Wood Sci Technol 48:937-948. DOI: 10.1007/s00226-014-0651-2

Oliveira V, Lauw A, Pereira H (2016) Sensitivity of cork growth to drought events: insights from a 24-year chronology. Climatic Change, 137 (1): 261-274. DOI: 10.1007/s10584-016-1680-7

Paniagua B, Vega-Rodríguez MA, Gómez-Pulido JA, Sánchez-Pérez JM (2011) Automatic texture characterization using Gabor filters and neurofuzzy computing. Int J Adv Manuf Technol 52:15-32.DOI: 10.1007/s00170-010-2706-3

Pereira CS, Marques JJF, San Romão MV (2000) Cork taint in wine: Scientific knowledge and public perception — A critical review. Crit Rev Microbiol 26:147-162. DOI: 10.1080/10408410008984174

Pereira H, Rosa ME, Fortes MA (1987) The cellular structure of cork from Quercus suber L. IAWA Bull 8: 213-218. DOI: 10.1163/22941932-90001048

Pereira H, Melo B, Pinto R (1994) Yield and quality in the production of cork stoppers. Holz Roh Werkst 52:211-214

Pereira H, Lopes F, Graça J (1996) The evaluation of the quality of cork planks by image analysis. Holzforschung 50: 111-115. DOI: 10.1515/hfsg.1996.50.2.111

Pereira H, Tomé M (2004) Cork oak. In: Evans J, Youngquist JA (eds) Encyclopedia of forest sciences. Elsevier, Oxford, pp 613-620

Pereira H (2007) Cork: biology, production and uses. Elsevier, Amsterdam

Pereira H (2015) The Rationale behind Cork Properties: A Review of Structure and Chemistry. Bioresources 10: 6207-6229.

Pinto-Correia T, Ribeiro N, Sá-Sousa P (2011) Introducing the *montado*, the cork and holm oak agroforestry system of Southern Portugal. Agroforest Syst 82:99-104. DOI: 10.1007/s10457-011-9388-1

Radeva P, Bressan M, Tovar A, Vitrià J (2002) Bayesian classification for inspection of industrial products. In: MT Escrig et al. (eds), Proceedings 5th Catalonian Conference Artificial Intelligence. Springer-Verlag, Heidelberg, pp 399-407

Ribeiro NA, Surový P, Pinheiro AC (2010) Adaptive Management on Sustainability of Cork Oak Woodlands. In: Manos B, Paparrizos K, Matsatsinis N, Papathanasiou J (eds) Decision Support Systems in Agriculture, Food and the Environment: Trends, Applications and Advances. Information Science Reference, Hershey, New York, pp 437-449. DOI: 10.4018/978-1-61520-881-4.ch020

Ribéreau-Gayon J (1933) Dissolution d'oxygène dans les vins. In: Contribution à l'étude des oxidations et réductions dans les vins. Application à l'étude de vieillissement et des cases. Delmas, Bordeaux, France.

Ridler TW, Calvard S (1978) Picture thresholding using an iterative selection method. IEEE Trans System, Man and Cybernetics SMC-8: 630-632

Rosa ME, Pereira H, Fortes MA (1990) Effects of water treatment on the structure and properties of cork. Wood Fiber Sci 22:149-164

Schindelin J, Arganda-Carreras I, Frise E, Kaynig V, Longair M, Pietzsch T, Preibissch S, Rueden C, Saalfeld S, Schmid B, Tinevez J-Y, White DJ, Hartenstein V, Eliceiri K, Tomancak P, Cardona A (2012) Fiji: an open-source platform for biological-image analysis. Nat Methods 9: 676-682. DOI: 10.1038/nmeth.2019

Silva MA, Julien M, Jourdes M, Teissedre P-L (2011) Impact of closures on wine post-bottling development: a review. Eur Food Res Technol 233:905-914. DOI: 10.1007/s00217-011-1603-9

Stängle SM, Brüchert F, Heikkila A, Usenius T, Usenius A, Sauter UH (2015) Potentially increased sawmill yield from hardwoods using X-ray computed tomography for knot detection. Ann For Sci 72:57-65. DOI: 10.1007/s13595-014-0385-1

Surová D, Pinto-Correia T (2008) Landscape preferences in the cork oak Montado region of Alentejo, southern Portugal: Searching for valuable landscape characteristics for different user groups. Landscape Research 33:311-330. DOI: 10.1080/01426390802045962

Surová D, Surový P, Ribeiro NA, Pinto-Correia T (2011) Integrating differentiated landscape preferences in a decision support model for the multifunctional management of the Montado. Agroforest Syst 82:225-237. DOI: 10.1007/s10457-011-9373-8

Taylor A, Plank B, Standfest G, Petutschnigg A (2013) Beech wood shrinkage observed at the micro-scale by a time series of X-ray computed tomographs (µXCT). Holzforsch 67:201-205. DOI: 10.1515/hf-2012-0100

Teixeira RT, Pereira H (2009) Ultrastructural observations reveal the presence of channels between cork cells. Microsc Microanal 15:1-6. DOI: 10.1017/S1431927609990432

Teixeira RT, Pereira H (2010) Suberized cell walls of cork from cork oak differ from other species. Microsc Microanal 16:569-575. DOI: 10.1017/S1431927610093839

Tran H, Doumalin P, Delisee C, Dupre JC, Malvestio J, Germaneau A (2013) 3D mechanical analysis of low-density wood-based fiberboards by X-ray microcomputed tomography and Digital Volume Correlation. J Mater Sci 48:3198-3212. DOI: 10.1007/s10853-012-7100-0

Ugliano M, Kwiatkowski M, Travis B, Francis IL, Waters EJ, Herderich M, Pretorius IS (2009) Post-bottling management of oxygen to reduce off-flavour formation and optimize wine style. Aust N Z Wine Ind J 24:24-28

Van den Bulcke J, Boone M, Van Acker J, Stevens M, Van Hoorebeke L (2009) X-ray tomography as a tool for detailed anatomical analysis. Ann For Sci 66:508. DOI: 10.1051/forest/2009033

Van den Bulcke J, Boone M, Van Acker J, Van Hoorebeke L (2010) High-resolution X-ray imaging and analysis of coatings on and in wood. J Coat Technol Res 7: 271-277.DOI: 10.1007/s11998-009-9182-4

Van den Bulcke J, Wernersson ELG, Dierick M, Van Loo D, Masschaele B, Brabant L, Boone MN, Van Hoorebeke L, Haneca K, Brun A, Hendriks CLL, Van Acker J (2014) 3D tree-ring analysis using helical X-ray tomography. Dendrochronologia 32:39-46. DOI: 10.1016/j.dendro.2013.07.001

Vega-Rodríguez MA, Sánchez-Pérez JM, Gómez-Pulido JA (2001) Cork Stopper Classification Using FPGAs and Digital Image Processing Techniques. In: IEEE Computer Society (eds), Proceedings of the Euromicro Symposium on Digital Systems Design, Washington, DC, pp 270-275

Vidal S, Aagaard O (2008) Oxygen management during vinification and storage of Shiraz wine. Aust N Z Wine Ind J 23:56-63

Vitrià J, Bressan M, Radeva P (2007) Bayesian classification of cork stoppers using class-conditional independent component analysis. IEEE Trans Syst Man Cybern Part C-Appl Rev 37:32-38. DOI: 10.1109/TSMCC.2006.876043

Vlassenbroeck J,Dierick M, Masschaele B, Cnudde V, Van Hoorebeke L, Jacobs P (2007) Software tools for quantification of X-ray microtomography at the UGCT. Nucl Instrum Meth Phys Res A 580:442-445. DOI: 10.1016/j.nima.2007.05.073

Waters E, Skouroumounis G, Sefton M A, Francis IL, Peng ZK, Kwiatkowski M (2001) The inherent permeability of corks to oxygen. In: Australian Wine Research Institute Annual Report, p 31

Webb A (2003) Introduction to biomedical imaging. John Wiley & Sons, Inc., Hoboken, New Jersey.

Wei Q, Leblon B, La Rocque A (2011) On the use of X-ray computed tomography for determining wood properties: a review. Can J For Res 41:2120-2140. DOI: 10.1139/x11-111

Wieland S, Grünewald T, Ostrowski S, Plank B, Standfest G, Mies B, Petutschnigg A (2013) Assessment of mechanical properties of wood-leather panels and the differences in the panel structure by means of X-ray computed tomography. BioResources 8:818-832.